Universitat Autònoma de Barcelona

Advanced control techniques for the heart rate during treadmill exercise

Ali ESMAEILI

Universitat Autònoma de Barcelona

UNIVERSITAT AUTÒNOMA DE BARCELONA

DOCTORAL THESIS

Advanced control techniques for the heart rate during treadmill exercise

Author:
Ali ESMAEILI

Supervisor:
Dr. Asier IBEAS

A thesis submitted in partially fulfillment of the requirements for the degree of Doctor of Philosophy

in

Electrical Engineering and Control Science
Department of Telecommunication and Systems Engineering

September 10, 2019

Declaration of Authorship

I, Ali ESMAEILI, declare that this thesis titled, "Advanced control techniques for the heart rate during treadmill exercise" and the work presented in it are my own. I confirm that:

- This work was done wholly or mainly while in candidature for a Doctor of Philosophy degree at Universitat Autonoma de Barcelona (UAB) University.
- Where any part of this thesis has previously been submitted for a degree or any other qualification at UAB University or any other institution, this has been clearly stated.
- Where I have consulted the published work of others, this is always clearly attributed.
- Where I have quoted from the work of others, the source is always given. With the exception of such quotations, this thesis is entirely my own work.
- I have acknowledged all main sources of help.
- Where the thesis is based on work done by myself jointly with others, I have made clear exactly what was done by others and what I have contributed myself.

Signed:

Date:

Declaration of Supervisor

I, *Asier Ibeas*, as principal supervisor of Ali ESMAEILI, confirm that I have read this thesis and in my opinion, this thesis is sufficient in terms of scope and quality for the defense of the degree of Doctor of Philosophy at Universitat Autonoma de Barcelona (UAB).

Signed: _____

Date: _____

"Thanks to my solid academic training, today I can write my final thesis with hundreds of words and sharing all of the information and achievement that I have gotten from these four years. I hope that it's getting useful for future works."

Ali Esmaeili

UNIVERSITAT AUTÒNOMA DE BARCELONA

Abstract

Department of Telecommunication and Systems Engineering

Doctor of Philosophy

Advanced control techniques for the heart rate during treadmill exercise

by Ali ESMAEILI

The objective of this work is to design a heart rate (HR) controller for a treadmill so that the HR of an individual running on it tracks a pre-specied, potentially time-varying profile specified by doctors for the cardiac recovery of the person.

Initially, we consider a mathematical model relating the relationship between the speed of the treadmill and HR of the person running on it. An important issue in this model is the determination of its parameters. Thus, we first tackle the parameter estimation problem in this model which is formulated as an optimization one, that is solved through a heuristic technique known as Particle Swarm Optimization. This is the first time that this technique is used for the estimation of cardiac models and is a contribution of the thesis.

Afterward, a super- twisting sliding mode controller is designed to perform the robust control of treadmill's speed in the presence of potential unmodelled dynamics and parametric uncertainties. Numerical examples show that the estimation procedure is able to obtain accurate values for the system's parameters while the proposed control approach is able to obtain zero tracking error without chattering, definitely achieving the control objectives. In both cases, the range of treadmill's speed goes from 2 to 14 km/h, range that is not usually employed in previous studies.

Finally, in the last part of this work, the objective is to design a discrete-time robust controller. Initially, a feedback linearization-based controller is designed, but it has poor robustness properties. In order to solve this problem, we propose another method consisting in the Joint parameter-state estimation based-control. However, this approach does not identify the parameters and it offers some oscillations. To solve all of these problems and regarding the previous Chapter, we used the discrete-time sliding mode controller method to complete our study. In the first part of this Section, as designing a nonlinear model directly is hard, we decided to linearize the model and then discretize it. Furthermore, the continuous control is generated by a zero-order hold (ZOH). On the other hand, since the nonlinear model relationship describes a better relation between HR and speed, a nonlinear is used in the last part of this thesis. The final and best controller is a discrete-time super-twisting model that avoids chattering and achieves very good robustness and tracking in the system. The great systematic procedure to design of the controller, the perfect tracking and the avoidance of using an observer for this system are other advantages of this approach. The simulation results in this work that presented in the speed range of 2-14 km, a range that is not usually employed in previous studies to the control of the heart rate during treadmill exercise.

Acknowledgements

This thesis is a result of almost four years of research activity that I have carried out at the Department of Telecommunication and Systems Engineering at Universitat Autonoma de Barcelona.

This result was carried out with the essential support of many people who helped me with their knowledge, their time and most of all, with their friendship.

Therefore, I wish to first express my gratitude to my great supervisor, Dr. Asier Ibeas, who tremendous support, inspiration, patience, knowledge, faith, and friendship made completion of my graduate studies possible and encouraged me to this Ph.D. thesis.

I am particularly grateful to my Dad Masood, My Mom Seyedeh Sedigheh and my one and only Sister Nazila, for their everlasting love, support, patience, and understanding. Their suggestions have been an invaluable source of inspiration to grow up and improve me.

Contents

Declaration of Authorship iii

Declaration of Supervisor v

Abstract ix

Acknowledgements xi

1 Introduction 1
- 1.1 Cardiac Rehabilitation . . . 2
- 1.2 Aim of the work . . . 4
  - 1.2.1 Methodology . . . 5
  - 1.2.2 Benefits of the work . . . 9
- 1.3 Techniques employed in the thesis . . . 9
  - 1.3.1 Parameter Estimation algorithm . . . 9
  - 1.3.2 Super-twisting Sliding Mode Control . . . 13
  - 1.3.3 Discrete-Time Control Systems . . . 17
  - 1.3.4 Euler Discretization . . . 18
  - 1.3.5 ZOH Discretization . . . 19
  - 1.3.6 Discrete-time Super Twisting Sliding Mode Control . . . 19
- 1.4 Description of the contributions of the thesis . . . 21
- 1.5 Structure of the thesis . . . 21

2 Identification of heart rate model parameters 23
- 2.1 Introduction . . . 23
- 2.2 Heart rate model . . . 24
  - 2.2.1 M-estimator . . . 26
- 2.3 Simulation results . . . 28
- 2.4 Conclusion . . . 33

3 Super-Twisting Sliding Mode Control 37
- 3.1 Introduction . . . 37
- 3.2 Classic Sliding Mode Control . . . 38
- 3.3 Super-twisting sliding mode control . . . 39
- 3.4 Simulation and results . . . 43
- 3.5 Conclusion . . . 45

4 Discrete-time Control 49
- 4.1 Introduction . . . 49
- 4.2 Feedback-Linearization Based Control . . . 50
  - 4.2.1 Discrete-Time model . . . 51
  - 4.2.2 Controller design . . . 52
  - 4.2.3 Observer design . . . 53

4.2.4 Stability analysis of the discrete-time closed-loop system 53
4.2.5 Stability of the continuous-time closed-loop system 55
4.2.6 Simulation Examples 55
4.3 Joint parameter-state estimation based-control 59
4.3.1 Joint Parameter-State Estimation 59
4.3.2 Simulation Examples 60
4.4 Discrete-time Sliding Mode Control 64
4.4.1 Problem Formulation 64
4.4.2 Linearization and ZOH discretization 64
4.4.3 Control Design 68
4.4.4 State Observer 69
4.4.5 Results and Simulation 69
4.4.6 Nonlinear Model 73
4.4.7 Discrete-time Super-twisting Sliding Mode Controller 73
4.4.8 Control Design 73
4.4.9 Results and Simulation 74
4.4.10 Conclusion 76

5 Conclusions **79**
5.1 Future View 80

List of Figures

1.1 Main causes of mortality in the world. . . . 1
1.2 Evolution of the main causes of mortality between 2009 and 2018. . . . 2
1.3 Forecast of the causes of mortality in the world, period 2018-2030. . . . 2
1.4 Whole components of the system. . . . 5
1.5 Main components of the thesis: treadmill's speed control. . . . 5
1.6 The process of moving particles in a group. . . . 11
1.7 The Chattering Phenomenon appearing in classical sliding mode control. . . . 15
1.8 The Saturation function used in classical SMC to over-come the chattering effect. . . . 16

2.1 PSO pseudocode employed to solve the optimization problem. . . . 27
2.2 Heart rate response for subject NO 3 (that shows in green points) with using PSO at speed of (2-14 km/h) . . . 30
2.3 Heart rate response with using PSO at speed of (2-14 km/h)- for 4 random subjects . . . 30
2.4 Evolution of estimated parameter for subject No.1 . . . 31
2.5 Evolution of estimated parameter for subject No.8 . . . 31
2.6 Actual values of parameters. . . . 32
2.7 Relative Error of estimated parameters. . . . 32
2.8 Comparing heart rate estimation results with PSO and M-estimator. . . . 33
2.9 Speed of the treadmill employed for estimation purposes. . . . 33
2.10 Evaluation of the cost function (2.5) with PSO and M-estimator. . . . 34
2.11 Fit-in error functions (2.13) and (2.14). . . . 35

3.1 General schematic implementation of the heart rate control loop system based on treadmill speed by super- twisting sliding mode Controller. . . . 43
3.2 Implementation of integral super-twisting sliding mode controller in order to avoid chattering phenomenon. . . . 44
3.3 Heart Rate provided by the STSMC controller. . . . 45
3.4 The first 150 seconds HR provided by the STSMC controller. . . . 46
3.5 Speed provided by the STSMC controller. . . . 46
3.6 Heart rate tracking error with STSMC and PID. . . . 47
3.7 Treadmill speed coresponding to the application to each controller. . . . 47
3.8 Evaluation of the cost function with STSMC and PID. . . . 48

4.1 Actual heart rate and reference signal. . . . 56
4.2 Error between the actual heart rate and reference signal. . . . 56
4.3 Evolution of the observation error, $\tilde{x}_{2,k}$. . . . 57
4.4 Control command: speed of the treadmill. . . . 57
4.5 Actual heart rate and reference signal in the presence of parameters mismatch. . . . 58

4.6 Error between the actual heart rate and reference signal in the presence of parameters mismatch. 58
4.7 Actual heart rate and reference signal. 61
4.8 Tracking error between the actual heart rate and the reference signal. . 62
4.9 Observation error for the $x_2(t)$ variable. 62
4.10 Evolution of the estimated parameters $\hat{a}_1$, $\hat{a}_2$ and $\hat{a}_6$. 63
4.11 Evolution of the estimated parameters $\hat{a}_3$, $\hat{a}_4$ and $\hat{a}_5$. 63
4.12 Speed of the treadmill. 63
4.13 Heart rate provided by the DTSMC controller 70
4.14 Speed provided by the DTSMC controller 70
4.15 Observer estimation error of DTSMC 71
4.16 Tracking error of DTSMC 71
4.17 Comparing Heart rate provided by the DTSMC controller and PID . . 72
4.18 Comparing tracking error of DTSMC and PID 72
4.19 Heart rate provided by the DTSTSMC controller. 75
4.20 Speed provided by the DTSTSMC controller. 75
4.21 Tracking error of DTSTSMC. 76
4.22 Evaluation of the Tracking errors of DTSTSMC, DTSMC, Joint-parameter and Feedback-Linearization. 77
4.23 Zoom evaluation of the Tracking errors of DTSTSMC, DTSMC, Joint-parameter and Feedback-Linearization. 77

List of Tables

2.1 Actual parameters of subjects 1 - 5. 28
2.2 Actual parameters of subjects 6 - 10. 29
2.3 Estimated parameters obtained by running the PSO algorithm of subjects 1 - 5. 29
2.4 Estimated parameters obtained by running the PSO algorithm of subjects 6 - 10. 29

Dedicated to my lovely family, my Father Masood, my Mother Seyedeh Sedigheh and my lovely one and only sister Nazila.

Chapter 1

Introduction

Ischemic Heart Disease (IHD) is a progressive disorder of the arteries that may end with narrowing or complete occlusion. Among its clinical consequences, we can find angina pectoris, myocardial infarction, chronic ischemic heart disease, and sudden death. Cardiovascular diseases, and in particular ischemic heart disease, represent the main cause of mortality in the world, [**1**] as can be seen in Figure 1.1 according to data from the World Health Organization (WHO), [**2**]. Furthermore, its importance has increased during the last decade as illustrated in Figure 1.2 and it will continue to be the main cause of mortality in the world in the year 2030, see Figure 1.3, according to WHO, [**1**]. Figure 1.3 shows that Ischaemic Heart Disease is one of the diseases that most strongly affects the quality and life expectancy of people, [**2**].

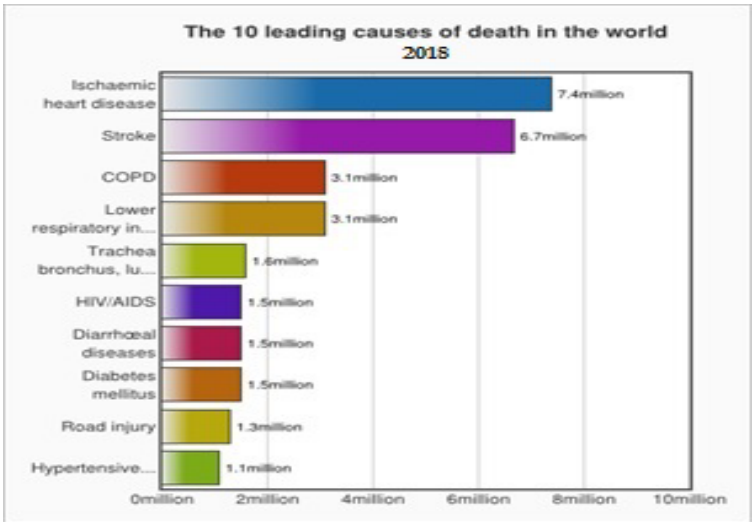

FIGURE 1.1: Main causes of mortality in the world.

One of the main medical priorities after suffering an episode of Ischaemic Heart Disease is to try to prevent it from recurring (secondary prevention), as well as to improve the quality of life of the patient in order to recover the maximum functional capacity, to control the cardiovascular risk factors, achieve social and labor reintegration, decrease the mortality associated with new cardiac events and decrease the frequency and severity of post-infarct depression. In these cases, Cardiac Rehabilitation (CR) has proven to be a highly effective tool in the recovery of patients and their ability to return to a normal life. In fact, cardiac rehabilitation is defined as the set of activities necessary to assure the people that suffer from the heart an optimal physical, mental and social condition, [**1**]. CR is recommended not only in patients who have suffered from IHD but in a wide range of situations such as in patients with coronary artery bypass grafting and after angioplasty, after heart transplantation,

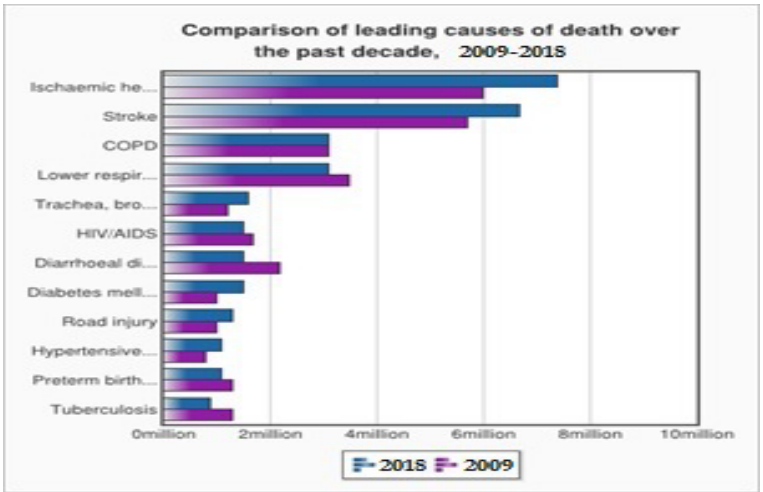

FIGURE 1.2: Evolution of the main causes of mortality between 2009 and 2018.

2018					2030	
Disease or injury	% total deaths	Rank		Rank	% total deaths	Disease or injury
Ischaemic heart disease	12.6%	1	→	1	13.1%	Ischaemic heart disease
Cerebrovascular disease	9.7%	2	→	2	10.3%	Cerebrovascular disease
Lower respiratory infections	6.9%	3	→	3	8.7%	HIV/AIDS
HIV/AIDS	4.8%	4	→	4	7.9%	Chronic obstructive pulmonary disease
Chronic obstructive pulmonary disease	4.8%	5	→	5	3.5%	Lower respiratory infections
Perinatal conditions	4.3%	6	→	6	3.1%	Diabetes mellitus
Diarrhoeal diseases	3.3%	7	→	7	3.0%	Trachea, bronchus, lung cancers
Tuberculosis	2.7%	8	→	8	2.8%	Road traffic accidents
Trachea, bronchus, lung cancers	2.2%	9	→	9	2.4%	Tuberculosis
Road traffic accidents	2.1%	10	→	10	2.1%	Perinatal conditions
Diabetes mellitus	1.7%	11	→	11	1.8%	Stomach cancer
Malaria	1.6%	12	→	12	1.8%	Hypertensive heart disease
Hypertensive heart disease	1.6%	13	→	13	1.5%	Self-inflicted injuries
Self-inflicted injuries	1.5%	14	→	14	1.3%	Nephritis and nephrosis
Stomach cancer	1.5%	15	→	15	1.3%	Liver cancer
Cirrhosis of the liver	1.4%	16	→	16	1.2%	Diarrhoeal diseases
Nephritis and nephrosis	1.2%	17	→	17	1.2%	Colon and rectum cancers
Colon and rectum cancers	1.1%	18	→	18	1.1%	Cirrhosis of the liver
Liver cancer	1.1%	19	→	19	1.1%	Violence
Measles	1.1%	20	→	20	1.0%	Oesophagus cancer
Violence	1.0%	21	→	23	0.80%	Malaria
Oesophagus cancer	0.8%	24	→	42	0.40%	Measles

FIGURE 1.3: Forecast of the causes of mortality in the world, period 2018-2030.

in patients with operated valve disease, in congenital defects and in heart cardiac failure [3], [5]. Numerous studies reveal that cardiac patients undergoing cardiac rehabilitation have better long-term survival as well as fewer future complications [5], [6]. In addition, the incorporation of a patient into cardiac rehabilitation programs can considerably reduce secondary costs, mainly re-hospitalizations. Therefore, one of the main actions in the field of health and one of the fundamental measures of secondary prevention for coronary patients is cardiac rehabilitation.

1.1 Cardiac Rehabilitation

Cardiac rehabilitation programs are multidisciplinary programs that include different elements, among which we can find health education talks (to advise on changes in life habits), smoking cessation courses (if applicable), relaxation techniques and

training in skills to control stress. However, the most important element is a progressive program of physical exercises (mainly aerobic) to improve physical fitness and functional capacity. This transversal CR program is carried out by a team of professionals that includes cardiologists, nurses, psychologists, psychiatrists, nutritionists and social workers, [**3**].

The CR program is divided into three phases: (I) hospital, (II) ambulatory and (III) autonomous (throughout the patient's life) which is monitored through periodic visits to the health center. The key piece in rehabilitation consists of aerobic exercise on a bicycle, treadmill, or other devices that allows indoor exercise. The team responsible for the rehabilitation carries out a protocol that establishes exercise guidelines that is communicated to the patient for its execution (exercise intensity, time, etc.). The protocols are adjusted for each patient through an evaluation of the cardiac capacities at the beginning of the recovery, with one of the most known evaluation protocols being the so-called BRUCE, [**7**]. There are several clinical studies worldwide that show the effectiveness of CR in the coronary recovery of patients. In [**8**] - [**10**] it is shown that participation in CR programs results in a very significant reduction in mortality from any cause (21-34 Percent lower). In addition, studies [**9**], [**10**] show a decisive influence of the duration of CR on its long-term effects. The longer the duration of the CR program, the lower the mortality rate. A decrease in mortality of 19 percent was shown in patients who had received at least 25 sessions while patients who participated in 36 sessions had a 47 percent lower risk of death and 31 percent less risk of myocardial infarction than the patients who participated in a single session.

After phase II of CR (ambulatory) phase III of CR (autonomous), also called home-based, [**8**] is initiated. The studies [**11**], [**12**] conclude that the forms of home-based CR and centers-based CR are equally effective in improving the clinical and health outcomes related to the quality of life and the choice between one and the other is a reflection of each patient's individual preference. However, CR in centers continues to be the preferred option for many patients due to the fact that they perceive a sense of security by having access to specialists from different disciplines and having more elaborate individual work programs, [**8**].

Despite the numerous clinical evidence of the beneficial effects of CR programs, these are, generally, not very widespread in the world. In Spain, in 1995, the estimated CR only reached 2 percent of patients with myocardial infarction. In 2003, studies showed that the figure had not changed significantly, [**5**], [**8**]. The situation in South America and the Caribbean is very similar, having been documented that the number of CR programs seems to be insufficient for a population with a high and growing burden of cardiovascular diseases, [13], [**14**]. The situation in other European and North American countries is very unequal. In Austria, one of the countries where CR is most developed, 95 percent of the affected population has phase II coverage, which is reduced to 6 percent in the Netherlands and 30 percent in Denmark [**15**]. In the United Kingdom, in 1998 there were 300 CR programs, although there was underutilization and great variability in the practice and organization of them, [**6**] and in Italy, there were around 111 centers, [**15**]. In the US, around 10-20 percent of patients who meet criteria participate in CR programs, [**16**]. Despite these figures, there are not many studies that analyze the reasons for the poor implementation of these programs in the world. As an example, [**14**] sheds light on these causes in South America: lack of qualified personnel, financial restrictions and lack of physical space.

At this point we can reach the following conclusions in relation to CR programs:

• There are numerous clinical evidence that prove its usefulness in the rehabilitation and secondary prevention of coronary diseases, in particular ischemic heart disease.

• Clinical evidence has been shown that CR at home allows obtaining beneficial effects similar to CR in specialized centers. Even so, many patients prefer to do it in centers instead of autonomously.

• The convenience of maintaining a sustained CR over time, with a number of sessions as high as possible, has been demonstrated.

• CR programs have, generally, little implantation in the world. Particularly in the European Union there is a great dispersion in terms of its implementation in different countries.

• The possible causes of the low average implantation can be the absence of the required professionals, financial reasons and lack of space and specialized centers.

1.2 Aim of the work

This work is aimed at making easier the access to CR programs and at spreading its use by the design of a computerized system that allows the patients to develop the physical exercise recommended by the specialists (rehabilitation protocol) in a programmed, safe, autonomous, and above all, effective ways on a treadmill. Usually, when we get on a treadmill, we specify the speed and inclination of the treadmill in such a way that the subject runs in those conditions. The heart responds to this exercise according to its natural dynamics.

The monitoring of the heart rate allows the subject to know if he works in an adequate range of values that allow effective rehabilitation. These values are provided by the hospital's CR work team individually to the patient during phase II of rehabilitation, while in the autonomous phase (III), [**17**], which provides protocols, is an extended manual providing general guidelines for all the patients in a generalized way. When the heart rate does not meet the rehabilitation goals, the speed and/or inclination of the treadmill must be modified manually in order to return the heart to the appropriate recovery interval. The manual manipulation of the speed of the treadmill supposes an element of fear in the patients, who due to the fear to overcome a certain level of pulsations maintain a sub-optimal exercise with respect to the necessary one for its optimal recovery, [**18**][**19**]. Additionally, it implies concern and stress in patients that can be avoided with the development of an automatic computerized system.

The aim of the project is the design of a robust control system that automatically determines the speed of a treadmill based on the measurement of the patient's heart rate in such a way that allows the heart to follow a heart rate profile established as a reference by the specialists for the coronary rehabilitation of the subject.

In Fig 1.4 the whole system is shown. Basically, the system has different components such as the control system part, and the monitoring of the data which is getting controlled by the doctors. These components are getting connected to each other with a telecommunication server that can get the data from the control system and send them to the monitoring system.

In addition, the control system may also be completed with a telematic communication that will transmit personalized routines to the patients, store the performance data obtained by them and be able to perform a statistical, preventive and anticipatory analysis of the data in order to look for patterns that allow anticipating a future ailment, [**19**][**20**][**21**].

Likewise, if at the time of the exercise a dangerous situation occurs for the patient, this will be communicated in the form of an alarm to the pertinent health services.

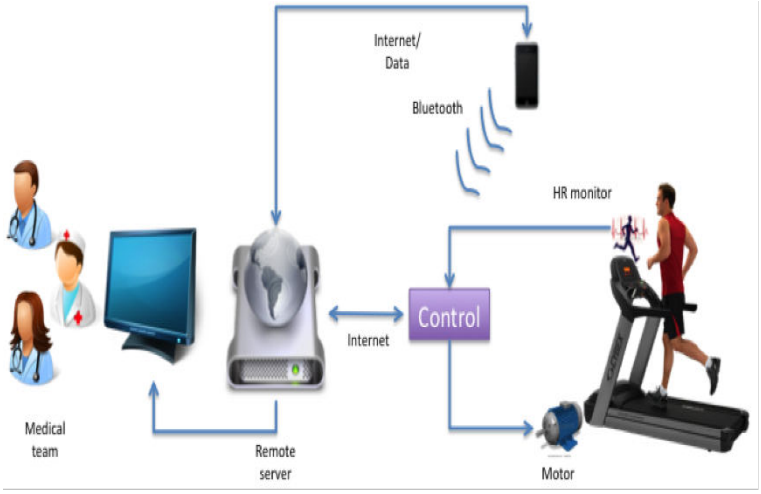

FIGURE 1.4: Whole components of the system.

However, the main objective of the work is not to set up the whole system but only the speed control part, that is represented in Figure 1.5.

FIGURE 1.5: Main components of the thesis: treadmill's speed control.

In the following section, we are introducing the steps performed to achieve such a goal.

1.2.1 Methodology

In particular, the project will develop the steps detailed below.

The **first step** is to model the relationship between the HR and the treadmill's speed. This step implies the model structure and parameter estimation. A literature review has been done in order to analyze the structure of the different models. These models are parametrized by a number of parameters and a parameter estimation

algorithm will be proposed in this work since this will allow having a personalized and individualized model for each person. So the controller can be adapted for each patient and also we can have a starting point for the design of the controller.

Currently, there are several models that allow establishing the relationship between HR and speed, essentially nonlinear. In fact, nonlinearity is one of the most representative characteristics of the behavior of the heart and a model capable of representing it will be necessary nonlinear in order to have a sufficiently precise benchmark for the control action. Nonlinear models have been proposed in the form of Hammerstein models, formed by an input non-linearity and a linear dynamic system in [**18**], [**20**], [**24**].

However, a dynamic non-linear model (nonlinearity is dynamic in this case and not only static as in the Hammerstein models) seems more appropriate for the representation of coronary behavior, as proposed in [**19**], [**21**] - [**23**], [**25**] - [**27**]. This model is appropriate for our purposes since it captures by means of a reduced number of parameters and equations the global behavior of the HR.

Once a nonlinear system has been chosen as a model, the design of the controller will be done as a **second step**. Usually, many controllers have been used in many studies these days but we decided to choose sliding mode control (SMC), and especially a method which is called super-twisting sliding mode.

The SMC has revealed very useful in the robust control of multiple systems, enhance the examples of SMC to real systems such as pneumatic cylinder as actuators for robot manipulators, and the hydraulic dynamics of the manipulator, [**18**][**20**]. However, this is the first time that SMC is used to control the HR during treadmill exercise since previous works used different control techniques.

In [**18**], [**20**], [**21**], [**27**] the authors start from a Hammerstein model to make such a design. In [**18**], [**27**] a compensation scheme is proposed that uses an approximate inverse model of non-linearity in order to cancel it and then design a predictive controller based only on the linear part. In parallel, in [**20**], [**24**] the static non-linearity is inverted while a LQ and H_∞ control is subsequently designed for the linear part.

In [**21**] a robust control is designed through LMIs by minimizing a certain function that contains the state of the system. A common feature of these works is that they carry out the design in continuous time and on a common model for all patients, that is, they do not distinguish the possible variability of conditions between them. The proposed dynamic nonlinear model is used, for example to synthesize feedback controller based on Lyapunov techniques in [**23**], [**25**], [**26**]. The main contribution of these works is the use of the complete dynamic model although they continue to design the controller in continuous time and for fixed models (the same for all patients).

Previous works in the area suffer from the following disadvantages, which will be mitigated in the development of this project:

i) They carry out a continuous design when the implementation will be carried out in discrete-time. Therefore, it would be convenient to take this fact into account from the beginning of the design.

ii) The design is the same regardless of the patient, so the specific behavior of the patient in the design is not taken into account, it is not an individualized design.

iii) Most of the designs are made for linear models when it would be advisable to make a design on an initially non-linear model.

In this regard, different approaches are proposed that improve the disadvantages existing in the literature:

The first type of control will be the design of a robust control based on SMC for the selected nonlinear model. At the beginning of the CR of a given patient, an effort

test will be performed that serves as the basis for the design of the rehabilitation protocol (this is a usual procedure, [**5**]). During the stress test, the parameters of the nonlinear model representing the particular heart of the patient can be identified. These parameters are incorporated into an individualized dynamic model.

The aim of this objective is to design a control procedure that automatically tunes an ad-hoc robust controller for the model provided by the patient. The controller will be individualized and its robust character will allow it to resist small drifts of the heart model during training and/or time.

Among all of the Sliding Mode Controllers, I choose Super twisting sliding mode one, because of good tracking properties and chattering avoidance. The super-twisting sliding mode control is encountering growing attention in the control research community. The objective of this part is to show that the super-twisting sliding mode approach is an effective solution to the cited drawbacks and constitutes a good candidate for solving a wide range of important practical problems.

Especial attention will be devoted to the chattering effect since this is a crucial aspect in biomedical applications. To this end, a super-twisting based sliding mode controller is designed instead of a traditional SMC. The super-twisting approach will allow avoiding the undesired oscillations that a classical sliding mode controller may cause. The stability and finite time convergence characteristics of the used algorithm have been recently proved by means of Lyapunov functions [**34**–**37**], so the stability analysis of the proposed controller can be performed in the same way. Simulation results will show that our approach definitely improves the accuracy of the model parameter estimation for the treadmill speeds, (up to 14 km/h) these range of speeds have not been considered in the previous studies. In section 1.3.2 more details will be given on super-twisting sliding mode control.

Most models, as well as control strategies based on them, have been presented in the literature in continuous time [**19**] - [**21**], [**23**] - [**27**] with few examples in -time, [**22**], and restricted to a linearized system with the limitations that fact implies. Nevertheless, for implementation of the controllers and the design of an individualized rehabilitation system, it would be more convenient to have discrete models. The design of control systems from discrete models offers the attractiveness of dealing with the aspect of the selection of the sampling period initially (which is a great advantage compared to the continuous time designs that are later discretized) since many of the primary properties of a feedback control system depend strongly on its value, [**28**], [**40**]. In this way, as a **third phase** of the project, we will proceed to obtain a discrete model of the heart by discretizing the continuous nonlinear model chosen as a starting point. The problem of discretization of continuous systems is well solved in the case of linear systems through very lax conditions in the input signal, for example through the use of zero-order holds (ZOH), but it remains an open research topic for non-linear systems, [**28**][**89**]. In section 1.3 I will explain with more details the techniques to obtain a discrete model of the system. Once we had a discrete model of the system, a discrete-time controller will be designed.

The **final** step is to design a discrete-time and controller for the heart rate during treadmill exercise. To this end, two approaches will be followed:

The **first approach** is to obtain a discrete-time *linear* system and design a for it. Actually, many designs have already been presented in CT. However, controllers are implemented in Discrete-time these days. It is better, thus, to the design of the controller in discrete-time.

The **second approach** is to diversity discretize the nonlinear CT model to obtain a nonlinear discrete-time one. To this end, the development of Yuz and Gudvin, [**36**] will be followed.

The design of the robust controller is tackled in discrete-time in order to explicitly take into account the effect of the sampling time during the design process. Moreover, the fact of using a discrete-time model to face the control design problem will allow us to obtain more accurate controllers than designing a continuous-time one and then sampling it at a low rate. Finally, the implementation of the proposed controller will be straightforward since most controllers are implemented in digital platforms nowadays.

To this end, a feedback linearizing control law is designed for the discrete-time system. Therefore, the nonlinear model, originally proposed in continuous-time, is discretized to obtain a suitable model for control design purposes. It will also be proved under which circumstances the so-obtained discrete model is positive. Then, As a consequence, a reduced-order observer is deployed to obtain the missing state variable. Once the discrete-time control is generated, the continuous-time signal is obtained by using a zero-order hold (ZOH). It will be shown that this control command is indeed a linear state-feedback control so that a linear controller is enough to achieve perfect output tracking under the frame of feedback linearization. The main drawback of the obtained control law is that it requires both state variables to generate the control command. However, only one of them is measured in practice. But the big problem that this method has is its poor robustness properties. In order to solve this problem, we are using another model which is called Joint parameter-state estimation based-control. The algorithm provides an estimation of unknown/ unmeasurable values, which are then used in the control law calculation. Nevertheless, the approach still presents problems regarding its complexity and estimation issues. Another problem appears in this system that does not identify the parameters and it offers some oscillations.

In this work, thus, a discrete-time sliding mode controller (SMC) is designed for the heart rate control in treadmill exercise. Sliding mode controllers have the advantage to provide a superb performance irrespective of the potential uncertainties in the model, [**32**][**57**].

Additionally, SMC also offers other advantages such as a simple design procedure and good robustness properties. Since more and more modern control systems are implemented by computers, the study of SMC in the discrete-time has been an important topic in the SMC literature, [**93**]. The development of the SMC theory in discrete-time also needed a revision of how the continuous-time algorithms are adapted to sampled systems. This fact has led researchers to approach discrete-time sliding-mode control from two directions. The first one is the emulation, that focuses on how to map continuous-time algorithms to discrete-time ones so that the switching term can be preserved, [**100**][**102**]. The second approach is based on the equivalent control design and disturbance observer, [**98**][**115**].

Initially, I will linearize the system, discretize it and design a SMC for the linear discrete system. This swill allows us to analyze the sampling-time.

On the other hand, in the following Section of Chapter 4, the nonlinear model has been employed.

The **final approach** is to design a super-twisting discrete-time controller for the nonlinear system.

An approach to design discrete-time robust control systems to using the fast output technique is considered when the system states are not needed online in [**101**]. Although in [**102**] a sort of discretization has been applied on high order sliding mode controllers, the results are not reported in the literature so far, which deals with the concept of high-order discrete-time sliding mode control (HDSM). The idea of super-twisting sliding mode control in discrete-time systems will be introduced in

terms of a certain class of discretizations. Based on the available conditions, we employ a new strategy to develop a discrete-time Super-Twisting- algorithm (DSTA), [**70**]. Despite the successful development of the classical SMC, in the eighties, a new control technique, called super-twisting sliding mode control, have been investigated. Its main idea is to reduce to zero, not only the sliding function but also its higher derivatives.

In the final part of my thesis, a super-twisting sliding mode controller for solving the problem has been presented. In this section, to solve these issues the controller has been designed a control system without using a state observer, and have a great robustness. In this case, the chattering and robustness in the controller are almost zero. So, I achieved a personalized controller that works without chattering and with good tracking properties.

1.2.2 Benefits of the work

By developing this system, the following benefits will be achieved that result in greater incidence and effectiveness of cardiac rehabilitation programs, by allowing:

• Expand the incidence of CR. It will no longer be necessary to have a CR center near home since these automated treadmills can be available in centers (sports clubs, gymnasiums) to which those people affected can easily go. This solves the problem of the poor incidence of CR in multiple regions of the world.

• Individually supervise each individual. The patient performs a CR on their own but the procedure is individualized and the telematics connection of the data guarantees that the doctors have access to their complete medical history. In addition, the system itself warns if a problem occurs that requires immediate attention. In this way, the patient feels the qualified control and less fear to undertake a CR on their own and maintain it over time as an additional healthy habit of life.

• Increase the quality of life of patients. As CR is prolonged, so do its positive effects on patients. This fact allows the physician to achieve greater functional recovery by providing them with improved quality of life.

• Reduce the costs of CR. The same team can supervise multiple patients, which optimizes the use of resources and covers a wider spectrum of patients with the same level of investment. In addition, the cost of the system is relatively low, a low-cost computer (Raspberry Pi costs around 35 euros) and affordable material today (heart rate monitor, etc.).

In short, it will increase the quality of life of patients, reduce costs for the health system and contribute to the extension of CR programs by homogenizing the incidence of programs between countries.

It is important to note that we are not developing the complete system, in this thesis we are just focused to obtain a HR controller for the speed of the treadmill.

1.3 Techniques employed in the thesis

This section will introduce the main techniques used to carry out the steps mentioned in Methodology Section 1.2.1.

1.3.1 Parameter Estimation algorithm

The first step is parameter identification. Heart rate treadmill models are parameterized by a number of parameters that capture the individual HR response to exercise. It is vital, thus, to design parameter estimation procedures that allow us to have a

personalized model for each individual from measured data. In this work, parameter estimation is set up as an optimization problem whose solution leads to the estimated model parameters. The optimization problem is solved by using a Particle Swarm Optimization (PSO) algorithm. Which is the first time where this method is used for the problem at hand. The parameter estimation will be focused in the range of treadmill speeds from 2 up to 14 km/h (2-14 km/h). In many studies, [**81**], [**82**], the usual range of speed is (2-8 km/h), or (2-10 km/h). Therefore, the proposed methodology is applicable in the large range of speeds from 2 to 14 km/h. Despite this range is popular in many rehabilitation and training exercises, it is the first time considered in this problem.

Previously, researchers used different methods in some studies such as the M-estimator, recursive least squares (RLS) method, and model Hessian to solve the parameter estimation problem, [**50**][**51**]. These methods are effective, from the statistical point of view, to obtain an adequate estimation of the parameters. However with PSO, we get better behavior than the previous approaches, since the accuracy of the estimation parameter is increased by using PSO.

The advantages of the basic particle swarm optimization algorithm are:

(1)PSO is based on the intelligence. It can be applied into both scientific research and engineering use.

(2)PSO algorithm has no overlapping and mutation calculation. The search is carried out by the speed of the particle. During the development of several generations, only the most optimistic particle can transmit information onto the other particles, and the speed of the researching is very fast.

(3)The calculation in PSO is very simple. Compared with the other developing calculations, it occupies the bigger optimization ability and it can be completed easily.

(4) PSO adopts the real number code, and it is directly by the solution. The number of the dimension is equal to the constant of the solution.

The PSO method is based on swarm intelligence. The research on it is just at the beginning. Far from the Genetic algorithm (GA) and the simulated annealing (SA) approach, the PSO has no systematical calculation method and it has no definite mathematic foundation. On the other hand, besides the interest in evolutionary procedures that governed EAs (Evolutionary Algorithms), new paradigms from nature were subjected to investigation. The first PSO models introduced the novelty of using difference vectors among population members to sample new points in the search space. This novelty diverged from the established procedures of EAs, which were mostly based on sampling new points from explicit probability distributions. Additional advantages of PSO were its potential for easy adaptation of operators and procedures to match the specific requirements of a given problem, as well as its inherent decentralized structure that promoted parallelization, [**52**]. PSO has gained much attention nowadays and has wide applications in different fields such a fitness distance ratio, [**53**], adaptive mutation and inertia weight, [**54**], and parameter identification in magnet synchronous motors, [**55**], hybrid neural network and the level of seismic inversion, [**56**].

Particle swarm optimization (PSO) algorithms are nature-inspired population-based metaheuristic algorithms originally accredited to Eberhart, Kennedy, and Shi [**56**]. These algorithms mimic the social behavior of birds flocking and fish schooling. Starting to form a randomly distributed set of particles (potential solutions), the algorithms try to improve the solutions according to a quality measure (fitness function), [**48**][**52**]. The improvement is performed through moving the particles around the search space by means of a set of simple mathematical expressions which model

some interparticle communications. These mathematical expressions, in their simplest and most basic form, suggest the movement of each particle towards its own best-experienced position and the swarm's best position so far, along with some random perturbations. There is an abundance of different variants using different updating rules. In Fig 1.6 the process of moving particles in a group is shown. However, despite being generally known and utilized as an optimization technique, PSO has its roots in image rendering and computer animation technology where Reeves [54] defined and implemented a particle system as a set of autonomous individuals working together to form the appearance of a fuzzy object like a cloud or an explosion. The idea was to initially generate a set of points and to assign an initial velocity vector to each of them. Using these velocity vectors, each particle changes its position iteratively while the velocity vectors are being adjusted by some random factors. Reynolds [55] added the notion of inter-object communication to Reeves' particle system to introduce a flocking algorithm in which the individuals were able to follow some basic flocking rules such as trying to match each other's velocities. Such a system allowed modeling more complex group behaviors in an easier and more natural way.

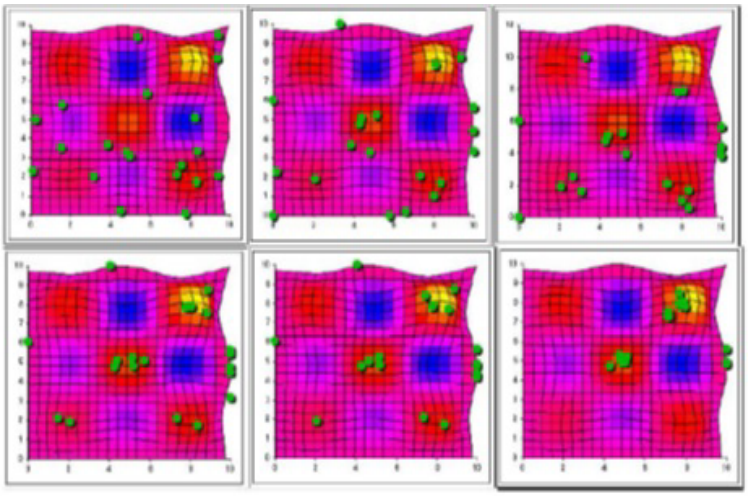

FIGURE 1.6: The process of moving particles in a group.

Kennedy and Eberhart **[54]** while trying to "graphically simulate the graceful but unpredictable choreography of a bird flock" came across the potential optimization capabilities of a flock of birds. In the course of refinement and simplification of their paradigm, they discussed that the behavior of the population of agents that they were suggesting follows the five principles of swarm intelligence articulated by Millonas **[56]**. First is the proximity principle: the population should be able to carry out simple space and time computations. Second is the quality principle: the population should be able to respond to quality factors in the environment. The third is the principle of diverse response: the population should not commit its activities along excessively narrow channels. The Fourth is the principle of stability: the population should not change its mode of behavior every time the environment changes. The fifth is the principle of adaptability: the population must be able to change behavior mode when it is worth the computational price. They also mention that they compromisingly call their massless volume-less population members particles in order to make the use of concepts like velocity and acceleration more sensible.

As a development of PSO Kennedy and Eberhart [**54**] indicated appropriately particle swarm optimization is probably best presented and understood by explaining its conceptual development. Hence, the algorithm's transformation process from its earliest stages to its current canonical form is briefly reviewed in this section. Future discussion on the main aspects and issues would be more easily done this way.

The earliest attempt to use the concept for social behavior simulation carried out by Kennedy and Eberhart [**56**] resulted in a set of agents randomly spread over a torus pixel grid which used two main strategies: nearest neighbor velocity matching and craziness. At each iteration, a loop in the program is determined for each agent which other agent was its nearest neighbor, then assigned that agent's X and Y velocities to the agent in focus, [**52**][**53**]. As it is predictable, it has been viewed that sole use of such a strategy will quickly settle down the swarm on a unanimous, unchanging direction. To avoid this, a stochastic variable called craziness was introduced. At each iteration, some change was added to randomly chosen X and Y velocities. This change introduced enough variation into the system to give the simulation a "life-like" appearance. The above observation points out one of the most necessary features of PSO which indicates its seemingly unalterable nondeterministic nature: incorporation of randomness.

Kennedy and Eberhart took the next step by replacing the notion of "roost" (a place that the birds know previously) in Heppner and Grenander [55] by "food" (for which the birds must search) and therefore converted the social simulation algorithm into an optimization paradigm. The idea was to let the agents (birds) find an unknown favorable place in the search space (food source) through capitalizing on one another's knowledge. Each agent was able of remembering its best position and knowing the best position of the whole swarm. The extremum of the mathematical function to be optimized can be thought of as the food source.

Regarding the *parameters*, like any other metaheuristic algorithm, PSO's performance is dependent on the values of its parameters. The optimal values for the parameters depend mainly on the problem at hand and even the instance to deal with and on the search time that the user wants to spend in solving the problem [**73**]. In fact the main issue is to provide balance between exploration and exploitation tendencies of the algorithm. Total number of particles, total number of iterations, inertia weight and/or constriction factor, and cognition and social behavior coefficients (c_1 and c_2) are the main parameters that should be considered in a canonical PSO. The total number of iterations could be replaced with a desired precision or any other termination criterion.

In general, the search space of an n-dimensional optimization problem can be conceived as an n-dimensional hypersurface. The suitable values for a metaheuristic's parameters depend on relative ruggedness and smoothness of this hyperspace. For example, it is imaginable that in a smoother hyperspace, a fewer number of particles and iteration numbers will be required. Moreover, in a smoother search space, there will be fewer local optimal positions and less exploration effort will be needed, while in a rugged search space, a more thorough an exploration of the search space will be advisable, [**74**]-[**75**].

Generally speaking, there are two different strategies for parameter value selection, namely, off-line parameter initialization and online parameter tuning [**73**]. In off-line parameter initialization, the values of different parameters are fixed before the execution of the metaheuristic. These values are usually decided upon through empirical study. It should be noted that deciding about a parameter of a metaheuristic algorithm while keeping the others fixed (i.e., one-by-one parameter selection) may result in misleading observations since the interactions of the parameters are

not taken into account. However, it is the common practice in the literature since examining combinations of the algorithm parameters might be very time-consuming. To perform such an examination, when desired, a meta-optimization approach may be performed, i.e., the algorithm parameters can be considered as design variables and be optimized in an overlying level.

The main drawback of the off-line approaches is their high computational cost since the process should be repeated for different problems and even for different instances of the same problem. Moreover, appropriate values for a parameter might change during the optimization process. Hence, online approaches that change the parameter values during the search procedure must be designed. Online approaches may be classified in two main groups [**72**]: dynamic approaches and adaptive approaches. In a dynamic parameter updating approach, the change of the parameter value is performed without taking into account the search progress. The adaptive approach changes the values according to the search progress.

Attempts have been made to introduce guidelines and strategies for selection of PSO parameters. Shi and Eberhart [**88**] analyzed the impact of inertia weight and maximum allowable velocity on the performance of PSO and provided some guidelines for selecting these two parameters. For this purpose, they utilized different combinations of w and V_{max} parameters to solve the Schaffer's f6 test function, [**75**][**88**], while keeping other parameters unchanged. They concluded that when V_{max} is small ($<= 2$ for the f6 function), an inertia weight of approximately 1 is a good choice, while when Vmax is not small ($>= 3$), an inertia weight $w = 0.8$ is a good choice. They declared that in absence of proper knowledge regarding the selection of Vmax, it is also a good choice to set V_{max} equal to X_{max}, and an inertia weight $w = 0.8$ is a good starting point. Furthermore, if a time-varying inertia weight is employed, even better performance can be expected. I will follow these guidelines when I use the PSO to solve my parameter optimization problem.

Many different online tuning strategies are also proposed for different PSO parameters. For inertia weight, methods such as random inertia weight, adaptive inertia weight, sigmoid increasing/decreasing inertia weight, linear decreasing inertia weight, chaotic inertia weight and chaotic random inertia weight, oscillating inertia weight, global-local best inertia weight, simulated annealing inertia weight, natural exponent inertia weight strategy, logarithm decreasing inertia weight, and exponent decreasing inertia weight are reported in the literature, [**56**]. All of these methods replace the inertia weight parameter with a mathematical expression which is either dependent on the state of the search process (e.g., the global best solution, the current position of the particle, etc.) or not. Bansal et al. [**55**] examined the abovementioned inertia weight strategies for a set of five mathematical problems and concluded that chaotic inertia weight is the best strategy for better accuracy, while random inertia weight strategy is best for better efficiency. This shows that the choice of a suitable inertia weight strategy depends not only on the problem under consideration but also on the practitioner's priorities.

Chapter 2 will describe how the PSO algorithm is adapted to the HR model parameter estimation.

1.3.2 Super-twisting Sliding Mode Control

Following the steps mentioned in section 1.2.1, the other objective of this work is to use Sliding Mode Control to design our control system, which is for the first time that this method is used for this kind of systems. The aim is the robustness of the system and having minimum chattering during the control process. On the other

hand, in this work Sliding Mode Control is divided into two parts: the first part is super twisting sliding mode technique and discretization of a controller by ZOH method in linear part, and the second part is about discretization of super twisting sliding mode.

To this end, a super-twisting based sliding mode controller will be designed instead of a traditional SMC, [**59**], [**60**]. The super-twisting approach will allow avoiding the undesired oscillations that a classical sliding mode controller may cause. Estimated control simulation results will show that our approach definitely improves the accuracy of the model parameter estimation for these treadmill speeds, (up to 14 km/h) and the SMC also improves the heart rate control which has not been considered in the past.

These techniques are capable of guaranteeing the attainment of the control objectives in spite of modeling errors and/or parameter uncertainties affecting the controlled plant. Among the existing methodologies, the Sliding Mode Control (SMC) turns out to be characterized by high simplicity in design and robustness. Essentially, SMC utilizes discontinuous control laws to drive the system state trajectory onto a specialed surface in the state space, the so-called sliding or switching surface, and to keep the system state on this manifold for all the subsequent times, [**61**].

In order to achieve the control objective, the control input must be designed with an authority sufficient to overcome the uncertainties and the disturbances acting on the system. The main advantages of this approach are two: first, while the system is on the sliding manifold it behaves as a reduced order system with respect to the original plant; and, second, the dynamic of the system while in sliding mode is insensitive to model uncertainties and disturbances, [**77**].

The control of dynamical systems in the presence of uncertainties and disturbances is a common problem to deal with when considering real plants. The effect of these uncertainties on the system dynamics should be carefully taken into account in the controller design phase since they can worsen the performance or even cause system instability. For this reason, during recent years, the problem of controlling dynamical systems in the presence of heavy uncertainty conditions has become an important subject of research. As a result, considerable progress has been attained in robust control techniques, such as nonlinear adaptive control, model predictive control, backstepping, sliding model control and others, [**86**][**95**].

The uncertainty in the model is divided into two general categories, [**97**][**101**]:

1. The structural or parametric uncertainty that may be due to system uncertainties and the inaccuracies in the parameters in the model, such as uncertain system parameters.

2. Non-structural uncertainties or unmodeled dynamics that can be related to the purposeful simplification of system dynamics and the inaccuracy of system rank or estimation error, for example, in linear modeling of friction. Inaccuracy in modeling can have adverse effects on nonlinear systems. Therefore, in any practical design, they must be explicitly addressed. To control the uncertain systems, controller design is required to be robust in the presence of uncertainties.

However, in spite of the claimed robustness properties, the real-life implementation of SMC techniques presents a major drawback: the so-called chattering effect, i.e., dangerous high-frequency vibrations of the control signal that excite oscillation in the system's output. This phenomenon is due to the fact that, in real-life applications, it is not reasonable to assume that the control signal can switch at infinite frequency. On the contrary, it is more realistic, due to the inertias of the actuators and sensors and to the presence of noise and/or exogenous disturbances, to assume that it switches at a very high, but finite, frequency. Chattering and the need for

discontinuous control constitute two of the main criticisms to sliding modes control techniques.

The control input designed in the first-order sliding mode includes the sign function. Since the implementation of the sliding mode controller is not ideal and the triggers are not able to switch the moment and it may delay, so the presence of this function in the control input forces the trigger to momentarily switch. Thus, the size of the sliding variable, which is the total weight of the error, is not infinitely accurate, and the phenomenon of shrinking (vibration or Unwanted oscillation) appears.

The form of this phenomenon is shown in Fig. 1.7. First, the path of the mode moves to the sliding surface $S = 0$ in the region $S > 0$ and first hits the point. Ideally, in the control of the ideal sliding mode, the path should begin to slide on the surface from this point; at this moment, the sign function of the mark is changed, and the control must be switched. In practice, there is a delay between the change of the sign function and the switching control. This delay causes the path to passing from the sliding surface and goes to the area $S < 0$, while the control is switched and the direction is changed and directed to the sliding surface to collide with it, and the function of the change sign marks, and the delay in two the switching control, makes the route cross the sliding surface. By repeating this action, a "zigzag" movement will arise. This phenomenon is called unwanted fluctuation or chattering, [**72**][**76**].

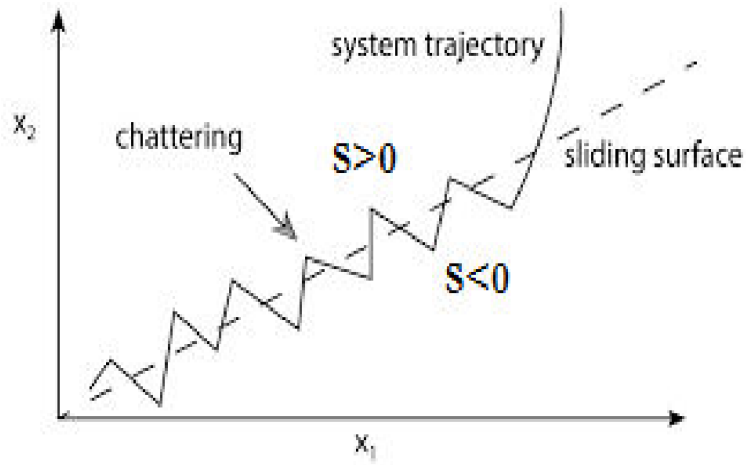

FIGURE 1.7: The Chattering Phenomenon appearing in classical sliding mode control.

Only few exceptional exceptions can be accepted, and sliding control rules can be good, [**86**]. But in general, chattering is very unfavorable because it has the following disadvantages:

- It provides a lot of control activity.
- It may stimulate high-frequency unmodeled dynamics.
- Reduces control accuracy.
- Increases heat loss in electrical circuits and increases electrical energy consumption.
- Increases wear and tear in mechanical parts and stimulants.

These disadvantages reduce system performance and may lead to unsustainability.

There are several ways to smooth the chattering. One of these methods is to smooth out the control discontinuity in the narrow boundary layer in the adjacent

sliding surface by a continuous approximation of the discontinuous slider mode controller. The continuous approximation or boundary layer method is the mostly employed methods in which the bucket function replaces the sign with the saturation function, [**98**].

The function is close to the sign function which is showed in Fig 1.8.

In addition to the saturation function, we can use other functions such as the continuous function in which the parameter ψ in the Figure 1.8 determines the width of the boundary layer. Due to the approximation, the use of continuous approximation in each case reduces the control accuracy. But it can be increased by controlling the accuracy of the boundary layer width as a variable with time. In a special case, the gradient of the saturation function on the boundary layer can be considered as X variable by increasing this parameter.

Higher-order sliding modes are endowed with attractive dynamical properties, such as finite-time convergence and insensitivity to matched perturbations. We refer the interested reader to the work of Fridman for a survey of recent developments and open problems on sliding mode control and observation, [**122**]. The super-twisting algorithm (STA) is a finite-time stable algorithm. The works of Moreno showed that the class of systems containing the STA inherits the Lyapunov stability properties of an associated continuous-time smooth linear system. In turn, Polyakov and Poznyak provided a methodology for designing Lyapunov functions for the super-twisting algorithm, via the solution of a partial differential equation and prove the finite-time convergence of such an algorithm. A different approach toward the Lyapunov stability analysis of the super-twisting algorithm may be found in the work of Poznyak where the authors availed of discontinuous Lyapunov functions to estimate its convergence time, [**120**].

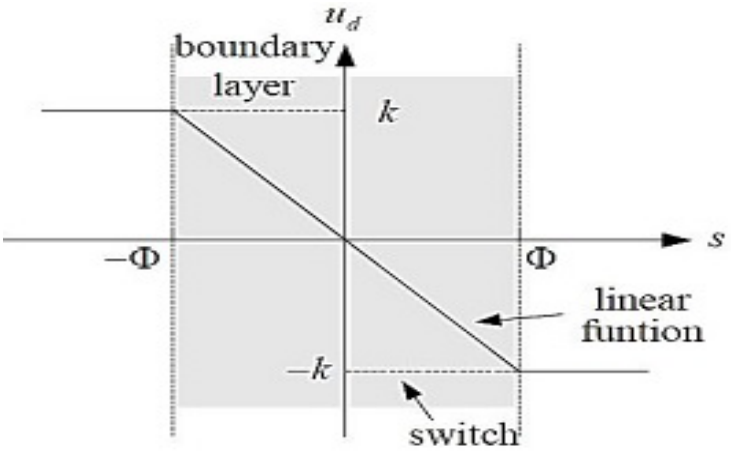

FIGURE 1.8: The Saturation function used in classical SMC to overcome the chattering effect.

The first attempt to extend the super-twisting algorithm to an algorithm with several inputs and outputs may be found in the work of Nagesh and Edwards, [**70**]. There, the authors studied the Lyapunov stability of a particular case of the multivariable super-twisting algorithm and described the class of perturbations that preserve the stability of the origin. Recently, Levant and Livne presented the extension of a scalar algorithm to a multivariable framework based on the homogeneity property of the former one.

This approach concludes that the properties of the scalar case are extended to the multivariable case. In turn, Basin proposed both a scalar and multivariable algorithm that may be regarded as an extension of that in the work of Nagesh and Edwards, [**60**]. The key feature of their system is the addition of terms that ensure the convergence of the trajectories to the origin before a time that is independent of the initial condition; such a stability trait is denoted as fixed-time stability. In the work of Vidal, [**61**], a multivariable STA with time-varying gains was proposed such that it preserves the global robust stability of the original despite an uncertain symmetric input matrix. In the work of Fan and Tian, [**59**], the authors availed of a multivariable STA with time-varying gains to design an observer for a hypersonic vehicle model.

In continuous time systems, the Super-twisting Sliding Mode have been extensively studied and it is shown that preserves the main characteristics of classical SM while avoiding the undesirable chattering effect. The main purpose to introduce and use this technique for the HR design problem is to avoid chattering and we use this technique for this aim.

1.3.3 Discrete-Time Control Systems

According to the methodology section 1.2.1, the design of the robust controller in our study is also tackled in discrete-time in order to explicitly take into account the effect of the sampling time during the design process.

In the first Section of chapter 4, the main purpose is to ease off the design of controllers by using a feedback-linearizing control approach that will be shown to lead to linear state feedback controllers able to achieve perfect tracking under potentially arbitrary reference signals.

For the second Section of chapter 4, a Joint parameter-state estimation based control is designed. The identified values are then used in the controller design feedback-linearization in the last section. This is a two-step procedure since the identification is firstly performed and afterward, in a second step, the controller is designed. In addition, some control algorithms need the values of both states in order to implement the control law. Since the second state variable is unmeasurable, it is generally needed to employ a state observer.

The main problems of this method are complexity and difficulty of estimation. Also the oscillation of this method was another problem that we face when implementing this algorithm. Regarding result and great performance of the sliding mode control in Chapter 3 we will use this design to overcome all these difficulties. In order to design a discrete-time sliding mode control (DT-SMC), we will do it first in the linear system and finally the nonlinear design which will present in Section 4.4.

So far, there are several key discretization methods that are used in industrial applications, such as the zeroth-order-hold (ZOH), Euler method, and the Tustin method, [**89**]. However, ZOH has been frequently used in practice, particularly in feedback control implementation. Moreover, the fact of using a discrete-time model to face the control design problem will allow us to obtain more accurate controllers than by designing a continuous-time one and then sampling it at a certain rate. Finally, the implementation of the proposed controller will be straightforward since most controllers are implemented in digital platforms nowadays, [**94**][**112**].

According to the aforementioned discussion, the characteristic feature of a continu ous-time SMC system is that sliding mode occurs on a prescribed manifold, where switching control is employed to maintain the state on the surface. When a sliding mode is realized, the system exhibits some superior robustness properties

with respect to external matched uncertainties. However, the realization of the ideal sliding mode requires switching with an infinite frequency.

Discrete-time sliding mode control has been extensively studied to address some basic questions associated with the sliding mode control of discrete-time (DT) systems with relatively low switching frequencies. Having said that, the quest of in-depth understanding of the complex dynamical behaviors due to the discretization of continuous-time SMC systems has to be further explored, [**114**]. The discretization behaviors of SMC systems as well as some intrinsic properties of discretized SMC systems are investigated in this section.

This very feature deteriorates the elegant invariance property enjoyed by most, if not all continuous-time SMC systems. For Discrete-time systems, it is often assumed that the sampling frequency is sufficiently high to assume that the closed-loop system is continuous-time [**89**]. However, the actual closed-loop cannot be driven into true sliding mode but quasi-sliding mode, which was defined in [**106**]. Obviously, the most apparent difference between a discrete-time system and its continues-time counterpart is the limited switching speed of the discontinuous control part. In DT SMC, because of the zigzagging behaviors, exact sliding on the intersection of predefined switching manifolds to some extent is impossible. To compensate for this disadvantage of DT-SMC, a new concept, sliding sector, was brought in and has been studied for quite a while [**105-107**].

Discretization is a major approach for industrial applications of control systems. In many cases, control design is based on continuous time system models due to their simplicity over their discrete-time counterparts, and the practical implementation is commonly done by using digital microprocessors or computers. There is a gap between the ideal dynamical performance anticipated based on the design from the theory for the continuous-time system models and the actual dynamical performance when the control system is discretized. The time delay in delivering control signals due to discretization is the key factor affecting the control performance.

This is particularly, when the control is discontinuous by its nature, such as the SMC. The "disruptive" switching may possibly cause incorrect actions due to the delay of delivering timely control signals. These behaviors may likely cause severe damage to industrial control devices such as actuators. In addition, the deteriorated invariance property may worsen the reliability of SMC systems, hence making controlled industrial processes vulnerable to unexpected environmental changes. The detail of this phenomenon has been intensively studied in [**120**][**121**].

There are two main methods for discretization, Euler discretization and ZOH discretization. In industries, simulations of control systems are usually done via Euler discretization while their implementation in practice is commonly done via ZOH discretization.

1.3.4 Euler Discretization

In [**122**][**123**], several important issues with regard to the discretization of SMC were discussed. A mathematical formulation of discretization using Euler's approximation was undertaken. It was shown that the solution trajectory must be attractive, so that the Euler's and the exact solutions can be consistent, as the sampling period decreases. In comparison with other control methods, the sampled SMC suffers more from the sampling process, as it would lose the high gain property near the vicinity of the switching surface. To compensate for this, disturbance prediction is indispensable, which is feasible under the hypothesis that the disturbance is slow

time-varying. In [**114**], the discretization behaviours of the most popular SMC systems using the Euler discretization were studied. It was shown that if the discretized SMC system is asymptotically stable then every trajectory converges to a period–2 cycle. Some symmetric features of the trajectory in steady state were explored and boundary conditions for the steady states were derived.

1.3.5 ZOH Discretization

ZOH has been frequently used in practice, particularly in feedback control implementation.

The use of a discontinuous control law in a system will cause a chattering phenomenon in the vicinity of the sliding manifold, hence leading to a boundary layer with thickness,[**101**][**118**]. In continuous-time SMC, smoothing schemes such as boundary layer (saturator) are widely used, which in fact results in continuous nonlinear feedback instead of switching control. Nevertheless, it is widely accepted by the community that this class of controllers can still be regarded as SMC. In such circumstance, the central issue is to guarantee the precision bound or the smallness of the error. Similarly, in discrete-time SMC, by substituting the switching term by means of a function that depends continuously on its arguments instead of being discontinuous such as the sign function, chattering can be eliminated, [**127**].

The nature and existence of DSM have been discussed in the literature [130], [**131**] and [**132**]. For discrete-time systems, sliding motions were first studied by Miloslavjevic in [**123**] the context of sampled data linear systems. In [**115**], some work has been reported for several classes of discrete-time linear systems. There are two schools of thought on discrete-time sliding mode control. In the first one [**126**], an equivalent control is proposed known as discrete-time sliding mode control (DSMC), that directs the states onto the sliding surface in one sampling period and subsequently helps to remain on it. This does not need any switching in control. The second one, it is based on the discretization of continuous reaching law. It is shown in [**118**], that the DSMC based on this, is switching type and it brings the trajectories, to the surface infinite time but unable to slide the trajectory along the surface. The convergence of error to a final ultimate bound, where the system overcomes the disturbance, could be called the DSM.

Based on the available conditions, we propose a new application of this method to develop a so-called discrete-time Super-Twisting sliding mode (DTSTSM). In this scheme, the system's trajectories enter into a boundary layer in the vicinity of the sliding mode and stay inside it forever. This name has been adopted considering the similarities between the Euler discretization applied on the continuous version of the super-twisting method.

1.3.6 Discrete-time Super Twisting Sliding Mode Control

The super-twisting algorithm (STA) is one of the most popular algorithms in the field of robust nonlinear control and observation. It is a second-order sliding mode algorithm for systems of relative degree one with respect to a defined sliding variable (output). One of its remarkable theoretical properties is the finite-time convergence of the output in the presence of matched Lipschitz perturbations. Compared to the first-order sliding mode controller, the STA generates a continuous control signal, which is desirable in many applications. Stability and robustness properties of the STA, as well as the closely related problem of convergence time estimation, have been extensively studied in the literature [**119**], [**120**] [**128**]. Using the STA as a state

observer and as a controller in an output feedback setting is discussed in [**134**]. Furthermore, from a practical point of view, the STA enjoys the advantage of simple implementation in a digital environment.

The robustness features are achieved by a discontinuity introduced in the second derivative of the system's output, which generates a sliding mode in the closed-loop system. An ideal sliding motion is understood as the limit of motions when switching imperfections vanish and the switching frequency tends to infinity, [**127**]. However, in a digital environment, the switching frequency is always limited because the sampling time is nonzero. This limitation leads to the so-called discretization chattering phenomenon, i.e., self-sustaining oscillations in the systems output and state variables, which diminish the control performance, [**135**].

In the case of the STA, the precision of the variable to be controlled is proportional to the square of the sampling time where the proportionality constant depends on the chosen controller parameters and the perturbations (Levant, 1993). This is in particular problematic in many practical applications, as the design of non-adaptive sliding mode controllers requires the knowledge of upper bounds of the uncertainty, which is not always known a priori. An overestimation of this bound leads to unnecessarily high control gains and consequently to large discretization chattering amplitudes. An adaptive sliding mode controllers, which do not require this information, special attention is usually paid to dynamic gain design. In that case, the gains are reduced if the amplitude of the perturbation decreases in order to avoid large chattering amplitudes, [**136**].

A discrete-time sliding mode controller is delicately constructed by designing a nonlinear sliding manifold based on the super-twisting sliding mode technique and also discrete-time control law based on the super-twisting algorithm. The rigorous stability is provided to show that the tracking errors converge to zero in discrete-time.

Since STW algorithm contains a discontinuous function under the integral, chattering is not eliminated but attenuated. Although they all can alleviate the high-frequency switching of control action more or less, only STW controller can reach the sliding mode manifold Discrete-time in the presence of uncertainties or disturbances. However, conventional super-twisting algorithm tracking controller usually can not acquire the discrete-time the convergence of tracking error for the system whose relative degree is more than one. In order to realize the discrete-time convergence of tracking errors, a so-called nonsingular terminal sliding mode (NTSM) control method has been proposed in [**129**]. With the special design of a nonlinear sliding manifold, the tracking errors converge to zero in discrete-time. Some novel methods have been proposed in [**118**] to realize the discrete-time convergence of tracking error for a system whose relative degree is more than one.

This method is applied and designed for the very first time in parameter estimation and control design. Here I explain the techniques that we use for the state of the art of controller. Based on the available conditions, we propose a new strategy to develop a discrete-time Super-Twisting- algorithm (DSTA). However, to the best of our knowledge, few discrete-time super-twisting versions of the controller have been proposed. The substitution of the signum function by a saturation, common trick to reduce the chattering for super-twisting SMC, has straightforward extension algorithm. It is then fair to assume that the explicit discretization was used to get a discrete-time super-twisting controller.

In this Section, entirely discrete-time versions of the STA are applied to the problems at hand. The difficulty of the oscillation of the parameters and great response of the super-twisting controller in Chapter 3, were great reasons to imply a new

method to solve these problems. Initially, instead of tackling the nonlinear problem we tackled the linear on in this section too. On the other hand, the main objectives of this method will offer great tracking properties, avoidance of state observer, no chattering, systematic design and robustness.

1.4 Description of the contributions of the thesis

The objective of this work is to design a heart rate (HR) controller for a treadmill so that the HR of an individual running on it tracks a pre-specified, potentially time-varying profile specified by doctors for the cardiac recovery of the person. The main contributions of the thesis are:

i) Design a new parameter estimation algorithm based on PSO. The estimation algorithm is able to obtain an accurate estimation of the parameters in an individual forms, which is the main aim is to be able and use for each person.

ii) The second contribution is to design a super-twisting sliding mode control for the continues-time system. I achieved a very good tracking response with tracking error of less than one percent. I choose a super-twisting sliding mode control method because of chattering avoidance and especially got a very good response in the wide range of the speed that was applied for the first time in this problem.

iii) The final contribution is the design of the robust discrete-time controller. For this purpose, we proposed first to design a feedback-linearization. A feedback linearization-based control law is designed to achieve the control objective but the obtained results have poor robustness. In Section 2 of Chapter 4, a Joint parameter-state estimation algorithm is developed to obtain an estimation of the parameter values to use for the control law calculation but due to the complexity of the algorithm and perfect performance of the super-twisting in Chapter 3 we decided to design a robust discrete-time controller. In Section 4.3 discrete-time sliding mode control has been described in two different new methods. instead of tackling the nonlinear problem we tackled the linear in Section 4.4 and the linearization system will discretize with Zero Hold-Order (ZOH) method. Finally for solving the problems such as chattering, robustness, perfect tracking and as mentioned great response of the super-twisting without an observer, a very new method which is called discrete-time super-twisting sliding mode control will be applied for the first time to solve the problem of robustness and chattering of the system.

1.5 Structure of the thesis

The thesis is organized as follows:

In Chapter 2, we explain the identification algorithm of a heart rate model parameters. The parameter estimation problem is formulated as an optimization one and solved by using Particle Swarm Optimization (PSO). In a section of this chapter, we compare our results with other techniques that were used before to solve this problem.

In Chapter 3, Sliding Mode Control, which is the method that we used for the first time in this work for designing our controller, is defined. Regarding the Sliding Mode control, they are some techniques that we used. The ZOH technique is one of the techniques that we used to design a discrete-time controller for the system at hand. This method will be explained in Chapter 4.

In Chapter 4, the explanation of robust Discrete-time Control can be seen. The important issue for using this technique is about it is chattering-free, the ability of

not needing an observer, robustness and perfect tracking for solving the problems. Actually, by using this technique we got a great response from our system that can be individualized by every person.

Finally, Chapter 5 summarizes the conclusions of the thesis.

Chapter 2

Identification of heart rate model parameters

In this chapter, the identification of the heart rate model parameters is presented. The PSO algorithm is used in this chapter to solve the parameter estimation problem for the first time and the results that we obtained are superb. Some methods previously have been proposed to solve the parameter estimation. We used the M-estimator method to compare our results because M-estimator is one of the best methods from the statistical point of view to solve the parameter estimation problem. Eventually, the results show that the PSO approach has a great response compared to the M-estimator.

2.1 Introduction

In order to meet the metabolic demand during exercise, the heart rate (HR) of an exerciser increases. Thus, the knowledge of how HR responds to exercise will improve our understanding of exercise physiology. In addition, it may also be useful for predicting cardiovascular disease mortality, [**40**]. The understanding of HR response with exercise may also lead to an improvement in developing training protocols for athletics, more efficient weight loss protocols for the overweight people, and in facilitating the assessment of physical fitness and health of individuals, [**41**]. For instance, this may give us some points in order to prevent heart attack during treadmill exercise.

Several models have been proposed in the works of literature to model the heart rate response to treadmill velocity, [**47**]. For instance, [**80**], proposes a Hammerstein model composed of a static non-linearity defined by a look-up table followed by a linear dynamical system while [**89**] proposes a non-linear dynamical model. Anyway, nonlinearity must be present in the model due to the nonlinear response of the heart rate to the exercise. A further discussion of models has been carried out in Section 1.3.1 of Chapter 1. The models are parameterized by a number of parameters that capture the individual HR response to exercise. It is vital, thus, to design parameter estimation procedures that allow us to have a personalized model for each individual from measured data.

In this work, parameter estimation is set up as an optimization problem whose solution leads to the estimated model parameters. The optimization problem is solved by using a particle swarm optimization (PSO) algorithm. The introduction to the PSO algorithm along with its use in the solution of optimization problems been done in Section 1.3.1 of Chapter 1. The proposed approach in comparison with the M-estimator procedure shows that PSO advice better behavior than the previous

approaches, while the accuracy of the estimation parameter is increased by using PSO.

In this study, the parameter estimation problem is solved by using the Particle Swarm Optimization (PSO) method, which is the first time where this method is used for the problem at hand. The parameter estimation will be focused in the range of treadmill speeds from 2 up to 14 km/h (2-14 km/h). In many studies, **[19][21][24]**, the usual range of speed is (2-8 km/h), or (2-10 km/h). Therefore, the proposed methodology is applicable in the large range of speeds from 2 to 14 km/h. Despite this range is popular in many rehabilitation and training exercises, it is the first time considered in this problem.

This chapter is organized as follows. Initially, the model of the system is considered in Section 2.2 . In this Section, the PSO algorithm used for solving the parameters estimation problem is also introduced. Finally, in the last section (Section 2.3) the results and comparisons with another parameter estimation method, called M-estimator method are presented.

2.2 Heart rate model

The following nonlinear model describes the relationship between speed and heart rate during treadmill exercise, [1], and it is the model that will be used through the thesis:

$$\dot{x}_1(t) = -a_1 x_1(t) + a_2 x_2(t) + a_3 u^2(t) \tag{2.1}$$

$$\dot{x}_2(t) = -a_4 x_2(t) + \phi(x_1(t)) \tag{2.2}$$

$$\phi(x_1(t)) = \frac{a_5 x_1(t)}{1 + \exp\left(-(x_1(t) - a_6)\right)} \tag{2.3}$$

$$y(t) = x_1(t) + HR_{rest} \tag{2.4}$$

Where $x(0) = [x_1(t), x_2(t)] = [0, 0]$ is the usual initial condition and a_1, ..., a_6 are positive scalars that are adjusted from real data to describe the particular response of each individual to exercise. The output $y(t)$ relates to the change of HR of the person, and HR_{rest} is the value of the Heart Rate at rest. The control input $u(t)$ describes the speed of the treadmill. The component $x_1(t)$ describes the change of HR from the heart rate at rest mainly due to the central response to exercise, whereas the component $x_2(t)$ describes the slower and more complex local peripheral effects. The positive feedback signal x_2, or a dynamic disturbance input to the x_1 subsystem, may be treated as a reaction of HR to the effects from the peripheral local responses or factors. In this case, the metabolites from the peripheral local metabolism further accelerate the HR during exercise. For instance, in the case of the peripheral local metabolism, the accumulated metabolic by-products, such as adenosine, K+, H+, lactic acid and other metabolites, cause vasodilatation and hyperemia inactive muscles, **[34]**. Vasodilatation in the active muscles causes a reduction in total peripheral resistance which in turn causes a decrease in mean arterial blood pressure. In order to regulate the blood pressure, the cardiac output needs to be increased, meaning that stroke volume and HR are increased via the baroreceptor reflex, **[34]**.

The nonnegative nonlinear function $\phi(x_1)$ has the property that $\phi(x_1) << 1$ when x_1 is small, whereas when x_1 is much larger than a_6, $\phi(x_1(t))$ approaches the linear function $x_1(t)$. If x_1 is small and a_6 is large, the variable x_1 is multiplied by a small factor(i.e. $\frac{a_4}{1+exp(-x_1(t)-a_6)} \approx 0$ in the second equation of (1), so x_2 becomes nearly independent of x_1 . If $x_1(0) = x_2(0) = 0$ which is typical initial condition and

the input $u(t)$ is small, the state $x_1(t)$ may not be large enough to make the factor $\frac{a_4}{1+exp(-x_1(t)-a_6)}$ significant, and $x_2(t)$ will remain close to zero. As a result, system (1) can be approximated by the system $x_1(t) = -a_1x_1(t) + a_3u^2(t)$ with $x_2(t) = 0$. On the other hand, if the input $u(t)$ is sufficiently large, the state $x_1(t)$ will be driven to a level that the factor $\frac{a_4}{1+exp(-x_1(t)-a_6)}$ is significant, and $x_2(t)$ is no longer independent of $x_1(t)$.

It is important to bear in mind that the objective of this chaper is twofold: 1) Propose a parameter estimation method based on PSO, and, 2) use M-estimator method to compare the results, both things used for the first time in this problem and also for speeds ranging from 2 to 14 km/h. In this way, the estimation of the model's parameters $X = (x_i) = [a_1.....a_6]$ is formulated as an optimization problem. Hence, the optimization of a cost function will provide an estimation of the parameters. The PSO algorithm will be used to solve the so-obtained optimization problem.

PSO consists of a population (or swarm) of M particles, each of which represents a n dimensional potential solution of the optimization problem. In our approach, $n = 6$ is the number of parameters to be estimated. Particles are assigned random initial positions and they change their positions iteratively to reach the global optimal solution. It is desired to minimize the fitness function as the PSO iterations progress.

The parameter estimation problem is cast into an optimization one so that the minimum of the fitness cost function will provide an estimation of the parameters of the system. The Squared Error Loss (SEL) is the most common cost function to be optimized for speed estimation problems and it is also the easiest to work with from a mathematical point of view. The SEL is linked with variance and bias of an estimator, so that the cost function is formulated for the estimated parameter vector $\hat{X}_k$ at iteration step k as :

$$I_k = Var(\hat{y}_k) + bias(\hat{X}_k) \tag{2.5}$$

where $\hat{y}_k$ is the estimated output. Both terms in Eq. (2.5) are nonnegative i.e. $Var(\hat{y}_k) > 0$, $Bias(\hat{X}_k) \geq 0$, so that the minimum of the cost function I_k is given by $I_k = 0$. Therefore, when the cost function I_k vanishes then $(Var\hat{y}_k = 0)$ and $bias(\hat{X}_k) = 0$ implying that the estimation of the parameters is performed adequately. The minimization of such cost function is done by using the PSO algorithm.

Each particle evaluates its fitness (given by Eq. (2.5)) **[34][46][49]**, and every particle $i = [1, ..., M]$ has a memory to store the value of its best own position $Pbest_{id}$, which is defined as the position where the particle has minimum fitness. Besides, the best of $Pbest_{id}$ of all particles, called $Gbest_d$, is stored too. At each iteration k, the PSO modifies each dimension of the position x_{id} in a particle by adding a velocity v_{id} and moves the particle towards the linear combination of $Pbest_{id}$ and $Gbest_d$ according to:

$$v_{id}(k+1) = w\, v_{id}(k) + c_1\, rand_1(p_{id} - x_{id}) + c_2\, rand_2(p_{gd} - x_{id}) \tag{2.6}$$

$$x_{id}(k+1) = x_{id}(k) + v_{id}(k+1) \tag{2.7}$$

In fact, according to Eqs. (2.6)-(2.7), some new particles may be out of the search space so that a projection to the boundaries of such space is included in the algorithm, **[46]**. Moreover, the most common approach to restrict the particle position in the search space is to set the violated components of the particle equal to the value of the violated boundary, **[34]**. In the problem at hand, the constraint violation appears

when the algorithm provides a negative value for the parameters. Consequently, the projection algorithm takes the form:

$$x_{id} = \begin{cases} 0 & x_{id} < 0 \\ \\ x_{id} & otherwise \end{cases} \tag{2.8}$$

In this way, we can guarantee that the estimated parameters are nonnegative and the velocity and position of each particle are updated by the equations until a termination condition is met and the algorithm finally stops.

Typically, the number of subsequent iterations without improvement of the best solution and/or the dispersion of the particles current (or best) positions in the search space has been used as indicators of search stagnation. Frequently, the aforementioned termination criteria are combined in forms such as:

$$IF \quad (|I_{k+1} - I_k| \leq \varepsilon) \quad OR \quad (k \geq k_{max}). \, Then \, Stop \tag{2.9}$$

where I_k is is the function to be optimized (in this case, (2.3)) and k stands for the iteration number, respectively, and ε is the corresponding user-defined tolerance. However, the search stagnation criterion can prematurely stop the algorithm even if the computational budget is not exceeded. Successful application of this criterion is based on the existence of a proper stagnation measure. The parameters c_1 and c_2 are the so-called cognitive and social parameters, respectively, and satisfy $0 < c_1, c_2 < 1$, **[56][34]**.

Finally, w is the inertia weight selected as $0.4 \leq w \leq 0.9$, the range where the algorithm provides the best results, **[54]**. Regarding Section 1.3.1 in Chapter 1, we used all these fixed parameters because they are the standard range employed in the algorithms to get a better result. Basically, in the previous studies, the researchers used different ranges, but they could improve the results obtained by these values. Finally, they discover that the best range for these parameters can be these ranges that we used in our study to get the best results.

Figure 2.1 displays the pseudocode of the PSO algorithm developed in our study. The PSO search is carried out by the speed of the particle. During the development of several generations, only the most optimistic particles can transmit information to the other ones. One of the advantages of the PSO method is that it can be applied to optimization problems of large dimensions, often producing quality solutions more rapidly than alternative methods, **[55]**.

2.2.1 M-estimator

Previously in some studies, researchers used different methods such as the to solve the parameter estimation problem, **[34][51]**. The comparison with the M-estimator procedure will show that PSO has better behavior than the previous approach, while the accuracy of the estimation parameter is increased by using PSO.

As it will be shown in section 2.3, the theory of M-estimation is introduced for comparison purposes. The previous researchers used robust performance of estimation for two main reasons, namely: 1)there may be outliers in the data, that are sample values considered very different from the majority of the sample and 2)the data may depart from the underlying distribution assumptions, **[51]**. This method is

FOR each particle i

Initialize position x_{id}

Initialize velocity v_{id}

End FOR

End FOR

Iteration k=1

DO

FOR each particle i

Calculate fitness value

IF fitness value is better than p_best_{id} in history set current fitness value as the p_best_{id}

END IF

End FOR

Choose the particle having the best fitness value as the g_best_d

FOR each particle i

Calculate the velocity according to the equation

$v_{id}(k+1)= w\ v_{id}(k)+c_1\ rand_1(p_{id} - x_{id})+c_2\ rand_2(p_g - x_{id})$

update particle position according to the equation

$x_{id}(k+1)=x_{id}(k)+v_{id}(k+1)$

IF $x_{id}=\begin{cases} 0, & x_{id} < 0 \\ x_{id} & Otherwise \end{cases}$ End IF

End FOR

IF $[I_{k+1} - I_k] \leq \varepsilon\ OR\ (k \geq k_{max})\ ThenStop$

k=$k+1$ while maximum iteration or minimum error are not acceded

FIGURE 2.1: PSO pseudocode employed to solve the optimization problem.

good for estimating the parameters, which is the reason why we compare our approach with this one. This method is effective, from the statistical point of view, to obtain an adequate estimation of the parameters. The class of M-estimators contains the maximum likelihood estimator (ML) as a special case. If we assume that the data come from the model distribution $F(\mu, \sigma)$ then the log-likelihood can be written as:

$$\sum_{i=0}^{n} \{log(f_0(\frac{x_i - \mu}{\sigma}) - log\sigma) \tag{2.10}$$

The first order condition for the M-estimator of μ is then given by:

$$\frac{1}{n} \sum_{i=0}^{n} \psi_M(\frac{x_i - \mu_M}{\sigma}) = 0 \tag{2.11}$$

while the M-estimator of scale verifies

$$\frac{1}{n}\sum_{i=0}^{n}\rho_M\left(\frac{x_i-\mu}{\sigma_M}\right)=1 \tag{2.12}$$

with $\psi_M(u)$ being the so-called score function, and $\rho_M(u)=\psi_M(u)u$. Under regularity conditions the ML estimators have a 100 percent efficiency, meaning that their asymptotic variance equals the inverse of the Fisher information, the lower bound of the Cramer-Rao inequality, **[34][51]**. The parameters are estimated by solving Eq. (2.12) with respect to x_i. The estimated parameters obtained by using the M-estimator are applied again to parametrize Eq. (2.1)-(2.4). In order to, we are calculating the fit-in error (since it is an error coming from a difference in the output of the models and actual data) in this part, that is only in open loop and it is only for estimation purposes. The fit-in errors are calculated as:

$$J_{1,k} = [r_k - p_k] \tag{2.13}$$
$$J_{2,k} = [r_k - m_k] \tag{2.14}$$

where : $r_k = reference, (HR\ output\ of\ \ data)$
$p_k = PSO\ output$
$m_k = M-estimator\ parameter\ output$
In the next section the results regarding the proposed algorithm are discussed.

2.3 Simulation results

This Section is composed of the estimation results obtained by means of the PSO algorithm. Secondly, the comparison results between the PSO and M-estimator parameter estimation procedures is presented.

Now, we will apply the PSO parameter estimation algorithm to the data described in tables below corresponding to ten subjects. These data are numerical data used for testing the algorithm and they do not correspond to real subjects. The parameters of the PSO algorithm are given by $c_1 = 0.87$, $c_2 = 0.67$, $w = 58$, $rand_1 = 0.1$, $rand_2 = 0.5$ and $\varepsilon \geq 0.15$. Then, tolerance is small and selected according to the criteria commented in section 2.2. The actual parameters of the ten subjects are given in Tables 2.1 and 2.2 and the estimated ones obtained from the PSO proposed approach are in Tables 2.3 and 2.4.

TABLE 2.1: Actual parameters of subjects 1 - 5.

Parameters	Subject 1	Subject 2	Subject 3	Subject 4	Subject 5
a1	2.512	2.791	2.683	2.592	2.611
a2	25.92	25.74	25.25	25.41	25.84
a3	0.81	0.85	0.79	0.8	0.81
a4	0.9021	0.9087	0.909	0.9011	0.9108
a5	0.038	0.041	0.035	0.039	0.042
a6	5.37	5.51	5.43	5.65	5.29
HRrest	64	69	66	68	69

As it can be noticed from Tables 2.1, 2.2, 2.3 and 2.4, the estimated parameters obtained by the proposed PSO approach are close to the actual ones. These results mean that the PSO algorithm performs very well.

TABLE 2.2: Actual parameters of subjects 6 - 10.

Parameters	Subject 6	Subject 7	Subject 8	Subject 9	Subject 10
a1	3.12	3.7	3.05	3.25	3.9
a2	21.25	21.95	21.1	21.55	21.8
a3	1.5	1.6	1.3	1.4	1.7
a4	1.9	1.8	1.8	1.25	1.9
a5	1.01	1.21	1.16	1.09	1.25
a6	8.15	8.35	8.5	8.6	8.3
HRrest	62	67	64	68	61

TABLE 2.3: Estimated parameters obtained by running the PSO algorithm of subjects 1 - 5.

Parameters	Subject 1	Subject 2	Subject 3	Subject 4	Subject 5
a1	2.508	2.789	2.681	2.588	2.615
a2	25.88	25.69	25.2	25.48	25.71
a3	0.849	0.855	0.788	0.798	0.809
a4	0.9011	0.9079	0.9088	0.9019	0.9098
a5	0.04	0.043	0.039	0.032	0.04
a6	5.41	5.49	5.47	5.59	5.59

TABLE 2.4: Estimated parameters obtained by running the PSO algorithm of subjects 6 - 10.

Parameters	Subject 6	Subject 7	Subject 8	Subject 9	Subject 10
a1	2.95	3.15	2.8	2.95	3.5
a2	20.8	21.5	20.5	20.85	21.25
a3	1.1	1.2	0.95	1.15	1.2
a4	1.5	1.3	1.2	0.95	1.5
a5	0.8	0.9	1.0	0.85	1.0
a6	7.75	7.9	8.2	8.1	7.9

Figure 2.2 shows the actual heart rate corresponding to one of our subjects (subject No.3) along with the output of the estimated model obtained by using the PSO algorithm described in Section 2.2. As it can be observed in this figure, the estimated model captures the dynamics of the heart rate of this person. It means that the PSO algorithm has a good response. Moreover, PSO is able to provide accurate parameter values and able to reproduce the behavior of the heart rate. Figure 2.3 displays the HR generated by the original model parametrized by the parameters in Table 1 along with the values obtained when the estimated parameters values are used to obtain the HR response according to (2.1)-(2.4). The potential mismatch between the actual and the estimated outputs comes from the estimation errors, that in this case are very low, as Figure 2.7 will be shown. In a real case, this mismatch may come from an uncertain unmodeled dynamics that could come from the real system as well as parametric errors coming from an estimation error.

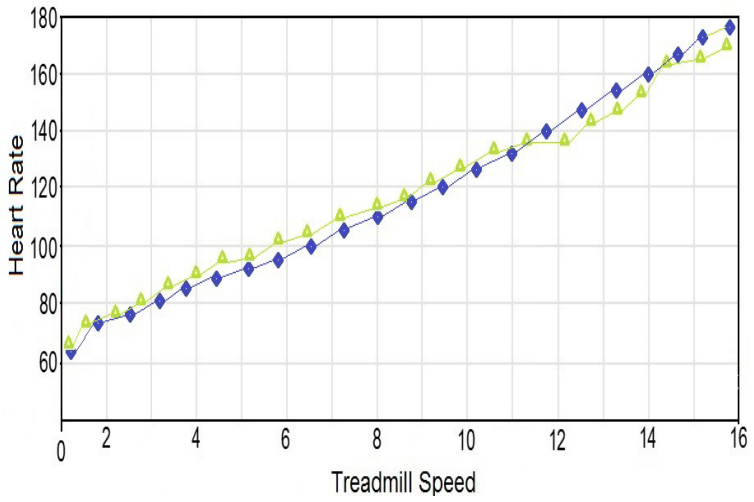

FIGURE 2.2: Heart rate response for subject NO 3 (that shows in green points) with using PSO at speed of (2-14 km/h)

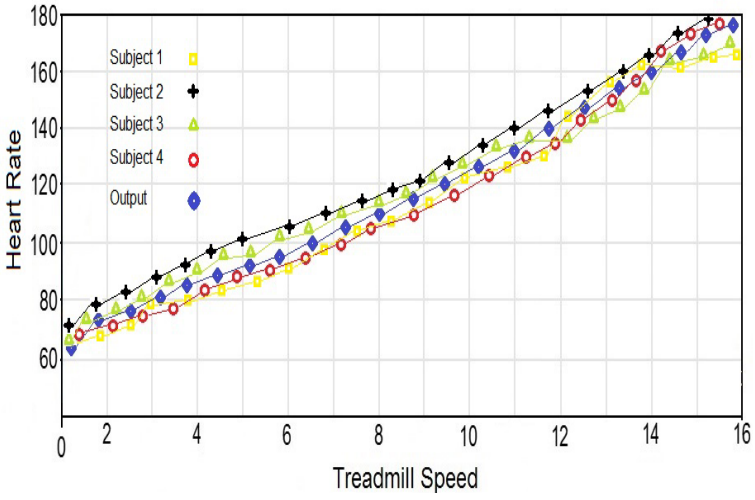

FIGURE 2.3: Heart rate response with using PSO at speed of (2-14 km/h)- for 4 random subjects

The following figures (Fig.2.4 and Fig.2.5) display the evolution of the estimated parameters for subjects No.1 and No.8 of Table 2.1 and the estimated ones. These figures show that after a small number of iterations the estimated parameters are close to the actual ones, a fact that is displayed numerically in Tables 2.2, 2.3 and 2.4.

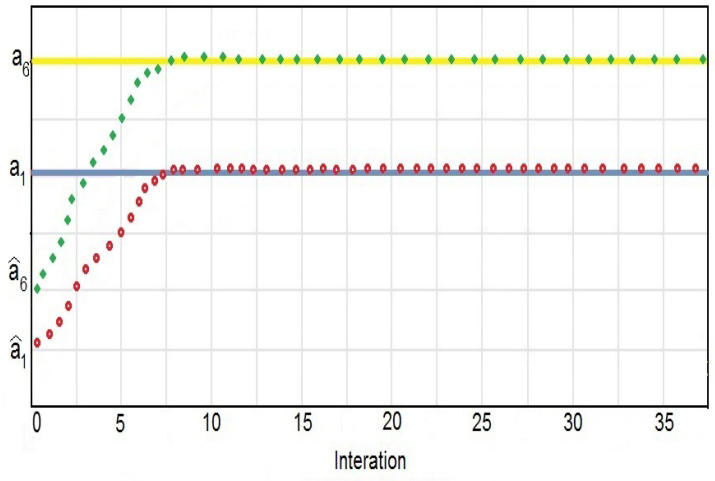

FIGURE 2.4: Evolution of estimated parameter for subject No.1

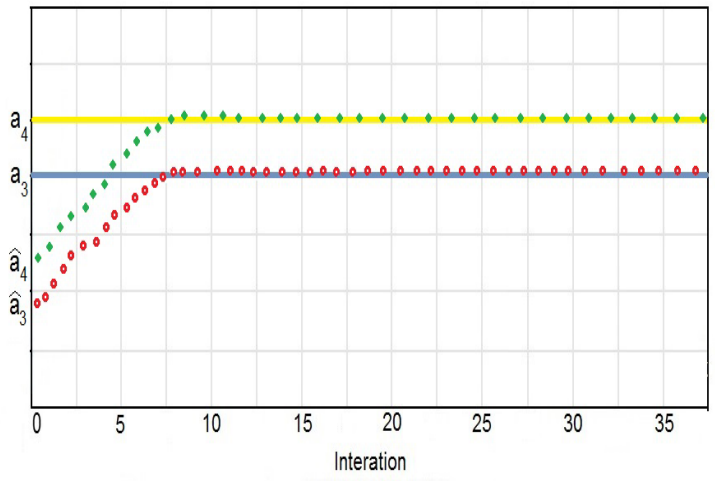

FIGURE 2.5: Evolution of estimated parameter for subject No.8

The following Figure 2.6 displays the actual value of parameters for the ten subjects. Since the value of the actual parameters exhibits a large variability, we can conclude that the algorithm works for people in a diversity of situations being described by very different parameters value. Therefore, Figure 2.7 shows the relative error of the estimated parameters. As it can be observed, the proposed PSO algorithm is able to achieve a superb estimation since the relative error, given by $\frac{a-a_{estimation}}{a} \times 100$, which is very low and the proposed algorithm with this high variability for the parameter values has a superb response.

Figure 2.8 shows the fit-in results of the output of the PSO and M-estimator. Thus, it is shown demonstrates that in many points the output of PSO intersects with

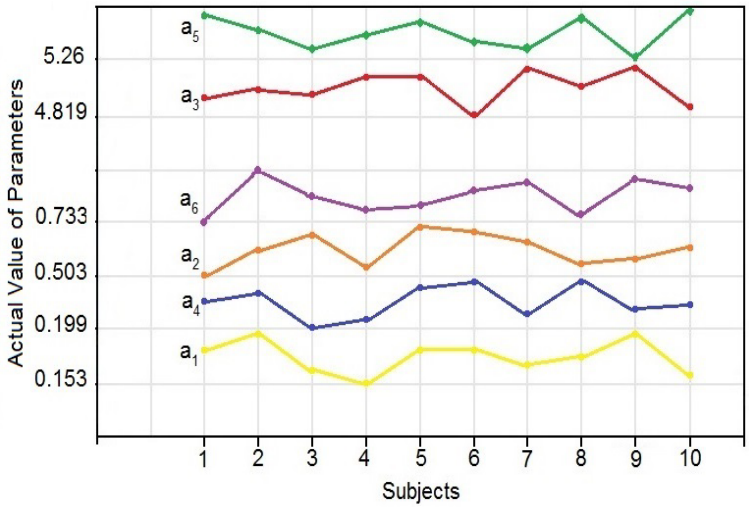

FIGURE 2.6: Actual values of parameters.

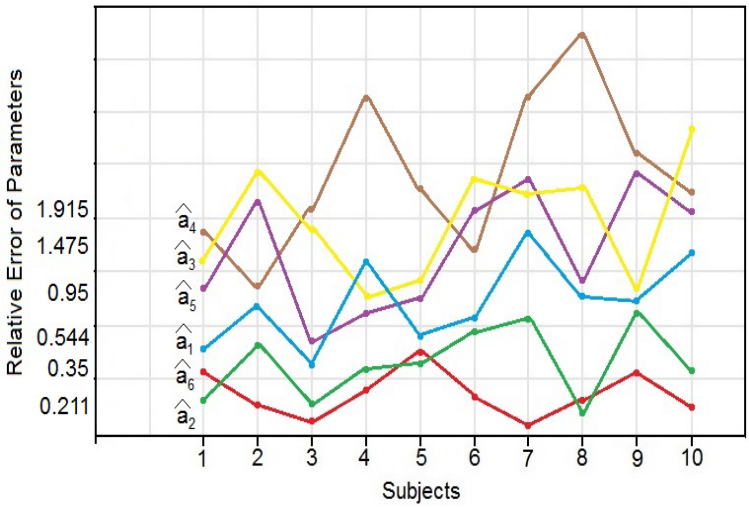

FIGURE 2.7: Relative Error of estimated parameters.

the reference signal and it means that PSO estimation is really close to the reference. On the other hand, the M-estimator displays an output that intercepts at some points with the reference, it has many variations in most of the points and this is not as effective as PSO. Therefore, PSO outperforms M-estimator. As it can be seen at the beginning of the process in Figure 2.9, PSO after 500 seconds starts definitely better than the M-estimator and it slightly goes better afterward. Both of these models have a good response, but PSO performs better during the speed process. On the other hand, PSO has a lower error against the M-estimator. The speeds that are presented to this figure (2.9) is not the same for all the parameters.

In Fig. 2.10 the value of the cost function (Eq. (2.5)) in Particle Swarm Optimization and M-estimator are displayed. The cost function (2) in the PSO after 5 iterations reduces faster than the M-estimator. So this fact can be interpreted as that estimation is performed faster in PSO method than by the M-estimator, and this fact is reflected in the quality of estimation.

Finally, in Figure 2.11 the evaluation of the fit-in error of the M-estimator with

respect to the PSO has been shown. It is one of the main reasons that we choose the M-estimator method to compare with PSO. on the other hand, it proves that this method (M-estimator) has a good response by itself and works well too. As it is clear, the M-estimator evaluation and PSO are having a very good response with respect to the reference signal.

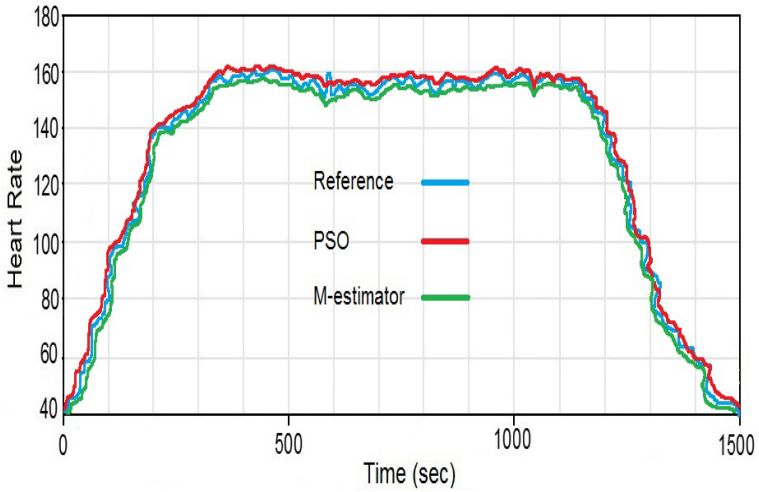

FIGURE 2.8: Comparing heart rate estimation results with PSO and M-estimator.

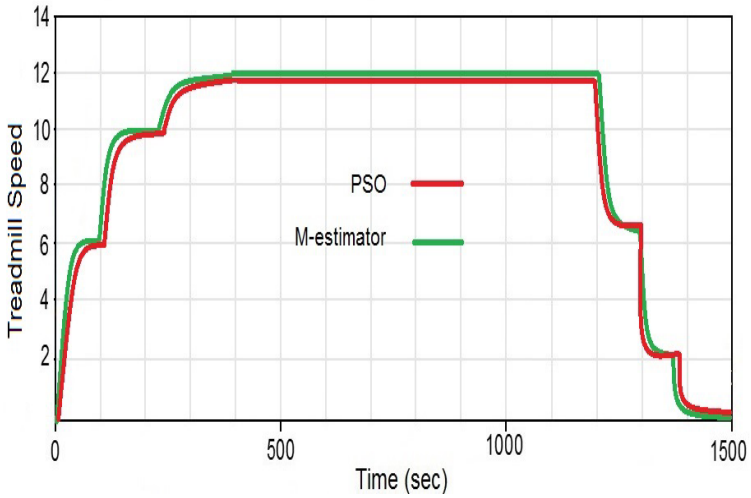

FIGURE 2.9: Speed of the treadmill employed for estimation purposes.

2.4 Conclusion

In this chapter, we introduced a new method to solve the parameter estimation problem for the heart rate model which is formulated as an optimization one and solved by using Particle Swarm Optimization (PSO). PSO also has been proposed to obtain an accurate estimation of the model parameters. Numerical examples show that the

estimation procedure is able to obtain accurate values for the system's parameters. In this case, the range of treadmill's speed goes from 2 to 14 km/h, the range that is not usually employed in previous studies.

In order to compare better our results, we decided to use the M-estimator method which is one of the best methods for solving the parameter estimation. At the end of this chapter, in Section 2.3, results have been shown. As it is clear that our method (PSO) had a great response compared to the M-estimator and our system performed greatly with the PSO algorithm.

In Chapter 3, the design of a sliding mode controller (SMC) for the HR control during treadmill exercise is explained and any small disfluency of the obtained parameters is compensated by using the SMC.

The material contained in this Chapter has been publihed in [**88**] and partly in [**34**].

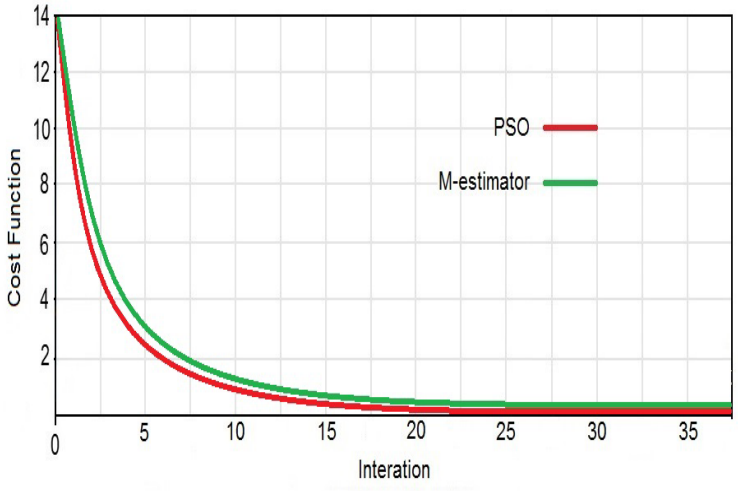

FIGURE 2.10: Evaluation of the cost function (2.5) with PSO and M-estimator.

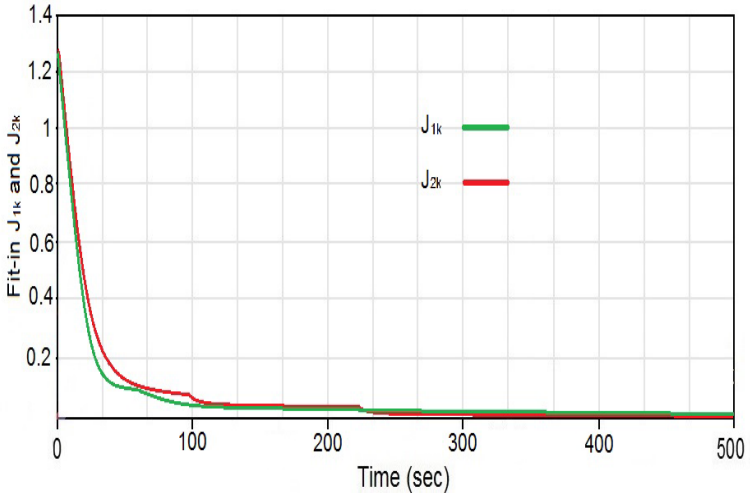

FIGURE 2.11: Fit-in error functions (2.13) and (2.14).

Chapter 3

Super-Twisting Sliding Mode Control

The objective of this chapter is to design a heart rate (HR) controller for a treadmill so that the HR of an individual running on it tracks a pre-specified, potentially time-varying profile specified by doctors for the cardiac recovery of the person. The technique that we are using to design the controller is Sliding Mode. In this way, a super-twisting sliding mode controller is designed to perform the robust control of treadmill's speed in the presence of potentially unmodelled dynamics or parametric uncertainties. Numerical examples show that the proposed control approach is able to obtain zero tracking error without chattering, definitely achieving the control objectives.

3.1 Introduction

Despite the estimation procedure developed in the previous chapter, some uncertainty and external disturbances may still appear in the system, so it is interesting to develop a robust controller for this type of systems.

The Variable Structure Control (VSC) is a general approach for designing robust control systems and it is composed by a series of continuous subsystems with a suitable logic switching. This type of control has taken on a growing importance over the years since it is suitable to control a wide range of systems such as linear and nonlinear, time-invariant and time-variant systems, single input single output systems (SISO) or multi-input multi-output systems (MIMO), continuous or discrete time systems, [**61**].

Nowadays the Super-twisting Sliding Mode Control (STSMC) has increased its spread thanks to the emergence of new classes of problems and the progress in switching components. The STSMC is a control technique very renowned due to its robustness property with respect to the parameters variation of the system and the external disturbances, and it is a very good technique for chattering avoidance. Thus, a Super-twisting Sliding Mode Controller (SMC) approach is adopted to design the controller.

Sliding mode controllers at large have revealed very useful in the robust control of multiple systems, such as pneumatic cylinder as actuators for robot manipulators, [**59**] and the hydraulic dynamics of the manipulator, [**60**]).However, this is the first time that SMC is used to control the HR during treadmill exercise. A survey on previous work has been done in Section 1.3.2 of Chapter 1. Especial attention will be devoted to the chattering effect since this is a crucial aspect in biomedical applications, [**62**], and also bear in mind that the super-twisting have got some applications in the past,[**61**][**67**][**70**]. To this end, a super-twisting based sliding mode controller

will be designed instead of a traditional SMC, [**57**]. The super-twisting approach will allow avoiding the undesired oscillations that a classical sliding mode controller may cause. In Section 3.4 of this Chapter, simulation results will be presented. In our approach, the accuracy of the model of parameter estimation for treadmill speeds has been improved. On the other hand speed range is (up to 14 km/h) which has not been considered in the previous studies.

In the next section, I will introduce the foundations of SMC in order to afterward illustrate the design of the super-twisting algorithm.

3.2 Classic Sliding Mode Control

Sliding mode control is a combination of linear feedback and Lyapunov methods with a particular variable shift. To illustrate this, consider the following equation:

$$x^{(n)} = f(X) + b(X)u \tag{3.1}$$

where $f(X) = f_{un} + f_{nom}$ is a non-linear function that is not fully identified, in which f_{un} is the unmodeled unknown part and f_{nom} is the nominal, known part, $b(X)$ is control and u is control input. In the system (3.1), the control input appears in the nth derivative of $x(t)$ and therefore the relative degree of the system is equal to n.In controlling the standard sliding mode, for simplicity in design, we should first define it with a variable weighted error in a variable, which is called the sliding variable. A particular form for the sliding variable is :

$$S(t) = \left(\frac{d}{dt} + \lambda\right)^{(n)} \tilde{x}(t) = \tilde{x}^{\{n)} + ... + \lambda^{n-1}\tilde{x} \tag{3.2}$$

Where $\lambda > 0$ is the weighting factor, $\tilde{x}$ is the variables of the state, x is state variable error and x_r is reference. So $\tilde{x}$ is defined as follows:

$$\tilde{x} = x_r - x \tag{3.3}$$

In the following, the objective of controlling the sliding variable is to stabilize and converge to zero $(S(t) \to 0)$. To do this, we have the derivative of the sliding surface:

$$S(t) = \frac{d^n(\tilde{x})}{dt^n} + ... + \lambda^n\tilde{x} = \tilde{x}^n + ... + \lambda^n\tilde{x} \tag{3.4}$$

By placing (3.2) and (3.3) in (3.4) we will have:

$$\begin{aligned} S(t) &= x^n - {x_r}^n + ... + \lambda^n(x - x_r) \\ &= f(x) + u - {x_r}^n + ... + \lambda^n(x - x_r) \end{aligned} \tag{3.5}$$

As it can be seen, the control input appears in the first derivative of the sliding variable, and so the relative degree of this system is equal to one. Therefore, changing the variable and defining the sliding variable, systems with a relative degree n turn into problems with a relative degree of one. Now, for the control of this first-order system, we use the Lyapunov stability theory. For this purpose, the following Lyapunov candidate candidate function is considered:

$$V(t) = \frac{1}{2}S(t)^2 \tag{3.6}$$

Which is a positive definite function. According to the theory of the stability of Lyapunov, if the derivative of this function is negative, the stability will be asymptotic. But in sliding mode control theory, to ensure the congestion of the slippery time limit, the condition (3.7) is considered, which is known as sliding condition.

$$\dot{V}(t) = S(t)\dot{S}(t) \leq -\eta \left|S(t)\right| \tag{3.7}$$

Where η is a positive constant. By integrating both sides of (3.7) we have:

$$S(t)\frac{dS(t)}{dt} \leq -\eta \left|S(t)\right| \tag{3.8}$$

$$\int_{S(0)}^{S(t)} \frac{S(t)}{|S(t)|} dS \leq \int_{0}^{t_r} -\eta dt \tag{3.9}$$

$$\begin{cases} t_r \leq \frac{|S(0)|}{\eta}, S(t) > 0 \\ t_r \leq \frac{-|S(0)|}{\eta}, S(0) < 0 \end{cases} \tag{3.10}$$

Therefore, the duration of the convergence of the sliding variable can be calculated from the following equation (3.11):

$$t_r \leq \frac{|S(0)|}{\eta} \tag{3.11}$$

To establish the above condition (3.7), the sliding mode controller consists of two parts $u_{sliding}$ and $u_{equivalent}$ which $u_{sliding}$ counteracts the uncertainties of the system and $u_{equivalent}$ is the so-called equivalent control, and will mathematically describe the definition of the super-twisting algorithm.

In Section 3.3 the design of the controller in the non-linear system is tackled by the Super-twisting sliding mode control. Also, keep in mind that this technique is very new for this kind of systems and it is for the very first time that is designed.

3.3 Super-twisting sliding mode control

This section contains the design of the super-twisting sliding mode control for the HR system. Thus, define the tracking error as:

$$e = R - y \tag{3.12}$$

where R denotes the reference signal (that is, the HR profile to be tracked) and y is the output of our system $e(t)$ denotes, therefore, the tracking error. The role of the controller is to ensure that the system's output accurately tracks the reference signal R. Bear in mind that R is known in advance since it is defined by the medical team for the appropriate recovery of the patient, (see Chapter 1) and consequently $\dot{R}$ is also known in advance.

When the system is perturbed or uncertain, the finite-time stabilization is not ensured. Hence, a reaching law based discontinuous control is developed which rejects the uncertainties of the system and ensures that the control objectives are fulfilled. Also, the nominal parameters come from Chapter 2 and are individualized

for each person. The uncertainties in our system can be modeled as:

$$\begin{aligned} \dot{x}_1(t) &= -a_1 x_1(t) + a_2 x_2(t) + a_3 u(t)^2 + f_{uncer1}(x) \\ \dot{x}_2(t) &= -a_4 x_2(t) + \phi(x_1(t)) + f_{uncer2}(x) \\ \phi(x_1(t)) &= \frac{a_5 x_1(t)}{1 + \exp\left(-(x_1(t) - a_6)\right)} \\ y(t) &= x_1(t) + HR_{rest} \end{aligned} \tag{3.13}$$

where $f_{uncer1}(x)$ and $f_{uncer2}(x)$ account for the unmodelled dynamics and parametric uncertainty in each of the model equations. On the other hand, we need to consider the following assumptions.

Assumption 1. $f_{uncer1}(x)$ and $f_{uncer2}(x)$ are upper-bounded .

Assumption 2. One upper-bound for each one of these terms is known.

These are common assumptions in SMC, **[62]**, and it is feasible to know these bounds in this problem. For instance, the uncertainties in the parameters maybe upper-bounded by the values and techniques exposed in chapter 2. Also, there are some approaches for which the bounds may be unknown and are estimated by the algorithm itself, **[61]** in an adaptive way. The sliding mode controller is composed of two parts:

$$u = u_{equiv} - u_{sliding} \tag{3.14}$$

where u_{equiv} is the so-called equivalent control used to remove certain terms while the sliding term $u_{sliding}$ is the term used to counteract the uncertainties of the system and will be of the super-twisting type, **[60]**. This approach will also help us avoid the chattering effect, that would be very harmful in the control system. Initially, the equivalent control will be derived while the final control law will be obtained by incorporating the super-twisting sliding term.

The following sliding manifold with the integral term is proposed:

$$S(t) = e(t) + \lambda \int_0^t e(\tau) d\tau \tag{3.15}$$

where λ is a strictly positive constant. The equivalent control is obtained by derivating with respect to time and then equating the so-obtained derivative to zero. In this way we have:

$$\begin{aligned} e(t) &= R(t) - y(t) = R(t) - x_1(t) + HR_{rest} \\ \dot{e}(t) &= \dot{R}(t) - \dot{x_1}(t) + H\dot{R}_{rest} \\ &= \dot{R}(t) + a_1 x_1(t) - a_2 x_2(t) - a_3 u^2(t) + f_{uncer1}(t) \end{aligned} \tag{3.16}$$

Thus, if we substitute the above expressions into (3.16) and simplify it, the derivative of the sliding manifold reads:

$$\begin{aligned} \dot{S}(t) &= \dot{e}(t) + \lambda e(t) \\ &= \dot{R} - \dot{y} + \lambda e(t) = \dot{R} - \dot{x_1} + \lambda e(t) \\ &= \dot{R} - (-a_1 x_1 + a_2 x_2 + a_3 u^2 + f_{uncer1}) + \lambda e(t) \end{aligned} \tag{3.17}$$

If $\dot{S}(t) = 0$ we have:

$$\dot{R} + a_1 x_1 - a_2 x_2 - a_3 u^2 - f_{uncer1} + \lambda e(t) = 0 \tag{3.18}$$

Now, if we isolate u^2 we obtain:

$$a_3 u^2 = \dot{R}(t) + a_1 x_1 - a_2 x_2 - f_{uncer1} + \lambda e(t) \tag{3.19}$$

$$u^2(t) = \frac{1}{a_3}(\dot{R}(t) + a_1 x_1 - a_2 x_2) + \lambda e(t) \tag{3.20}$$

The uncertain terms f_{uncer1} do not appear in (3.20) since they are unknown. Therefore, they do not appear in the equivalent control part. The super-twisting sliding term is given by, **[80]**

$$u_{sliding} = K|S|^{\alpha} sign(S) \tag{3.21}$$

It is important to point out that the total control command is given by (3.15) while being composed of the sum of (3.21). Therefore, the value of both state variables x_1 and x_2 is needed to calculate the control law. The heart rate x_1 can be measured easily, as there exist multiple devices to measure the HR of an individual in real time. However, the peripherical effects x_2 cannot be measured. As a consequence, a state observer is needed in order to implement the control command in practice. The state observer is given by:

$$\dot{\hat{x}_2}(t) = -a_4 \hat{x}_2(t) + \phi(x_1(t)) \tag{3.22}$$

With arbitrary initial condition $\hat{x}_2(0)$, since x_2 is infusible to obtain and f_{uncer1} is unknown. The final control law reads:

$$u(t) = \frac{1}{a_3}\left(\dot{R}(t) + a_1 x_1(t) - a_2 \hat{x}_2(t) + \lambda e(t)\right) - K|S|^{\alpha} sign(S) \tag{3.23}$$

Despite the observer works with arbitrary initial conditions, a judicious choice is given by $\hat{x}_2(0) = 0$ since at the beginning for the exercise, the peripherical effects are small and the initial value of the state variable is close to zero. In this way, the initial observation error would be zero and will maintain close to zero during all the observation. Therefore, the following Assumption 3 is feasible.

Assumption 3. The observation error $(\tilde{x}_2(0) = \hat{x}_2(0) - x(0))$ at the initial time is bounded and an upper-bound for it is known.

On the other hand, the need for a state observer will be relaxed in Chapter 4, where a robust discrete-time controller is designed. The switching gain K has to be selected so as to guarantee the stability and reference tracking of the closed-loop system. In order to obtain a guideline for its tuning we consider the following Lyapunov function candidate:

$$V(t) = \frac{1}{2}S^2 \tag{3.24}$$

Its time-derivative is given by:

$$\begin{aligned}\dot{V}(t) &= S\dot{S} = S\left(\dot{R} - \dot{x}_1(t) + \lambda e(t)\right) \\ &= S\left(a_2\hat{x}_2(t) - a_2x_2(t) - Ka_3|S|^{\alpha}sign(S) - f_{uncer1}(x)\right) \\ &= S\left(a_2\tilde{x}_2(t) - Ka_3|S|^{\alpha}sign(S) - f_{uncer1}(x)\right) \\ &= -Ka_3|S|^{\alpha+1} + S\left(a_2\tilde{x}_2(t) - f_{uncer1}(x)\right) \end{aligned} \tag{3.25}$$

where $(\tilde{x}_2(t) = \hat{x}_2(t) - x_2(t))$, represents the observation error. In order to ensure the appropriate operation of the controller, the time derivative (3.25) should be negative-definite, fact that is achieved if:

$$Ka_3 > |a_2\tilde{x}_2(t) - f_{uncer1}(x)| \tag{3.26}$$

Condition (3.26) can be further elaborated in the following way. The dynamics of the observation error is obtained by Eq. (3.22), whose result is:

$$\dot{\tilde{x}}_2(t) = -a_4\tilde{x}_2(t) - f_{under2}(x) \tag{3.27}$$

The solution to this equation is given by:

$$\tilde{x}_2(t) = e^{-a_4t}\tilde{x}_2(0) - \int_0^t e^{-a_4(t-\tau)}f_{uncer2}(x)d\tau \tag{3.28}$$

If the uncertain function f_{uncer2} is upper-bounded, i.e. $\sup|f_{uncer2}| < \infty$, fact that holds since according to Assumption 1 the uncertainty terms are bounded, then (3.28) can be upper-bounded accordingly as:

$$|\tilde{x}_2(t)| \leq e^{-a_4t}|\tilde{x}_2(0)| + \frac{1}{a_4}\sup|f_{uncer2}(x)|\left(1 - e^{-a_4t}\right) \tag{3.29}$$

$$\leq |\tilde{x}_2(0)| + \frac{1}{a_4}\sup|f_{uncer2}(x)| \tag{3.30}$$

for all $t \geq 0$. In this way, (3.26) is satisfied if the following condition holds:

$$Ka_3 > \left(a_2|\tilde{x}_2(0)| + \frac{a_2}{a_4}\sup|f_{uncer2(x)}| + \sup|f_{uncer1}(x)|\right) \tag{3.31}$$

since

$$\begin{aligned} & a_2|\tilde{x}_2(0)| + \frac{a_2}{a_4}\sup|f_{uncer2(x)}| + \sup|f_{uncer1}(x)| \\ \geq\ & a_2|\tilde{x}_2(t)| + \sup|f_{uncer1}(x)| \\ \geq\ & |a_2\tilde{x}_2(t) - f_{uncer1}(x)| \end{aligned} \tag{3.32}$$

Thus, the switching gain K must be selected to fulfill (3.32), a condition that depends on an upper-bound of the observation error, the nominal parameters of the system and upper bounds of the uncertainties. In the end, we must bear in mind that we are working with the square of the control signal so that the actual speed command is given by:

$$u_{actual} = \sqrt{max(0, u)} \tag{3.33}$$

In the case of recovery and training programs, the controller is able to make the heart

rate follow the predefined profile set up. In the next section, the simulation results showing the performance obtained by the control algorithm are presented.

Figure 3.1 shows the overall schematic of the implementation of the heart rate control loop system based on the treadmill velocity by the Super-twisting sliding mode controller in the Matlab's Simulink environment. Also in Fig.3.2, how to implement an integral sliding mode controller.

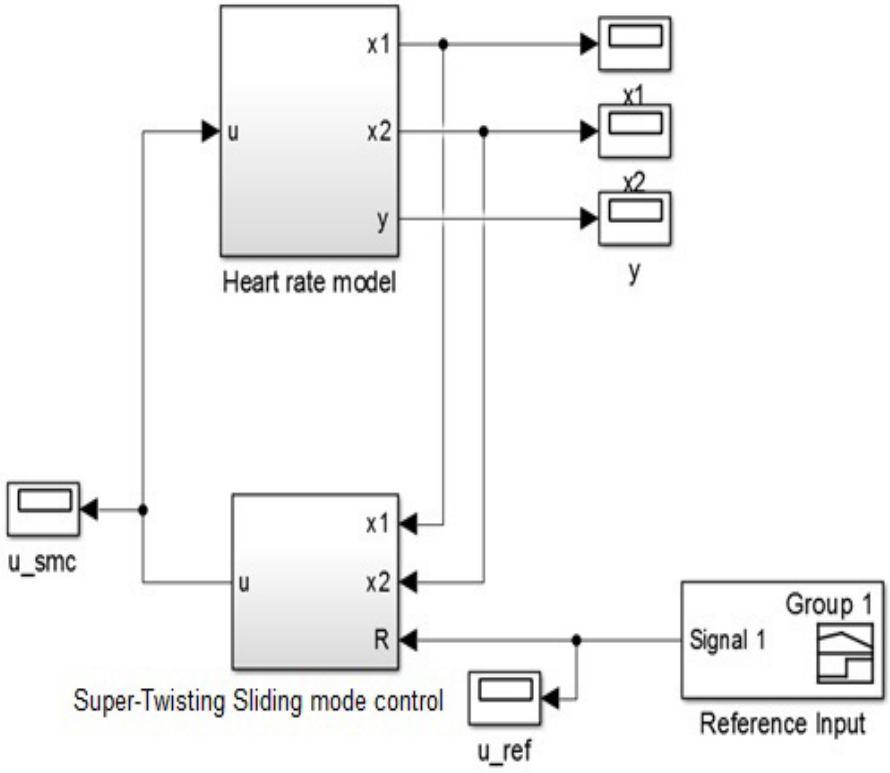

FIGURE 3.1: General schematic implementation of the heart rate control loop system based on treadmill speed by super- twisting sliding mode Controller.

3.4 Simulation and results

In this Section, we choose one person (subject No.3) from the Tables 2.1-2.4 shown in Chapter 2 to show the results achieved by the proposed controller. We want to highlight that similar good results are obtained for all the subjects. The controller parameters are $\alpha = 0.5$ and $K = 10$. It is important to note that, the selected K has been adjusted by trial-error, in this case, inspired by the results obtained in Chapter 2 for this subject. In Fig. 3.3, the actual Heart rate (HR) and the reference signal are shown. In this figure (Fig. 3.3), the output and the reference signal are superimpressed implying that the control objective has been achieved. The zoom of the first 150 seconds in the previous figure (Fig. 3.3) is shown in Figure 3.4. On the other hand, Figure 3.5 shows the speed calculated from the STSMC given by Eq. (3.17). In this case, the tracking error after the reaching phase is very small, despite the changes in the reference signal and it shows how the STSMC has a great response regards to the absence of chattering in the output and in the control command.

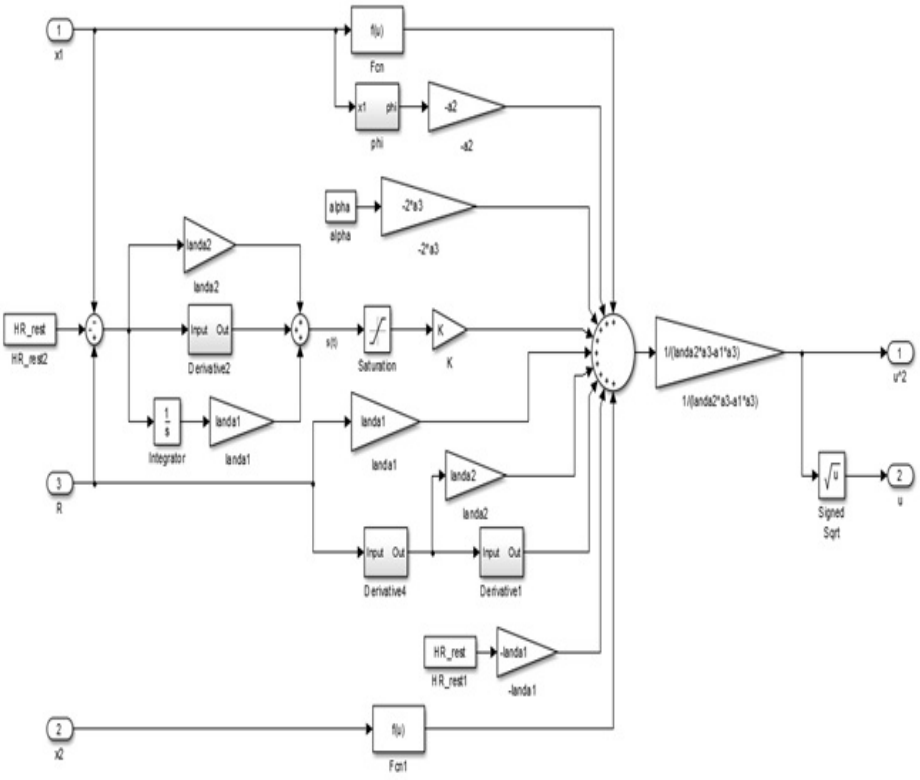

FIGURE 3.2: Implementation of integral super-twisting sliding mode controller in order to avoid chattering phenomenon.

The effect of the λ parameter in the outcome of the system is to help an SMC controller to have better performance.

On the other hand, PID is a common approach in the control of systems. For this reason, it is used to solve the control problem in many studies. The SMC control will be compared with the PID controller implemented in [**106**]. Since PID controllers are widely used in practice we will show the results achieved by the proposed controller in this scenario. In Fig. 3.6, the comparison of the actual HR obtained by using the STSMC and the PID controller is shown. As it is clear, the STSMC works much better than PID showing that it is able to obtain a zero tracking error despite the presence of uncertainties in the system's model. Overall, the presented method is able to obtain appropriate and superb closed-loop behavior.

In the Figure (3.7) treadmill speed coresponding to the application and each controller has been shown. Regarding the tracking signal, the super-twisting sliding mode has a better performance compare to PID one. The difference of the performance in STSMD and PID is not much but the signal of STSMC is closer to the reference and has a perfect response compare to the PID.

Figure (3.8) displays the evaluation of the cost function (which formulation appers in Chapter 2, Eq.2.5) between the PID and STSMC. As it can be seen at the beginning of the process in Figure (3.8), the Super-twisting controller after 500 seconds starts definitely better than the PID and it slightly goes better afterward. Both of these models have a great response, but STSMC performs better process. On the other hand, STSMC has a lower evaluation of the cost function to compare to the PID one.

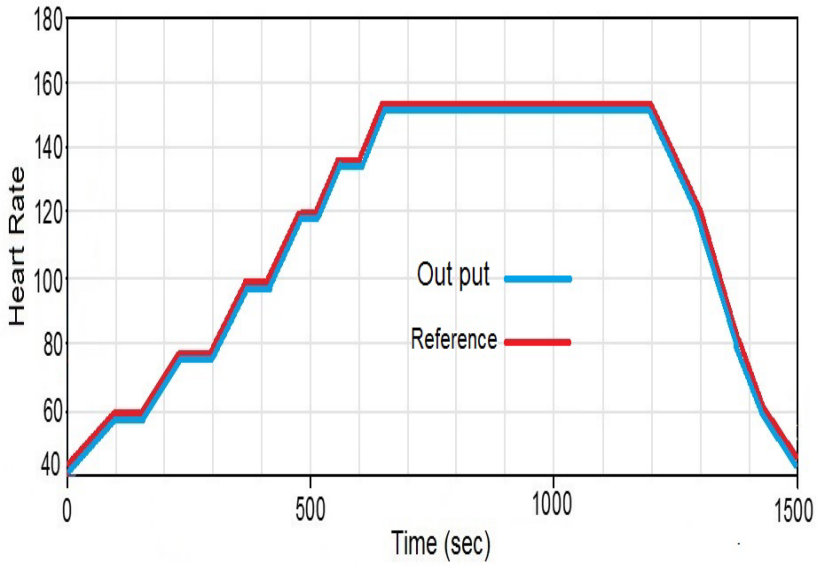

FIGURE 3.3: Heart Rate provided by the STSMC controller.

3.5 Conclusion

In this chapter, the design of a super-twisting based sliding control law has been performed for the system in order to counteract the remaining potential unmodelled dynamics or parametric uncertainties in the system. In all situations, the range of treadmill speeds goes from 2 up to 14 km/h, range not usually employed in previous studies. Simulation results show how the proposed SMC controller is capable of obtaining zero tracking error without chattering. The model proposed in our work includes parameters depending on miscellaneous environmental and personal items such as temperature and differ from one individual to another in respect to his physical and health conditions. The individualized model of each patient is used to design a super-twisting sliding mode controller able to regulate the speed of the treadmill in order to make the patient's heart rate.

The content of this Chapter has been published in the journal paper **[34]**.

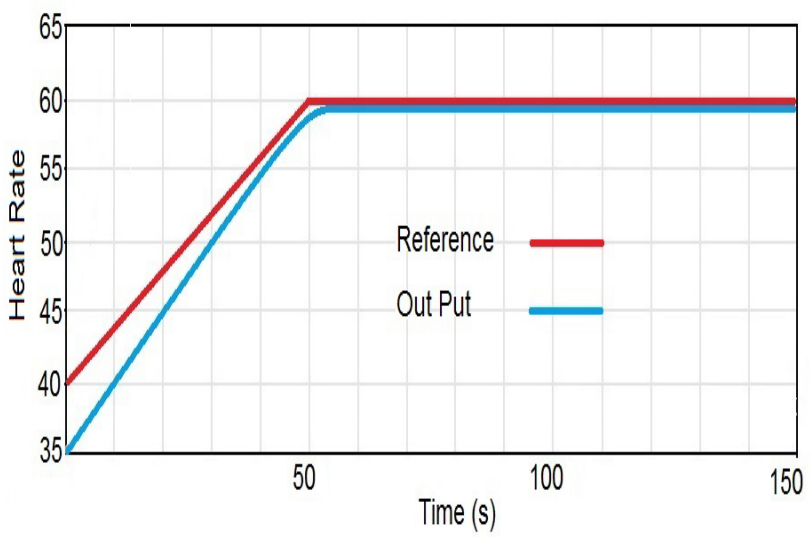

FIGURE 3.4: The first 150 seconds HR provided by the STSMC controller.

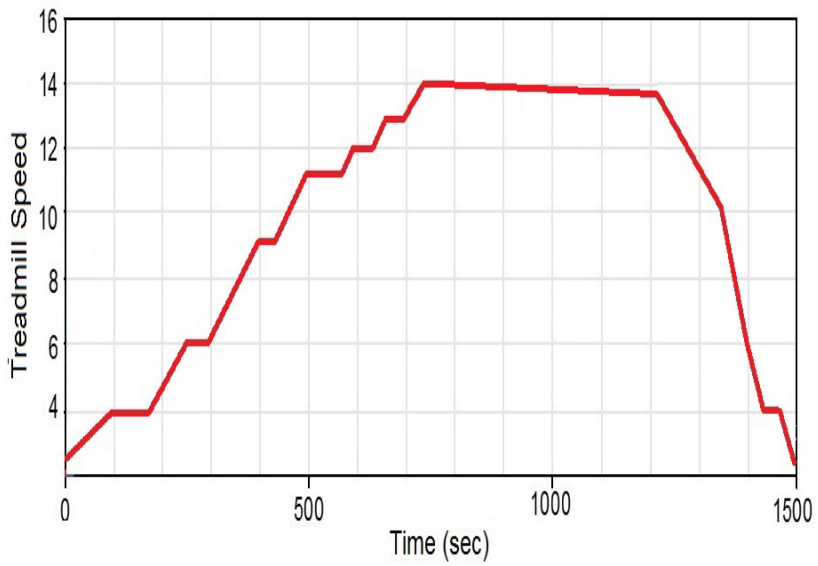

FIGURE 3.5: Speed provided by the STSMC controller.

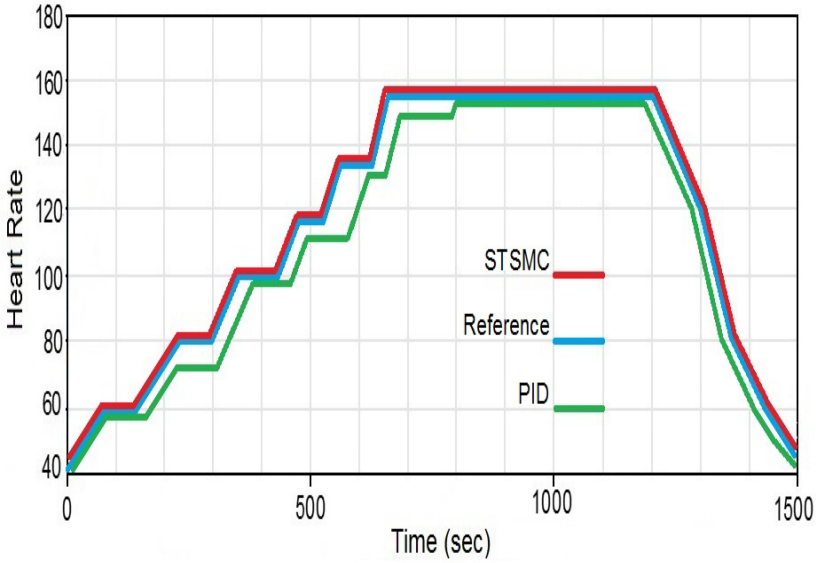

FIGURE 3.6: Heart rate tracking error with STSMC and PID.

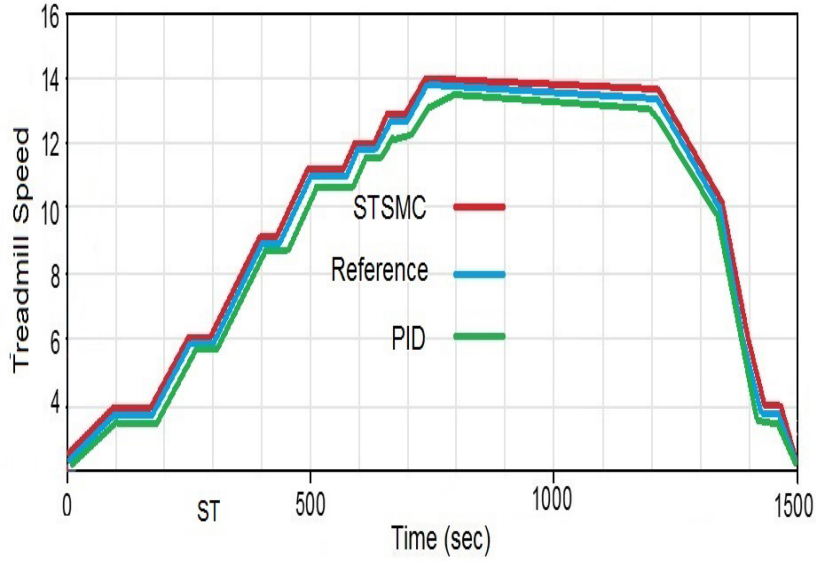

FIGURE 3.7: Treadmill speed coresponding to the application to each controller.

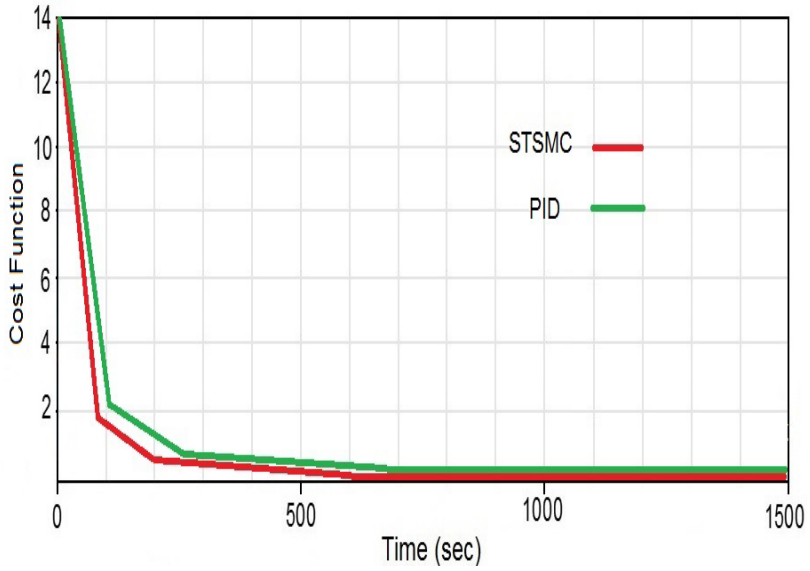

FIGURE 3.8: Evaluation of the cost function with STSMC and PID.

Chapter 4

Discrete-time Control

The objective of this Chapter is to design a discrete-time robust controller for the heart rate system. To this end, a feedback linearization-based controller is designed. It offers good results when the parameters of the system are known, but it has poor robustness properties. To solve this problem, the Joint parameter-state estimation algorithm is proposed, but it is complex, it does not identify parameters, it offers some oscillations and we already know that SMC offers a great response as Chapter 3 has shown.

Therefore, a discrete-time robust sliding mode controller is designed. Initially, we start by linearization SMC. Then it will be extended to the nonlinear case. The nonlinear system will offer great tracking properties, the avoidance of state observer, and it will offer a systematic design without chattering and great tracking and robustness properties.

4.1 Introduction

In this Chapter, a discrete-time sliding mode controller (SMC) is designed for the heart rate control in treadmill exercise. Sliding mode controllers have the advantage to provide a superb performance irrespective of the potential uncertainties in the model, [**95**]. Additionally, SMC also offers other advantages such as a simple design procedure and good robustness properties.

Since more and more modern control systems are implemented by computers, the study of SMC in the discrete-time has been an important topic in the SMC literature, [**101**][**102**]. The development of the SMC theory in discrete-time also needed a revision of how the continuous-time algorithms are adapted to sampled systems. This fact has led researchers to approach discrete-time sliding-mode control from two directions. The first one is the emulation, that focuses on how to map continuous-time algorithms to discrete-time ones so that the switching term can be preserved, [**105**]. The second approach is based on the equivalent control design and disturbance observer, [**123**].

This section is divided into six subsections. In the first Section, we are designing a feedback-linearization controller. The feedback-linearization system is a good strategy to design the controller but the obtained results have poor robustness so, in order to improve this point, we apply a Joint parameter-state algorithm in section 4.2. In this section, we tried to solve this problem and we got good promising feedback but due to the complexity of the algorithm, the problem with the estimation process and the good results obtained by the super twisting controller design in Chapter 3, we decided to design a sliding mode controller. Initially, instead of tackling the nonlinear problem we tackled the linear on in section 4.4. The results have a good response but the other problem that we face in this design was not identify the parameters and it offers some oscillation. Moreover, for solving this problem and

also other problems like chattering, robustness, perfect tracking, systematic design and not using any observer we decided to design a very new method which is called discrete-time super-twisting sliding mode control. The results that we achieved are great and we could solve all of these problems that we mentioned in the last controllers.

4.2 Feedback-Linearization Based Control

This section contains the design of a discrete-time state-feedback output tracking control for the heart rate during treadmill exercise. Initially, the nonlinear model describing the relationship between the heart rate and the speed of a treadmill is discretized. Afterward, a feedback linearization-based control law is proposed to achieve perfect output tracking. The control objective is to make the runner's heart rate follow a heart rate reference profile set by specialists as reference. The set-up of the problem in discrete-time allows taking into consideration the effect of sampling during the controller design procedure instead of relegating it to the implementation stage. It will be shown that a linear state feedback controller is enough to make the nonlinear model's output track the reference profile regardless of its possibly complex time variation. Since the full state is not available for measurement a reduced-order state observer is incorporated into the discrete-time control law. Then, the continuous control command is generated by using a zero-order hold (ZOH). The designed control system is tested on the original continuous-time nonlinear model by computer simulation to demonstrate the effectiveness of the proposed method to achieve the required objective.

Consider the nonlinear state space controlled system given in **[88]**[**34**]:

$$\dot{x}_1(t) = -a_1 x_1(t) + a_2 x_2(t) + a_6 w(t) \tag{4.1}$$

$$\dot{x}_2(t) = -a_3 x_2(t) + a_4 x_1(t)\phi(x_1(t)) \tag{4.2}$$

$$\phi(x_1(t)) = \frac{1}{1+\exp\left(-(x_1(t)-a_6)\right)} \tag{4.3}$$

$$y(t) = x_1(t) + HR_{rest} \tag{4.4}$$

The input variable $w(t) = u(t)^2$ corresponds to the square of the speed of the treadmill, $u(t)$. The state variable $x_1(t)$ represents the heart rate variation from the at-rest value $HR0$ and $x_2(t)$ represents the influence of local peripheral effects (like temperature, hydratation or sweat) on the heart rate. In this way, this model allows considering heart rate fluctuations not only with the running speed but also with environmental and physiological conditions. The output $y(t)$ is, thus, one-quarter of the actual heart rate of the exerciser given by the model from the at-rest heart rate value of this same person. The model parameters are given by the constants $a_i,\ i = 1, 2...6$ which may depend on each person.

The control problem is the design of a discrete-time speed controller making the output $y(t)$ follow as accurately as possible a specific given profile $r(t)$ (i.e. $y(t) \to r(t)$ as $t \to \infty$). The controller's role is to regulate the treadmill speed in order to change exercise intensity and, as a consequence, exerciser's heart rate. At this point it is worth recalling some structural properties of model (4.1)-(4.4), since they will be used afterwards in this Chapter **[88]**:

1) State variables $x_1(t)$ and $x_2(t)$ remain nonnegative for all time provided that parameters $a_i,\ i = 1, 2...6$ and initial conditions are nonnegative.

2) The function $\psi(x_1(t))$ is globally Lipschitz with Lipschitz constant k_f.

3) When treadmill speed is zero (i.e. $u = 0$) the heart rate deviation from the heart rate at rest quickly tends to zero provided that $\frac{a_1 a_3}{a_2 a_4} > \bar{m} = \min(1, k_f)$.

Assumption 1. It is assumed that Condition 3) holds for the model (4.1)-(4.4).

Assumption 1 implies that the considered model is supposed to be asymptotically stable. This is a feasible assumption based on the fact that the heart rate does not diverge in the absence of an external stimulus. Since the controller is to be designed in discrete-time, the next section deals with discretizing the original continuous-time system (4.1)-(4.4).

4.2.1 Discrete-Time model

The theory of dynamical systems discretization is well-developed for linear systems. However, the discretization of nonlinear systems is much harder. In this work, we follow the approach of **[88]** to obtain a nonlinear discrete-time model accurate to some order in the sampling period. To this end, we must first rewrite system (4.1)-(4.4) in normal form, **[98]**. A quick inspection reveals that its relative degree is unity so that it is already written in normal form. Thus, the discretization of (4.1)-(4.4) according to **[88]**[**98**], yields to:

$$x_{1,k+1} = x_{1,k} + h\left(-a_1 x_{1,k} + a_2 x_{2,k} + a_6 w_k\right) \tag{4.5}$$

$$x_{2,k+1} = x_{2,k} + h\left(-a_3 x_{2,k} + a_4 x_{1,k}\phi(x_{1,k})\right) \tag{4.6}$$

$$y_k = \frac{1}{4}\left(x_{1,k} + HR0\right) \tag{4.7}$$

where $h > 0$ denotes the sampling period and $x_{1,k}$ and $x_{2,k}$ are the discrete state variables. The reference signal, $r(t)$, and output signal $y(t)$ are also sampled at the sampling rate h to provide the sampled signals $r_k = r(kh)$ and $y_k = y(kh)$.

Assumption 2. The reference signal r_k is bounded and known one step ahead.

Assumption 3. The state variable $x_{1,k}$ is available through measurement.

These are feasible assumptions since the reference profile is fully determined for each individual beforehand and heart rate can be easily measured through pulsometers. Eqs. (4.5)- (4.6) are the starting point to design the controller. However, we will first show that the so-obtained discrete model retains the characteristic features of its continuous-time counterpart.

Theorem 1. The discrete-time model (4.5)-(4.6) has nonnegative solutions for all $k \geq 0$ provided that the parameters a_i, $i = 1, 2...6$ and initial conditions are nonnegative and the sampling period satisfies $0 < (1 - ha_3)$ and $0 < (1 - ha_1)$.

Proof. Equations (4.5) and (4.6) can be rewritten as:

$$x_{1,k+1} = (1 - ha_1)\, x_{1,k} + ha_2 x_{2,k} + ha_6 w_k \tag{4.8}$$

$$x_{2,k+1} = (1 - ha_3)\, x_{2,k} + ha_4 x_{1,k}\phi(x_{1,k}) \tag{4.9}$$

We can now proceed by total induction. The initial conditions $x_{1,0}$ and $x_{2,0}$ are nonnegative by hypothesis. Suppose now that $x_{1,k}$ and $x_{2,k}$ are nonnegative and we have to prove that so are $x_{1,k+1}$ and $x_{2,k+1}$. However, this fact can be proved straightforwardly since all the right-hand sides of Eqs. (4.8) and (4.9) are nonnegative because so are the parameters, $x_{1,k}$ and $x_{2,k}$, $w_k = u_k^2 \geq 0$ and $0 < (1 - ha_3)$ and $0 < (1 - ha_1)$. ■. Therefore, the discrete-time model retains the positivity of the original system.

Remark. 1. As a corollary of Theorem 1, the sampling period must be chosen such that:

$$0 < h < \min\left(\frac{1}{a_1}, \frac{1}{a_3}\right) \tag{4.10}$$

Moreover, the autonomous system is also asymptotically stable.

Theorem 2. Assume that the sampling time is selected such that Eq. (4.2) holds (so that the discrete-time system is positive). Then, the autonomous system (4.8)-(4.9) with $w_k = 0$ is asymptotically stable provided that Assumption 1 is met.

Proof. The autonomous nonlinear system (4.8)-(4.9) can be upper-bounded by using the fact $x_{1,k}\phi(x_{1,k}) \leq x_{1,k}$ as:

$$x_{k+1} \leq \begin{pmatrix} (1 - ha_1) & ha_2 \\ ha_4 & (1 - ha_3) \end{pmatrix} x_k \tag{4.11}$$

If the limiting system (4.2) is asymptotically stable so will be the discrete-time nonlinear system (4.9)-(4.8). The eigenvalues of the dynamics matrix of (4.11) are given by:

$$\lambda_{\pm} = 1 - \frac{h}{2}(a_1 + a_3) \pm \frac{h}{2}\sqrt{(a_1 - a_3)^2 + 4a_4a_2} \tag{4.12}$$

The limiting system is asymptotically stable provided that:

$$-1 < \lambda_{\pm} < 1 \tag{4.13}$$

Some algebra on Eq. (4.12) shows that condition (4.13) holds if $\frac{a_1a_3}{a_2a_4} > 1$, fact that is implied by Condition 3). Thus, the discrete-time system is asymptotically stable provided that the original continuous-time one is and the sampling period is chosen in such a way that the discretization preserves the positivity of the model. ■

Hence, the so-obtained discrete-time system retains the same properties as the continuous-time one. The next step is to design a controller for system (4.8)-(4.9).

4.2.2 Controller design

The controller is based on feedback linearization. Since the discrete-time system is expressed in normal form and its zero dynamics is stable[1], the control law reads:

$$w_k = \frac{1}{ha_6}\left(-(1 - ha_1)x_{1,k} - ha_2x_{2,k} + \nu_k\right) \tag{4.14}$$

which renders the nonlinear discrete-time system into the linear one:

$$x_{1,k+1} = \nu_k \tag{4.15}$$

If we now write the reference signal as $r_k = \frac{1}{4}\left(\hat{r}_k + HR0\right)$ and choose $\nu_k = \hat{r}_{k+1}$, then Eq. (4.15) becomes $x_{1,k+1} = \hat{r}_{k+1}$ and the reference signal is perfectly tracked by the output at all discrete time $t_k = kh$. Note that Assumption 2 has been used to define the reference signal and allows attaining the perfect tracking. Moreover, it can be

[1] The stability of the zero dynamics can be checked directly.

noticed that the feedback linearizing control law (4.14) can be cast into the form:

$$w_k = -\frac{1-ha_1}{ha_6}x_{1,k} - \frac{a_2}{a_6}x_{2,k} + \frac{1}{ha_6}v_k \tag{4.16}$$

$$= -Lx_k + Gv_k, \tag{4.17}$$

$$L = \left[\frac{1-ha_1}{ha_6}\ \frac{a_2}{a_6}\right],\ G = \frac{1}{ha_6} \tag{4.18}$$

which is a state-feedback control law. A direct consequence from this equation is that a linear controller is enough to perfectly track any reference signal for the nonlinear model of the heart rate response (when the parameters of the system are known). The only nonlinearity appearing in the control law will come from the quadratic relationship with the speed, $w_k = u_k^2$. Nevertheless, Eq. (4.18) needs the values of $x_{1,k}$ and $x_{2,k}$ in order to be realizable. $x_{1,k}$ is obtained from measurement as Assumption 3 states, but $x_{2,k}$ is not measured. Thus, we need an observer to obtain this value that is then used to implement the control command as it happened in Chapter 3. Therefore, a reduced-order observer will be designed in the next subsection with such a purpose.

4.2.3 Observer design

The observed state variable $\hat{x}_{2,k}$ is given by:

$$\hat{x}_{2,k+1} = (1-ha_3)\,\hat{x}_{2,k} + ha_4 x_{1,k}\phi(x_{1,k}) \tag{4.19}$$

with arbitrary nonnegative initial condition $\hat{x}_{2,0}$. This observer converges asymptotically to the actual value of $x_{2,k}$ since the substration of (4.9) and (4.7) leads to:

$$\tilde{x}_{2,k+1} = (1-ha_3)\,\tilde{x}_{2,k} \tag{4.20}$$

Hence, $\tilde{x}_{2,k} = x_{2,k} - \hat{x}_{2,k}$ converges asymptotically to zero (indeed, exponentially and monotically) provided that the sampling time satisfies $0 < (1-ha_3)$ which is guaranteed if (4.9) holds. Note that since $ha_3 > 0$ then $(1-ha_3) < 1$. Therefore, the actual control law reads:

$$w_k = \frac{1}{ha_6}\left(-(1-ha_1)x_{1,k} - ha_2\hat{x}_{2,k} + v_k\right) \tag{4.21}$$

while the speed of the treadmill is given by:

$$u_k = \sqrt{max\,(0, w_k)} \tag{4.22}$$

in order to generate a feasible speed. The continuous-time control signal is given by the ZOH reconstruction of u_k:

$$u(t) = u_k,\ t \in [kh, (k+1)h) \tag{4.23}$$

In the next subsection the stability analysis of the closed-loop system is performed.

4.2.4 Stability analysis of the discrete-time closed-loop system

The following result arises regarding the stability of the discrete-time closed-loop system.

Theorem 3. The state variables from the system (4.8)-(4.9) remain bounded for all discrete-time $t_k = kh$ provided that Assumptions 1, 2 and 3 hold, $||\tilde{x}_{2,0}||$ is bounded and the sampling time h is chosen satisfying equation (4.23).

Proof. Condition 3) from Section 4.2 guarantees the boundedness of state variables in the absence of an external source. Thus, we just need to prove the boundedness of state variables when a positive external signal (4.23) is actually applied to the system. In such a case, the discrete-time closed-loop is given by:

$$\begin{aligned} e_{k+1} &= ha_2\tilde{x}_{2,k} && (4.24)\\ \tilde{x}_{2,k+1} &= (1-ha_3)\,\tilde{x}_{2,k} && (4.25)\\ x_{2,k+1} &= (1-ha_3)\,x_{2,k} + ha_4 x_{1,k}\phi(x_{1,k}) && (4.26) \end{aligned}$$

where $e_k = x_{1,k} - \hat{r}_k$ is the tracking error. The solution to Eq. (4.25) is given by:

$$\tilde{x}_{2,k} = (1-ha_3)^k\,\tilde{x}_{2,0} \tag{4.27}$$

Since $||\tilde{x}_{2,0}||$ is bounded and $0 < (1-ha_3)$ thanks to Eq. (4.27), then $(1-ha_3)^k \to 0$ monotically as $k \to \infty$. Hence, $\tilde{x}_{2,k} \to 0$ as $k \to \infty$ and the observer provides an asymptotically exact observation of the state variable $x_{2,k}$. Moreover, $||\tilde{x}_{2,k}|| \leq ||\tilde{x}_{2,0}||$ for all $k \geq 0$. Therefore, from equation (4.24) we have:

$$||e_{k+1}|| = ha_2||\tilde{x}_{2,k}|| \leq ha_2||\tilde{x}_{2,0}|| < \infty \tag{4.28}$$

for all $k \geq 0$, implying that e_k is bounded at all time. Since the reference signal r_k (and, hence, $\hat{r}_k$) is bounded from Assumption 2, then $x_{1,k}$ is bounded at all time. Furthermore, from Eq. (4.7) it can also be concluded that the output y_k is bounded. On the other hand, the solution to Eq. (4.28) is given by:

$$x_{2,k} = (1-ha_3)^k\,x_{2,0} + ha_4\sum_{p=0}^{k-1}(1-ha_3)^{k-p-1}\,x_{1,p}\phi(x_{1,p}) \tag{4.29}$$

However,

$$0 < \psi(x_{1,k}) = \frac{1}{1+\exp\left(-(x_{1,k}-a_6)\right)} < 1 \tag{4.30}$$

for all $x_{1,k}$ and,

$$\sum_{p=0}^{k-1}(1-ha_3)^{k-p-1}\,x_{1,p}\psi(x_{1,p}) \leq \sum_{p=0}^{k-1}(1-ha_3)^{k-p-1}\,x_{1,p} \tag{4.31}$$

Moreover, since $x_{1,k}$ has been proved to be bounded, there exists a positive finite constant M such that $||x_{1,q}|| \leq M$ for all $q = 1, 2...k-p-1$, so that

$$\begin{aligned} \sum_{p=0}^{k-1}(1-ha_3)^{k-p-1}\,x_{1,p} &\leq M\sum_{p=0}^{k-1}(1-ha_3)^{k-p-1}\\ &= M\frac{1-(1-ha_3)^k}{ha_3} && (4.32) \end{aligned}$$

Thus, Eq. (4.32) can be upper-bounded as:

$$||x_{2,k}|| \leq (1-ha_3)^k\,||x_{2,0}|| + ha_4 M\frac{1-(1-ha_3)^k}{ha_3} \tag{4.33}$$

Since the right-hand side of Eq. (4.33) is bounded for all $k \geq 0$, then $x_{2,k}$ is also bounded and the proof is completed. ■

Notice that the observer provides an asymptotically exact estimation of $x_{2,k}$ regardless of the value the control signal. This fact can be used to intuitively show that the reference profile can be asymptotically perfectly tracked. Thus, there exists a finite integer k' such that $\hat{x}_{2,k} \approx x_{2,k}$ for all $k \geq k'$. In this way, Eq. (4.33) can be re-written as:

$$x_{1,k+1} = ha_6 L x_k + ha_6 w_k \tag{4.34}$$

When $w_k \geq 0$ and $u_k = \sqrt{w_k}$, then the error dynamics is represented by Eq. (4.33) that can be proved to converge to zero guaranteeing the perfect asymptotic tracking. On the other hand, when $u_k = 0$ because $\max(0, w_k) = 0$, then we have that $w_k = -Lx_k + G\nu_k < 0$, i.e. $Lx_k > G\nu_k$. In this case, Eq. (4.34) satisfies:

$$x_{1,k+1} > ha_6 G\nu_k = \hat{r}_{k+1} \tag{4.35}$$

Eq. (4.35) implies that the actual heart rate is bigger than the desired one. Therefore, the control input is zero and the system itself decreases the heart rate in order to track the reference value. Thus, in both cases the output tries to converge to the reference, and asymptotically attains the tracking.

4.2.5 Stability of the continuous-time closed-loop system

In this Section, the stability of the continuous-time system is addressed. The starting point is the stability of the discrete-time system proved in the previous Subsection 4.2.6. In this way, we already know that x_k, y_k and u_k are bounded for any integer $k \geq 0$. Therefore, the stability of the continuous-time system is guaranteed if we prove that model (4.1)-(4.4) does not have a finite escape time. Thus, state variables would not be able to diverge on any finite interval $[kh, (k+1)h)$. The absence of a finite escape time is granted provided that the nonlinear function $\psi(x_1(t))$ is *globally* Lipschitz. This is generally an overly conservative condition but, fortunately, is satisfied by the function at hand as Condition 2) in Section 4.2 states. As a consequence, state variables cannot diverge on any finite interval, and the continuous-time system signals are bounded at all time.

4.2.6 Simulation Examples

This Section contains some numerical simulation examples showing the results achieved by the proposed controller. The following particular values for the model, extracted from **[120]**, will be used in the examples:

$$\begin{aligned} a_1 = 2.2,\ a_2 &= 19.96,\ a_3 = 0.0831, \\ a_4 = 0.002526,\ a_5 &= 8.32,\ a_6 = 0.38 \end{aligned} \tag{4.36}$$

The heart rate at-rest is taken as $HR0 = 40$ bpm, the initial states are $x_0^T = [0\ 0]$ and the observer is initialized as $\hat{x}_{2,0} = 5$. This is a rather atypical initialization for the observer but a nonzero value has been selected in order to show the effectiveness of the control law in this less favorable case. The sampling time is $h = 0.1$s satisfying Eq. (4.11) since $0.1 < \min\left(\frac{1}{2.2}, \frac{1}{0.0831}\right) = 0.45$s. The maximum theoretical heart rate is 220 bpm[2]. This value means that there is one beat every 0.27 s. The selected

[2]The maximum theoretical heart rate for an individual of age A is usually taken as 220-A.

sampling time is enough to be able to measure the heart rate without aliasing. The simulations are performed in Matlab.

Figure 4.1 displays the reference signal used to test de controller along with the actual output of the system. It can be noticed that the output perfectly tracks the reference asymptotically. This fact is confirmed by Figure 4.2, that displays the error between both signals and vanishes asymptotically. During the first seconds of operation there is an error caused by the mismatch in the estimation of $x_{2,k}$ as Figure 4.3 displays. However, the error between the actual state variable and the observed one converges to zero asymptotically and monotically while the control law enforces the perfect tracking of the reference. Figure 4.4 depicts the speed of the treadmill acting as control command. It can be seen that the control is zero during the first seconds of simulation. Again, this fact is caused by the error in the estimation of $x_{2,k}$. In conclusion, the presented control law is able to make the heart rate follow the desired reference profile, achieving the proposed objective.

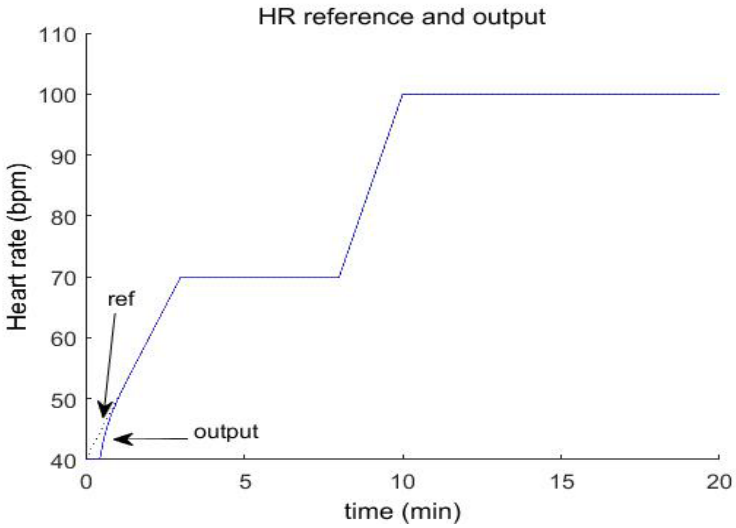

FIGURE 4.1: Actual heart rate and reference signal.

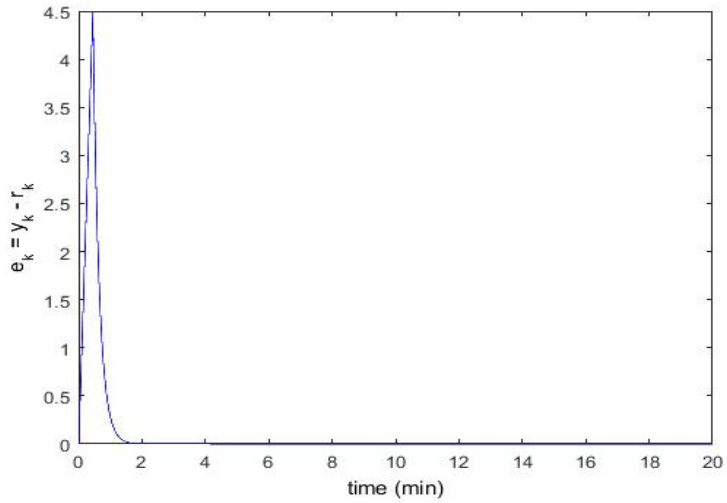

FIGURE 4.2: Error between the actual heart rate and reference signal.

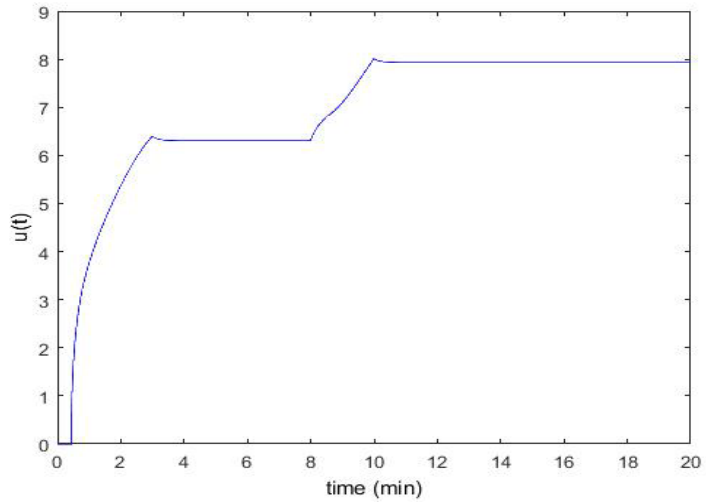

FIGURE 4.3: Evolution of the observation error, $\tilde{x}_{2,k}$.

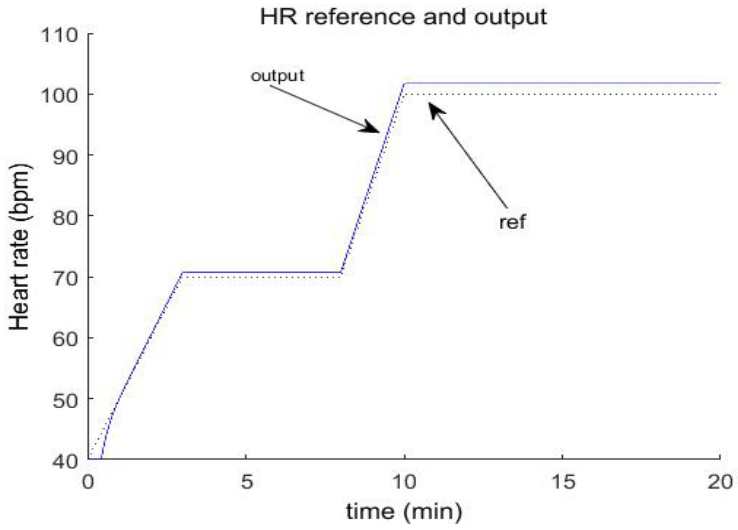

FIGURE 4.4: Control command: speed of the treadmill.

Robustness analysis

Now, the performance of the closed-loop is tested when the parameters of the system are not perfectly known. To this end, we will modify the parameters of the model used in the controller by adding an uncertainty of 10% to their nominal values. The same procedure is performed in the parameters used in the observer. The increment or decrement of each value is selected randomly. The particular values employed in the simulation are given by:

$$\begin{aligned} \hat{a}_1 = 2.42,\ \hat{a}_2 &= 21.956,\ \hat{a}_3 = 0.0748, \\ \hat{a}_4 = 0.0028,\ \hat{a}_5 &= 9.152,\ \hat{a}_6 = 0.418 \end{aligned} \tag{4.37}$$

In this way, Figure 4.5 displays the output of the system and the reference signal while Figure 4.6 depicts the tracking error. It can be concluded that the parameter mismatch generates a tracking error. However, as Figure 4.6 shows, the error lies between 1 and 2 bpm in the steady-state. If we take into account that the reference

value in the steady state is 100 bpm, the error is less than 2% of the value of the signal despite the parameter variation is of 10%. This performance, however, is not good enough for a rehabilitation system. Therefore, our future research goes in the direction of making the control law more robust while attaining a better closed-loop performance. Since the control system exhibits this robustness issues, we will study some approaches to improve the robustness.

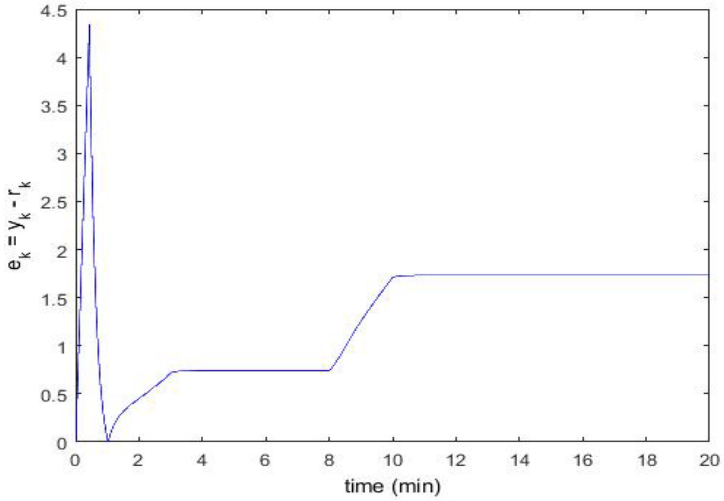

FIGURE 4.5: Actual heart rate and reference signal in the presence of parameters mismatch.

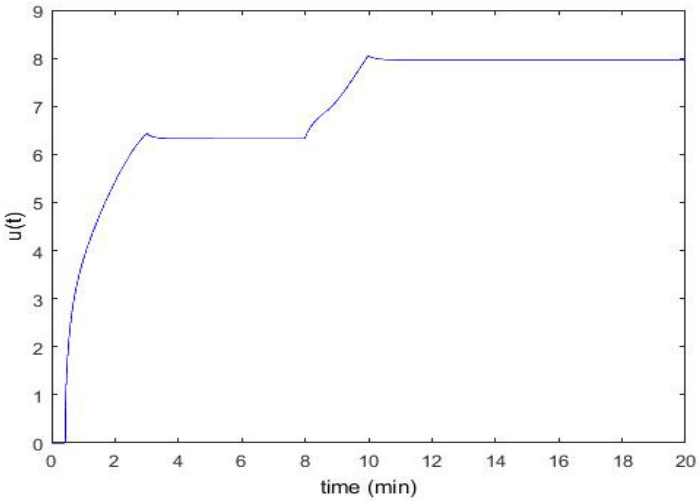

FIGURE 4.6: Error between the actual heart rate and reference signal in the presence of parameters mismatch.

The material of this Section was published in Conference paper [**88**].

In the next section, a joint parameter-state algorithm is employed to overcome the limitation of parameter mismatch that may come in this approach.

4.3 Joint parameter-state estimation based-control

In the previous Section, a feedback-linearization based control low has been designed but it suffered from robustness issues. The control command requires the values of the parameters of the model along with the states. Since both of them are unknown/unmeasurable, a joint parameter-state estimation algorithm is deployed in this subsection to obtain an estimation of their values, which are then used in the control law calculation. Simulation examples show the great response achieved by this approach in the control of heart rate during treadmill exercise.

Thus, we will design a feedback linearization-inspired control law based on the simultaneous parameter-state estimation of the treadmill heart rate model. In this way, the parameters of the model are estimated online without the need of an *a priori* parameter identification stage while the unavailable state is simultaneously observed. The design of such a system will make easier the development of personalized exercise routines for patients since it will avoid the beforehand identification procedure. Furthermore, the controller will always be able to apply an accurate control command despite the potential long-term variations through a time of the model. This fact adds reliability to the system. The simultaneous state-parameter estimation is one of the main problems in the control engineering field and many efforts have been devoted to it during the last years, **[104]**[**69**]. The discretized nonlinear model is given by Eqs. (4.6) and (4.8) will be the starting point of the design.Then, the approach adopted in **[132]** is used to simultaneously estimate the parameters and the unmeasurable state. The so-obtained values are finally used to calculate the feedback-linearization based control law Eqs (4.16-4.18) in order to control the patient's heart rate during treadmill exercise. To the best of author's knowledge, this is the first work in heart rate control during treadmill exercise that combines the simultaneous estimation of parameters and state.

4.3.1 Joint Parameter-State Estimation

This section contains the simultaneous parameter-state estimation algorithm for the discrete-time system (4.1)-(4.4). The approach presented in **[69]** and **[132]** is adopted for such a purpose. To this end, we first cast the nonlinear discrete-time system as:

$$x_{k+1} = f(x_k, w_k, a) \tag{4.38}$$

where $x_k = [x_{1k}\ x_{2k}]^T$ denotes the state, $a = [a_1\ a_2\ ...\ a_6]^T$ stands for the unknown parameters and:

$$f(x_k, w_k, a) = \begin{bmatrix} f_1(x_k, w_k, a) \\ f_2(x_k, w_k, a) \end{bmatrix} \tag{4.39}$$

$$= \begin{bmatrix} (1 - ha_1)x_{1k} + ha_2 x_{2k} + ha_6 w_k \\ (1 - ha_3)x_{2k} + ha_4 x_{1k}\psi(x_{1k}) \end{bmatrix} \tag{4.40}$$

Notice that equations (4.38)-(4.40) correspond to the system (2) in **[104]** with $A = 0$ and $\varphi = 0$. It can also be readily checked that the system satisfies all the technical assumptions required in **[69]** in order to apply the algorithm. Notice that the auxiliary output, $z_k = x_{1k} = [1\ 0]x_k = Cx_k$, will be used in the estimation. The joint estimator equations are given by:

$$\begin{aligned}
\hat{x}_{k+1} &= f(\sigma(\hat{x}_k), w_k, \hat{a}_k) + L(C\hat{x}_k - z_k) + \rho_k && (4.41)\\
\rho_k &= \lambda_{k+1}\left(\hat{a}_{k+1} - \hat{a}_k\right) && (4.42)\\
\lambda_{k+1} &= LC\lambda_k + \frac{\partial f}{\partial a}\left(\sigma(\hat{x}_k), w_k, \hat{a}_k\right),\ \lambda_0 = 0 && (4.43)\\
\hat{a}_{k+1} &= \hat{a}_k - \frac{\alpha}{\gamma} W_{k+1}^{-1} \lambda_k^T C^T \left(C\hat{x}_k - z_k\right) && (4.44)\\
W_{k+1} &= \left(1 - \frac{\alpha}{\gamma}\right) W_k + \frac{\alpha}{\gamma}\lambda_k^T C^T C \lambda_k,\ W_0 > 0 && (4.45)
\end{aligned}$$

where:

- L is the observer gain,
- $\sigma(\cdot)$ is the asymmetric saturation function:

$$\sigma(\xi) = \left(\sigma(\xi_1)\ \sigma(\xi_2)\right)^T \qquad (4.46$$

with:

$$\sigma_i(\xi_i) = \begin{cases} \xi_i & \underline{r}_i \le \xi_i \le \bar{r}_i \\ \bar{r}_i & \xi_i \ge \bar{r}_i \\ \underline{r}_i & \xi_i \le \underline{r}_i \end{cases} \qquad (4.47)$$

where $\underline{r}_i$ and $\bar{r}_i$ for $i = 1, 2$ are two real numbers such that $\underline{r}_i \le x_{ik} \le \bar{r}_i$ for $i = 1, 2$.

- α and γ are two positive numbers satisfying $0 < \alpha < \gamma$.

The way in which the control parameters should be selected and their influence in the estimation performance is discussed in **[132]**. The value of the gradient matrix involved in the calculations is given by:

$$\left(\frac{\partial f}{\partial a}\right)^T = \begin{pmatrix} -hx_{1k} & 0 \\ hx_{2k} & 0 \\ 0 & -hx_{2k} \\ 0 & hx_{1k}\psi(x_{1k}) \\ 0 & m(x_{1k}) \\ hw_k & 0 \end{pmatrix} \qquad (4.48)$$

with:

$$m(x_{1k}) = -ha_4 x_{1k} e^{-(x_{1k} - a_5)} \psi(x_{1k})^2 \qquad (4.49)$$

The parameter values along with the observed state $\hat{x}_{2k}$ are now used to implement the control command (4.45) as:

$$w_k = -\frac{1 - h\hat{a}_1}{h\hat{a}_6} x_{1k} - \frac{\hat{a}_2}{\hat{a}_6}\hat{x}_{2k} + \frac{1}{h\hat{a}_6}\nu_k \qquad (4.50)$$

4.3.2 Simulation Examples

This Section contains some numerical simulation examples showing the results achieved by the joint parameters-state estimation algorithm along with the feedback-linearization

controller. The parameters of the model are the same as in Section 4.2.6. The estimation algorithm is initialized with the following parameters:

$$\begin{aligned} \hat{a}_1 = 5,\ \hat{a}_2 &= 5,\ \hat{a}_3 = 5, \\ \hat{a}_4 = 5,\ \hat{a}_5 &= 0.5,\ \hat{a}_6 = 5 \end{aligned} \tag{4.51}$$

Notice that the estimated parameters are initialized with values that are very different from the actual ones in order to show the performance achieved by the approach. Moreover, $\alpha = 1$, $\gamma = 160$, $\bar{r}_1 = \bar{r}_2 = 100$, $\underline{r}_1 = \underline{r}_2 = 0$, $L = [0.2\ 0.05]^T$ and $\hat{x}_{20} = [0\ 0]^T$. Notice that this is a judicious choice for the initial estimated states since the exercise usually starts from the at-rest situation. Figure 4.7 displays the actual heart rate of the runner and the reference signal. It can be seen in this figure that both plots are practically superimposed, implying that the tracking objective is achieved with great accuracy. Moreover, Figure 4.8 shows the tracking error attained by the control scheme. As it can be observed in Figure 4.8 the error is less than 1 bpm (beat per minute) showing a good response from the control system.

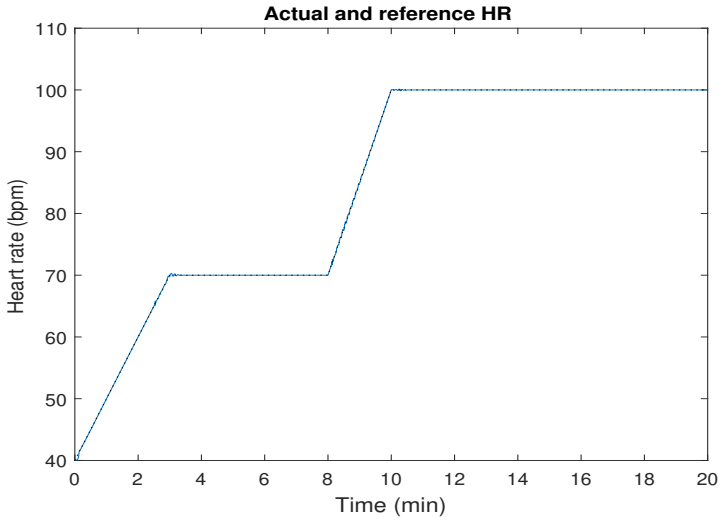

FIGURE 4.7: Actual heart rate and reference signal.

The behaviour of the state observer is depicted in Figure 4.9 where the observation error is shown. On the other hand, Figures 4.10 and 4.11 display the evolution of the estimated parameters. The final values for the estimated parameters are given by:

$$\hat{a}_{1end} = 0.60,\ \hat{a}_{2end} = -1.56,\ \hat{a}_{3end} = 5, \tag{4.52}$$

$$\hat{a}_{4end} = 5,\ \hat{a}_{5end} = 0.5,\ \hat{a}_{6end} = 0.515 \tag{4.53}$$

As it can be deduced from Figures 4.9, 4.10 and 4.11 and final values (4.23) and (4.24), neither the second state nor the parameters are identified correctly. Furthermore, parameter $\hat{a}_{2end}$ is even negative. However, the parameter identification is not needed to achieve a good closed-loop behaviour since state and parameter identification are only attained when certain persistent excitation conditions, which may not be accomplished in closed-loop control, are held. Notice that a_6 is the most critical parameter in the implementation of the control law (4.3.1). This parameter is adjusted by the algorithm in order to obtain an accurate closed-loop behaviour, finally attaining the control objective. It is also noticeable that parameters $\hat{a}_3$, $\hat{a}_4$ and

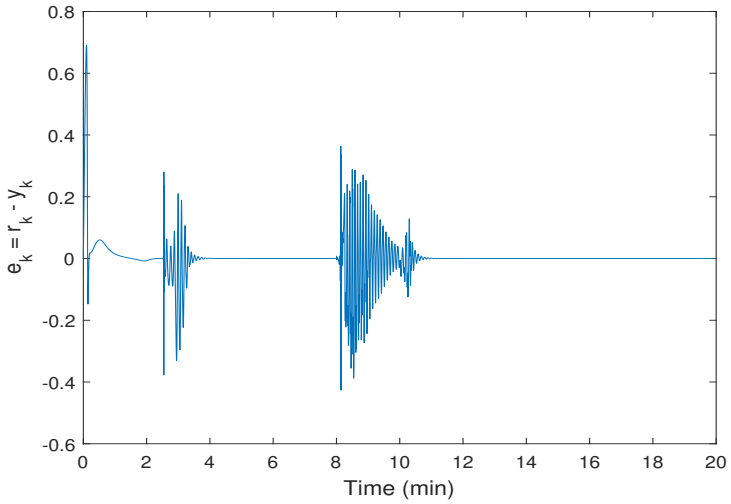

FIGURE 4.8: Tracking error between the actual heart rate and the reference signal.

$\hat{a}_5$ are not updated by the algorithm. Thus, the control objective is achieved by updating only the state and some of the parameters of the model. Finally, Figure 4.12 displays the speed of the treadmill, that is the calculated control law. To conclude, it is worth noticing the fact that the controller excites some low amplitude oscillation in the output, as it can be observed in Figure 4.8. The oscillation is caused by the transient behaviour induced by the change in the reference signal.

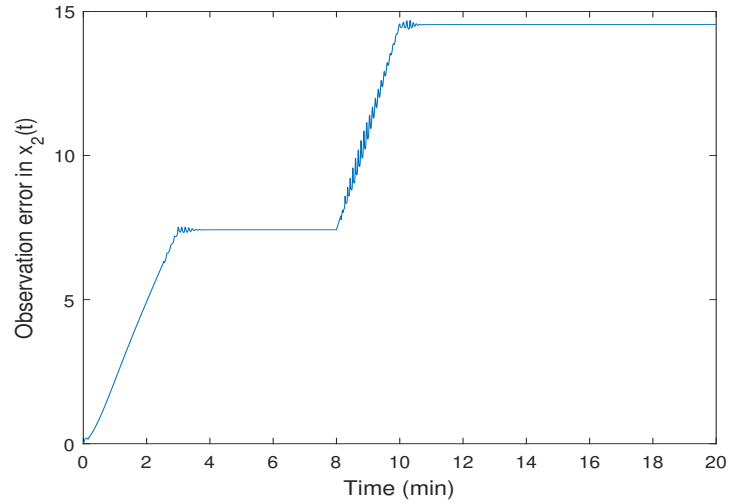

FIGURE 4.9: Observation error for the $x_2(t)$ variable.

Apart from the complexity and difficulty of estimation, the oscillation of this method was another problem that we face when implementing this algorithm. So we will use sliding mode control to finally overcome all these difficulties. In order to design a discrete-time sliding mode control (DT-SMC), we will do it first in the linear system and finally the nonlinear design which is presented in the following section (Section 4.4).

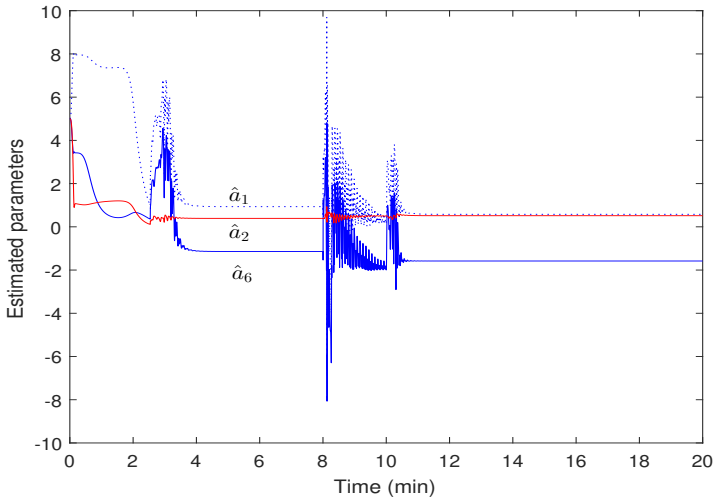

FIGURE 4.10: Evolution of the estimated parameters $\hat{a}_1$, $\hat{a}_2$ and $\hat{a}_6$.

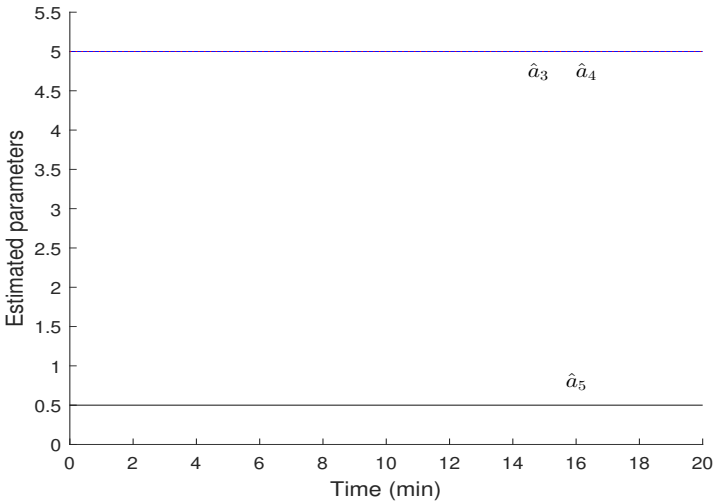

FIGURE 4.11: Evolution of the estimated parameters $\hat{a}_3$, $\hat{a}_4$ and $\hat{a}_5$.

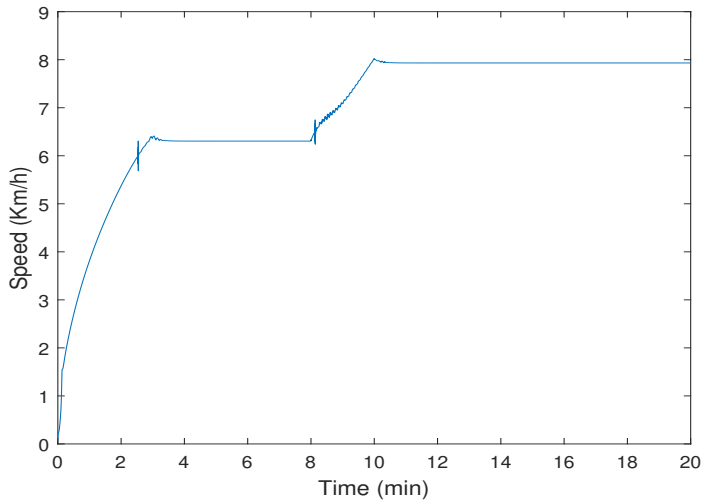

FIGURE 4.12: Speed of the treadmill.

4.4 Discrete-time Sliding Mode Control

Extensive research has been done over the last decades on the discrete-time sliding mode control (SMC) systems due to the fast developments of digital microprocessor-based control technology. There are two streams of SMC systems in discrete-time domain: one is that the dynamical systems are discretized first and a SMC is then designed for the discrete-time system; the other is that the SMC design is done in the continuous-time domain and then digitized for implementation. The latter has been shown to give rise to irregular discretization behaviors if the sampling rate is not selected properly. For example, irregular and complex periodic behaviors are found in zero-order-holder (ZOH) discretization of SMC systems and Euler's discretization of SMC system.

We will present a discrete-time sliding mode control to solve the difficulty and oscillation of the estimation that mentioned in the last section. Initially, the design will be in the linear case and afterwards the nonlinear case is considered. In the last subsection of this Section discrete-time, super-twisting sliding mode control will be present, which a very new method and it applies for the first time to solve these problems.

4.4.1 Problem Formulation

The following nonlinear model used in previous Sections is considered:

$$\dot{x}_1(t) = -a_1 x_1(t) + a_2 x_2(t) + a_3 u^2(t) + f_{u1}(x) \tag{4.54}$$

$$\dot{x}_2(t) = -a_4 x_2(t) + \phi(x_1(t)) + f_{u2}(x) \tag{4.55}$$

$$\phi(x_1(t)) = \frac{a_5 x_1(t)}{1 + \exp\left(-(x_1(t) - a_6)\right)} \tag{4.56}$$

$$y(t) = x_1(t) + HR_{rest} \tag{4.57}$$

Where $x(0) = [x_1(0), x_2(0)] = [0, 0]$ is the usual initial condition and a_1, ..., a_6 are positive scalars.

$f_{u1}(x)$ and $f_{u2}(x)$ account for the parametric and unmodeled dynamics of the system. The following Assumption will be done:

Assumption 2.1. The uncertain terms f_{u1} and f_{u2} are upper-bounded so that $Sup\,|f_{u1}| = k_1 < \infty$, $Sup\,|f_{u2}| = k_2 < \infty$.

The uncertainty-free model satisfies the conditions from Section 4.2.

Assumption 2.2 implies that autonomous-system is globally stable. Thus, this fact will allow us to obtain an upper bound of the discrete-time uncertainty in terms of the original continuous-time one. The method chosen in this Section is to linearize the nonlinear system and discretize the so-obtained linear system. This process is described in the next subsection. This will allow analyzing how the original uncertainty is propagated into the uncertainty of the discrete-time model.

4.4.2 Linearization and ZOH discretization

In order to linearize the equations (4.54-4.57), we must first obtain the system equilibrium point x_e. In operation, the equilibrium point will vary because of the treadmill's speed. Although there are different linearization approaches, we choose to linearize the system around the fixed point $(0, 0)$. Despite this point is not realistic in practical applications since the heart rate will be different from the heart rate at rest when speed is applied to the treadmill, it provides an easy model to design a

controller. The SMC will be then in charge of counteracting potential mismatches in the model including the one coming from the linearization. By setting the conditions $\dot{x}(t) = 0$, $u(t) = 0$, the system equilibrium point is $x_e = [0, 0]^T$. Through the linearization of equations (4.54-4.57) we have, around the equilibrium point:

$$\dot{x}(t) = Ax + Bw + F_l(t), \tag{4.58}$$

$$y = Cx + HR_{rest} \tag{4.59}$$

$$A = \nabla_x f|_{x_e,u_e} = \begin{bmatrix} \frac{\partial f_1}{\partial x_1} & \frac{\partial f_1}{\partial x_2} \\ \frac{\partial f_2}{\partial x_1} & \frac{\partial f_2}{\partial x_2} \end{bmatrix} = \begin{bmatrix} -a_1 & a_2 \\ \frac{a_5}{1+exp(a_6)} & -a_4 \end{bmatrix} \tag{4.60}$$

$$B = \nabla_u g|_{x_e,u_e} = \begin{bmatrix} a_3 \\ 0 \end{bmatrix}, \quad F_l = [f_{u1} \quad f_{u2}]^T + f_{lin} \tag{4.61}$$

$$C = [1 \quad 0] \tag{4.62}$$

where $x \in R^{2\times 1}$ is the state, $y \in R$ is the output, the control is $w(t) \in R$, with $w(t) = u(t)^2$, and the disturbance is $F_l \in R^{2\times 1}$. The state matrix is $A \in R^{2\times 2}$, the control matrix is $B \in R^{2\times 1}$, the output matrix is $C \in R^{1\times 2}$ and F_l accounts for the uncertainties in the linear model that contains the original uncertainty and the one coming from linearization, f_{lin}.

Proceeding further, the discretized counterpart of 4.54 is given by:

$$x_{k+1} = \Phi x_k + \Gamma w_k + d_k,\ x_0 = x(0),\ y_k = Cx_k + HR_{rest} \tag{4.63}$$

with:

$$\Phi = e^{AT} \tag{4.64}$$

$$d_k = \int_0^T e^{A\tau} F_l((k+1)T - \tau)d\tau, \quad x_k = x_{kT} \tag{4.65}$$

$$\Gamma = \int_0^T e^{A\tau} B d\tau \tag{4.66}$$

and $T > 0$ being the sampling period. Now, the uncertainty term d_k is upper-bounded as follows.

It is important to note that, we want to analyze how the original uncertainty translates into the uncertainty in discrete-time. Therefore, further calculations are deployed.

Since Assumptions 2.1 and 2.2 hold, the matrix A is Hurwitz and we have, [**87**]:

$$\left\| e^{At} \right\| \leq Ce^{-\rho t}, \quad C \geq 1, \quad \rho \geq 0 \tag{4.67}$$

In this way,

$$\begin{aligned} \|d_k\| &\leq \left\| \int_0^T e^{A\tau} F_l((k+1)T - \tau)d\tau \right\| \\ &\leq \int_0^T Ce^{\ \rho\tau} \|F_l((k+1)T \quad \tau)\| d\tau \\ &\leq C \underset{\tau \in [0,T]}{Sup} \|F_l((k+1)T - \tau)\| \int_0^T e^{-\rho\tau} d\tau \\ &\leq C \underset{\tau \in [0,T]}{Sup} \|F_l((k+1)T - \tau)\| \left(\frac{1 - e^{-\rho T}}{\rho} \right) \end{aligned} \tag{4.68}$$

Eq. (4.67) captures the uncertainty contained in F_l during the whole interval $[kT, (k+1)T])$ through the term $\sup_{\tau\in[0,T]} ||F_l(T-\tau)||$.

Eq. (4.68) can be further developed since:

$$\begin{aligned}
&\underset{\tau \in [KT, (k+1)T]}{Sup} \|F_l((k+1)T-\tau)\| \\
&= \underset{\tau \in [0, T]}{Sup} \|f_{lu}((k+1)T-\tau) + \|f_{lin}((k+1)T-\tau)\| \\
&\leq \underset{\tau \in [0, T]}{Sup} \|f_u((k+1)T-\tau)\| \\
&\quad + \underset{\tau \in [KT, (k+1)T]}{Sup} \|f_{lin}((k+1)T-\tau)\| \\
&\leq Max(k_1, k_2) + \underset{\tau \in [KT, (k+1)T]}{Sup} \|f_{lin}((k+1)T-\tau)\| \qquad (4.69)
\end{aligned}$$

Now the linearization term can be upper bounded as:

$$\sup_{\tau\in[kT,(k+1)T)} ||f_{lin}((k+1)T-\tau)|| \leq K_{lin} \qquad (4.70)$$

Now it will be shown that such a constant K_{lin} exists . As it is clear, the first equation (4.58) is linear. However, (4.54-4.57) is affected by the nonlinear term (3). In order to avoid this nonlinear dependence, the ϕ function can be inset between its two extreme values which are the limits of this function when $x_1(t)$ tends respectively to zero and to infinity :

$$\begin{aligned}
&\lim_{x_1\to 0} \phi(x_1) = \phi_1 = \frac{a_5}{1+exp(a_6)} \\
&\lim_{x_1\to \infty} \phi(x_1) = \phi_2 = 1 \qquad (4.71)
\end{aligned}$$

so that

$$\phi_1 \leq \phi(x_1(t)) \leq \phi_2 \qquad (4.72)$$

In this way, the above values define the following two extreme linear systems, given by Σ_0 and Σ_1:

$$\Sigma_0 : \begin{cases} \dot{x}_{10} = -a_1 x_{10}(t) + a_2 x_{20}(t) + a_3 w(t) \\ \dot{x}_{20} = -a_4 x_{20}(t) + \phi_1 x_{10}(t) \end{cases} \qquad (4.73)$$

$$\Sigma_1 : \begin{cases} \dot{x}_{11} = -a_1 x_{11}(t) + a_2 x_{21}(t) + a_3 w(t) \\ \dot{x}_{21} = \quad a_4 x_{21}(t) + \phi_2 x_{11}(t) \end{cases} \qquad (4.73)$$

Thus, the original nonlinear system, Σ, can be bounded as:

$$\Sigma_0 \leq \Sigma \leq \Sigma_1 \qquad (4.75)$$

Notice that the linearized system (4.58-4.62) corresponds to the extreme case Σ_1. Therefore, the maximum linearization error is given by the difference between Σ_1 and Σ_0. Hence, we have for Σ_1:

$$\Sigma_1 : \{\dot{x}_{21} = -a_4 x_{21}(t) + \phi_2 x_{11}(t) \qquad (4.76)$$

and for Σ_0:

$$\Sigma_0 : \{\dot{x}_{20} = -a_4 x_{20}(t) + \phi_1 x_{10}(t) \tag{4.77}$$

so that the original dynamical equation satisfies:

$$\dot{x}_{20}(t) \leq \dot{x}_2(t) \leq \dot{x}_{21}(t) \tag{4.78}$$

The systems Σ_0 and Σ_1 are asymptotically stable as a consequence of Assumption 2.2. Therefore, there exist finite positive constants δ_1 and δ_2 such that:

$$|x_{20}(t)| \leq \delta_1 \tag{4.79}$$

$$, \quad |x_{21}(t)| \leq \delta_2 \tag{4.80}$$

If we now choose $K_{lin} = \delta_1 + \delta_2$ we obtain an upper-bounding of the maximum error comitted by the linearization process. Thus, there exist a finite positive constant K_{lin} so that (4.70) holds.

In this way, we can upper-bound the discrete-time uncertainty as:

$$||d_k|| \leq \frac{C}{\rho} \left(max(k_1, k_2) + K_{lin}\right) \left(1 - e^{-\rho T}\right) \tag{4.81}$$

so that the final upper-bounding is given by (4.81).

Thus, we have been able to obtain an upper-bound of the discrete-time uncertainty from the uncertainty in CT.

Now we can expand the exponential term of (4.81) in a Mac-Laurin series to obtain:

$$\left(1 - e^{-\rho T}\right) = -\sum_{j=1}^{\infty} \frac{(-\rho T)^j}{j!} \tag{4.82}$$

$$= \rho T - \frac{\rho^2 T^2}{2} - \sum_{j=3}^{\infty} \frac{(-1)^j \rho^j T^j}{j!} \tag{4.83}$$

It is a well-known result on alternate series that when we truncate such a series up to a term, the error between the truncation and the original series is less in absolute value than the next term of the series (the first term neglected), **[132]**. Thus, we have:

$$(1 - e^{-\rho T}) = \rho T + \varepsilon(T) \tag{4.84}$$

This means that if we take (4.83) and use this approximation in (4.84), the approximation error satisfies:

$$|\varepsilon(T)| \leq \frac{\rho^2 T^2}{2} \tag{4.85}$$

This means that $\varepsilon(T) \in O(T^2)$ where $O(\cdot)$ stands for the Landau's Big O notation, **[132]**. Thus, a variable v is said to be $O(T^r)$ if, and only if, there is a $C > 0$ such that for any sufficiently small T the following inequality holds:

$$|v| \leq CT^r \tag{4.86}$$

where r is an integer. The so obtained equation (4.84) means that the upper-bounding of the uncertainties d_k with this approximation is correct up to $O(T^2)$, providing an estimation on how the selection of the sampling time influences the uncertainties upper-bound.

This subection is devoted to obtain a discrete-time model suitable to design a discrete-time sliding mode controller. Moreover, a relationship between the continuous-time and discrete-time uncertainties has been obtained. The following subsection describes how the controller is designed.

4.4.3 Control Design

The control objective is to design a discrete-time sliding manifold and a discrete-time Sliding Mode Control law for the sampled-data system (4.63).

Consider the discrete-time sliding manifold given by:

$$S_k = D_0(r_k - y_k) \tag{4.87}$$

where D_0 is a constant and $r_k \in \Re$. The objective is to force the output y_k to track the reference signal r_k. The control law is designed by incorporating a disturbance estimator given by, **[88]**:

$$\hat{d}_k = x_k - \Phi x_{k-1} - \Gamma u_{k-1} \tag{4.88}$$

The reaching equation is of SMC type and given by, **[132]**:

$$S_{k+1} - S_k = -qTS_k - \varepsilon T sgn(S_k) + d_k - d_0 - \delta_d sgn(S_k) \tag{4.89}$$

where q, ε are free design parameters that must be selected in such a way that the inequalities $0 < \varepsilon < 0.5$ and $0 < (1 - qT) < 1$ are satisfied while $\delta_d \geq \|d_k\|$, [89]. Thus, δ_d is selected based on (4.86).

The following assumption is necessary in order to calculate the control law.

Assumption 3.1. The reference signal must be known one step ahead, i.e. the value at $(k+1)$ should be known at k.

Considering $S_{k+1} = D(r_{k+1} - y_{k+1})$ and inserting the system equations (4.87) into the reaching rule, (4.89) is rewritten as follows:

$$\begin{aligned} Dr_{k+1} - DC(\Phi x_{2k} + \Gamma w_k) = (1 - qT)D(r_k - Cx_{2k}) \\ -(\varepsilon T + \delta_d)sgn(S_k) - d_0 + \hat{d}_k \end{aligned} \tag{4.90}$$

By using this equation, the control input for the system with equation (4.90) is obtained as:

$$\begin{aligned} w_k = (DC\Gamma)^{-1}\,[DC(\,\Phi - 1 + qT)x_{2k} + (1 - qT)D_{rk} \\ -Dr_{(k+1)} - d_0 - (\delta_d + \varepsilon T)sgn(S_k) + \hat{d}_k \end{aligned} \tag{4.91}$$

Given the relation Eq. (4.89) and the equation (4.90), the control input is now expressed as follows:

$$\begin{aligned} w_k = (DC\Gamma)^{-1}\,[DC(\,\Phi - 1 + qT)x_{2k} + (1 - qT)D_{rk} \\ -D_{r(k+1)} - \varepsilon T sgn(S_k) + qTDHR_{rest} + \hat{d}_k \end{aligned} \tag{4.92}$$

Using the disturbance estimation, Eq. (4.92), the actual Sliding Mode control law is given by

$$\begin{aligned} w_k = (DC\Gamma)^{-1}\,[DC(\,\Phi - 1 + qT)x_{2k} - \varepsilon T sgn(S_k) \\ + qTDHR_{rest}] \end{aligned} \tag{4.93}$$

Note that x_{2k} is not available from measurments. Thus, the next section describes a state estimator used to obtain an approximation to its value.

4.4.4 State Observer

The discrete-time model is given by:

$$x_k = \Phi x_{k-1} + \Gamma w_{k-1} + d_{k-1} \tag{4.94}$$

$$x_{2k} = \Phi_{21} x_{1k-1} + \Phi_{22} x_{2k-1} + \Gamma_2 w_{k-1} + d_{k-1} \tag{4.95}$$

so that the second equation reads:

Where Φ_{ij} stands for the elements of matrix Φ that only depends on the parameters that are unknown. The state estimator is given by:

$$\hat{x}_{2k} = \Phi_{21} x_{1k-1} + \Phi_{22} \hat{x}_{2k-1} + \Gamma_2 w_{k-1} \tag{4.96}$$

where $\hat{x}_{20} = 0$. Since x_{1k-1} is measureable, the nominal values for the matrices are given and the previous control signal is known, it is feasible to obtain an estimation of the second state variable, x_{2k}, from (4.96).

In the end, we must bear in mind that we are working with the square of the control signal so that the actual speed command is given by:

$$u_k = \sqrt{Max(0, w_k)} \tag{4.97}$$

In the case of recovery and training programs, the controller is able to make the heart rate follow the predefined profile set up. On the other hand, since we are applying a zero-order hold, the continuous-time control law takes the form:

$$u(t) = u_k, \; t \in [KT, (K+1)T) \tag{4.98}$$

In the next section, the results and response of discrete sliding mode control based on the design performed in this section are shown.

4.4.5 Results and Simulation

This Section contains some numerical simulation examples showing the results achieved by the proposed controller. The following particular values for simulation , extracted from [1][141], will be used in the examples:

$$\begin{aligned} a_1 = \quad 2.647 \quad , \quad a_2 = 25.87 \quad , \quad a_3 = 0.83 \\ a_4 = 0.904 \quad , \quad a_5 = 0.04 \quad , \quad a_6 = 5.23 \end{aligned} \tag{4.99}$$

and the nominal ones used for controller design purposes are given by:

$$\begin{aligned} \hat{a}_1 = \quad 1.85 \quad , \quad \hat{a}_2 = 23.15 \quad , \quad \hat{a}_3 = 0.79 \\ \hat{a}_4 = 0.855 \quad , \quad \hat{a}_5 = 0.038 \quad , \quad \hat{a}_6 = 4.7 \end{aligned} \tag{4.100}$$

The parameters are considered to be uncertain. Although, the average error in the parameters is 5 percent, the minimum error is 2 percent and the maximum error is about 9 percent. The heart rate at-rest is taken as HR = 65 bpm. The maximum theoretical heart rate is 220 bpm. The sampling time is given by $T = 0.27$ s. The selected

sampling time is enough to be able to measure the heart rate without aliasing. The simulations are performed in Matlab.

Figure 4.13 and 4.14 display the response of the discrete sliding mode controller and control signal of the treadmill speed based on the parameters of the model at the treadmill speed of 2-14 km / h. In this case, it is also observed that the controller has been able to ransfer the heart rate to a reference value without any overdrive for less than 10 seconds. Also, the control signal is applied quite smoothly. Therefore, the implementation of the controller in practice does not require a specific drive and implementation will be simple.

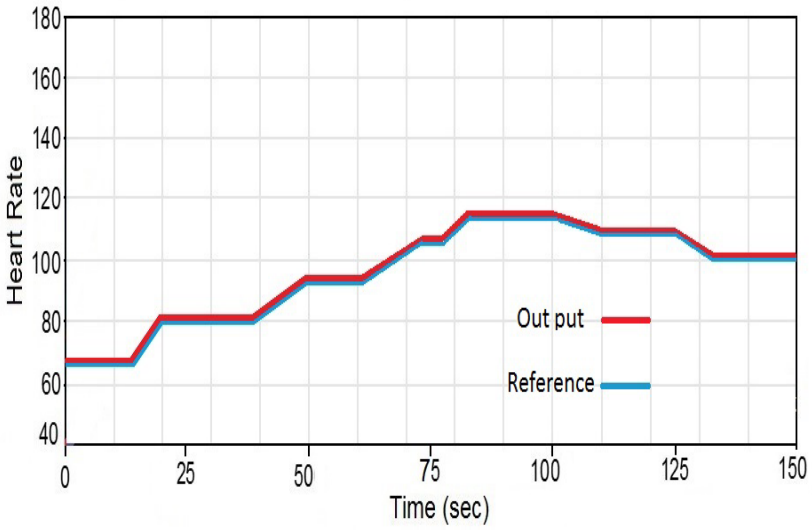

FIGURE 4.13: Heart rate provided by the DTSMC controller

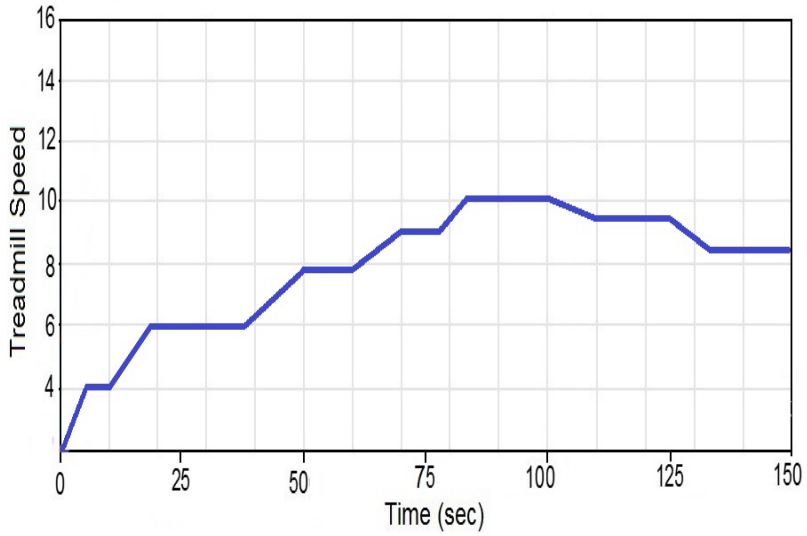

FIGURE 4.14: Speed provided by the DTSMC controller

On the other hand, 4.15 shows the heart rate estimation error by using the discrete time sliding mode control. As it can be seen, the error is decreasing and after few seconds and is close to zero.

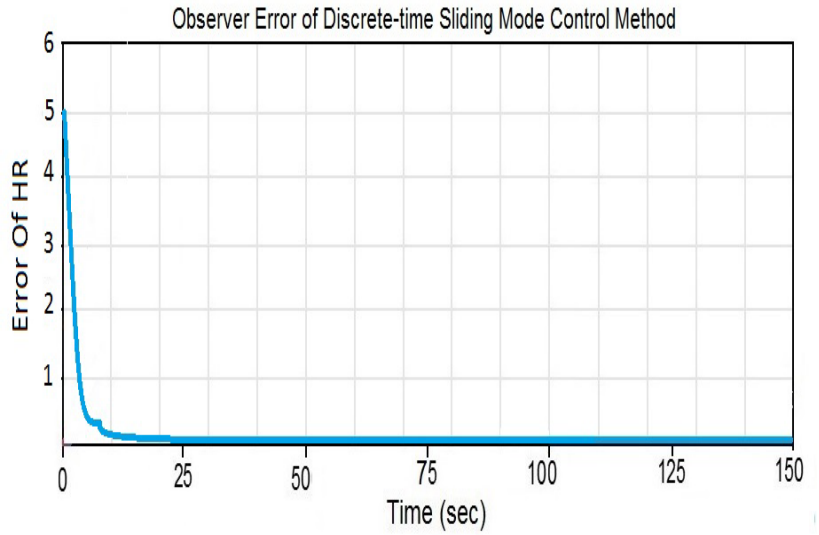

FIGURE 4.15: Observer estimation error of DTSMC

Figure 4.16 displays the observation error obtained by the state observer introduced in subection 4.4.3. This is the error between the actual state variable and the observed one. It is shown that it converges to zero asymptotically and monotonically while the control law enforces the perfect tracking of the reference.

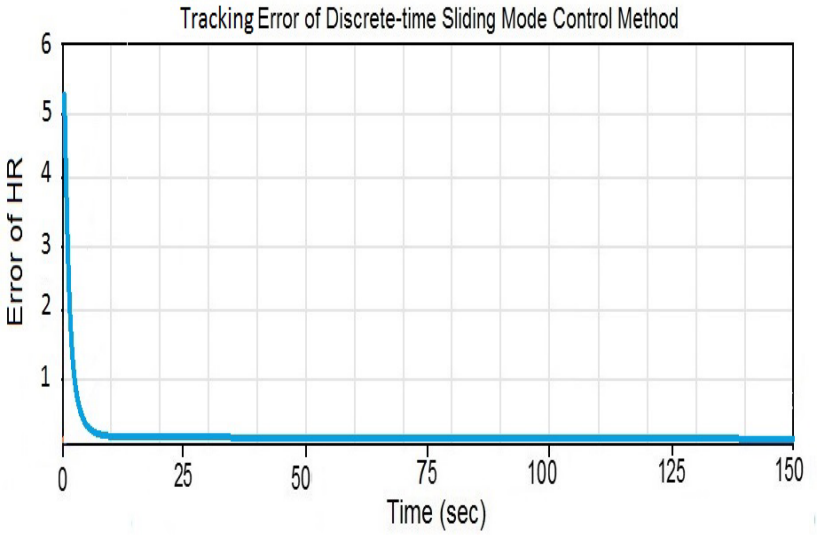

FIGURE 4.16: Tracking error of DTSMC

Regarding the comparation between discrete-time sliding mode control (DTSMC) and proportional–integral–derivative (PID), we are presenting 2 figures (4.17 and 4.18) that compare the performance between them.

In Fig.4.17 we are showing the heart rate provided by the DTSMC and PID controllers. Even though the PID controller has a quite good response, the DTSMC has a better response because it is closer to the reference signal.

Finally, 4.18 displays the tracking error comparison between our method (DTSMC) and PID controller. As it is clear, DTSMC is close to zero and after few seconds has a

better response compared to PID.

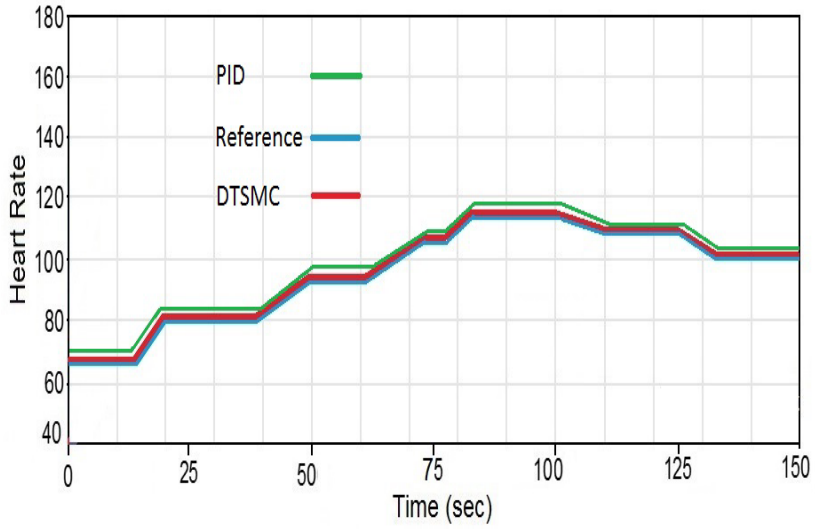

FIGURE 4.17: Comparing Heart rate provided by the DTSMC controller and PID

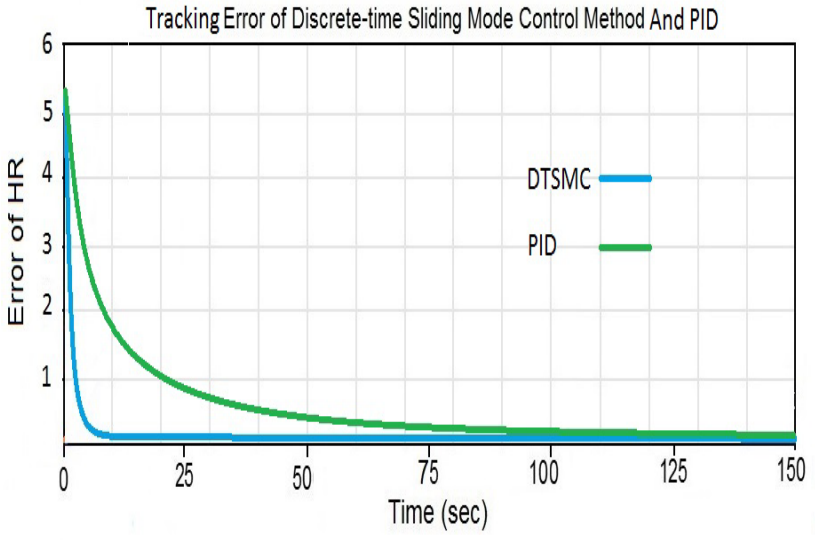

FIGURE 4.18: Comparing tracking error of DTSMC and PID

In the following Section, the nonlinear model will be present. This model has been designed for the first time to solve the difficulty and oscillation of the parameters that we had in our last results. In this method, we are using super-twisting sliding mode control and will be discretized. In this method, we will achieve a robust controller with avoiding the chattering and also having very good tacking results and without using any observer, which are the benefits of this model to compare it with the other models that we designed to reach to this model.

4.4.6 Nonlinear Model

The application of this control law is confronted with a serious problem. In fact, sliding mode necessitates an infinite switching frequency which is impossible to realize in practice because of the calculation time and of the sensors dynamics that can not be neglected, **[131][138]**.

Based on the available conditions, we employ a new strategy to develop a discrete-time Super-Twisting- algorithm (DSTA). Despite the successful development of the classical SMC, in the eighties, a new control technique, called super-twisting sliding mode control, have been investigated. Its main idea is to reduce to zero, not only the sliding function but also its high order derivatives.

This model has many benefits such as not using any observer. It also allows for avoiding any chattering and has a very good system design and great robustness compare to other models.

4.4.7 Discrete-time Super-twisting Sliding Mode Controller

The starting point is the nonlinear discrete model given in (4.5)-(4.7) reproduced here for convenience.

$$x_{1,k+1} = x_{1,k} + h\left(-a_1 x_{1,k} + a_2 x_{2,k} + a_6 w_k\right) \tag{4.101}$$
$$x_{2,k+1} = x_{2,k} + h\left(-a_3 x_{2,k} + a_4 x_{1,k}\phi(x_{1,k})\right) \tag{4.102}$$
$$y_k = \frac{1}{4}\left(x_{1,k} + HR0\right) \tag{4.103}$$

where $h > 0$ denotes the sampling period and $x_{1,k}$ and $x_{2,k}$ are the discrete state variables. The reference signal, $r(t)$, and output signal $y(t)$ are also sampled at the sampling rate h to provide the sampled signals $r_k = r(kh)$ and $y_k = y(kh)$.

The assumptions can be found in Section 4.2.1.

4.4.8 Control Design

Consider the following discrete-time reduced nonlinear system:

$$x_{k+1} = (1 - ha_1)x_k + ha_6 w_k + f_k \tag{4.104}$$

where $x = x_1$ and $x_k = x_{1,k}$, $u \in R$ is the control input and f represent the uncertainty and its continues.

This system is a simplification of the discrete-time system (4.101-4.102). When the whole model is reduced to just one equation representing HR. Thus, the system is reduced to a single-variable one and the remaining dynamics, given by the second state variable x_2, is considered as a perturbation on the system. In this way, a model is simplified to the price of increasing the amount of uncertainty of the model.

The discrete-time super-twisting algorithm is designed based on the approach of **[138]**.

Consider now the sliding surface given by:

$$S(k) = \quad r_k - x_k = S_k \tag{4.105}$$

Regarding the Eq. (4.103) and the sliding surface we have:

$$S_{k+1} = r_{k+1} - x_{k+1} = r_{k+1} - (1 - ha_1)x_k - ha_6 w_k - f_k \tag{4.106}$$

Eqs. (4.106) can be written as:

$$S_{k+1} = r_{k+1} - (1 - ha_1)x_k + (1 - ha_1)r_k - (1 - ha_1)r_k - ha_6 w_k - f_k \tag{4.107}$$

So that we have for the sliding surface:

$$S_{k+1} = (1 - ha_1)S_k + r_{k+1k} - (1 - ha_1)r_k - ha_6 w_k - f_k \tag{4.108}$$

In order to design the controller we make the definition:

$$V_k = r_{k+1k} - (1 - ha_1)r_k - ha_6 w_k \tag{4.109}$$

The control law is defined in terms of V_k as:

$$w_k = \frac{1}{ha_6}\left[r_{k+1} - (1 - ha_1)r_k - V_k\right] \tag{4.110}$$

According to **[138]**, the Controller can be processed as the following equations:

$$V_k = -k_1\phi_1(S_k) + \delta_k \tag{4.111}$$
$$\delta_{k+1} = \delta_k - k_2\phi_2(S_k) \tag{4.112}$$

Where

$$\phi_1(S_k) = |S_k|^{\frac{1}{2}} Sign(S_k) \tag{4.113}$$
$$\phi_2(S_k) = Sign(S_k) \tag{4.114}$$

It is important to mention that k_1 and k_2 are controller parameters and they are to be determinded, so as to obtain a good tracking response and robustness. Also $k_2 << k_1$, **[138]**.

In the end, we must bear in mind that we are working with the square of the control signal so that the actual speed command is given by:

$$u_k = \sqrt{Max(0, w_k)} \tag{4.115}$$

In the case of recovery and training programs, the controller is able to make the heart rate follow the predefined profile set up.

In the next section, the results and response of discrete sliding super-twisting sliding mode control based on the design performed in this Section are shown.

4.4.9 Results and Simulation

This Section contains some numerical simulation examples showing the results achieved by the proposed controller. The particular values for simulation, extracted from **[133]**, are the same as the values that we used in Section 4.2.6.

Figure 4.19 displays the response of the discrete super-twisting sliding mode controller and control signal of the treadmill HR based on the parameters of the model at the large range of treadmill speeds. In this case, it is also observed that the controller has been able to transfer the heart rate to a reference value without any overdrive for less than 10 seconds. Also, the control signal is applied quite smoothly. Therefore, the implementation of the controller in practice does not require a specific drive and implementation will be simple.

Figure 4.20 shows the treadmill speed of the controller without any chattering. On the other hand, Figure 4.21 shows the heart rate tracking error by using the discrete super-twisting sliding mode control time. As it can be seen, the error is decreasing and after few seconds and is close to zero.

Finally in Fig.4.22 the evaluation of the tracking errors between all the techniques that we used to this Chapter has been shown. As it is clear, the tracking error of the DTSTSMC has a very great response compared with the other techniques and it proves that the discrete-time super-twisting sliding mode control is the best controller with these comparisons. Eventually, Fig 4.23 shows the zoom of the evaluation tracking errors of all techniques to present better the more details.

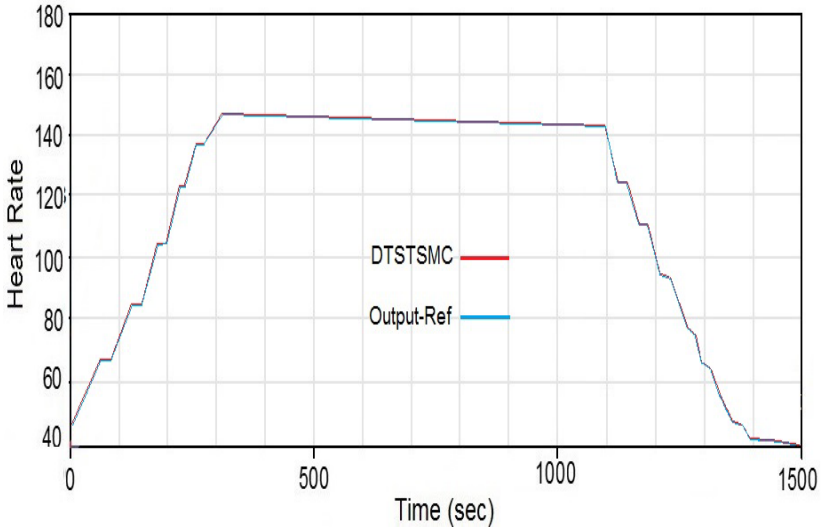

FIGURE 4.19: Heart rate provided by the DTSTSMC controller.

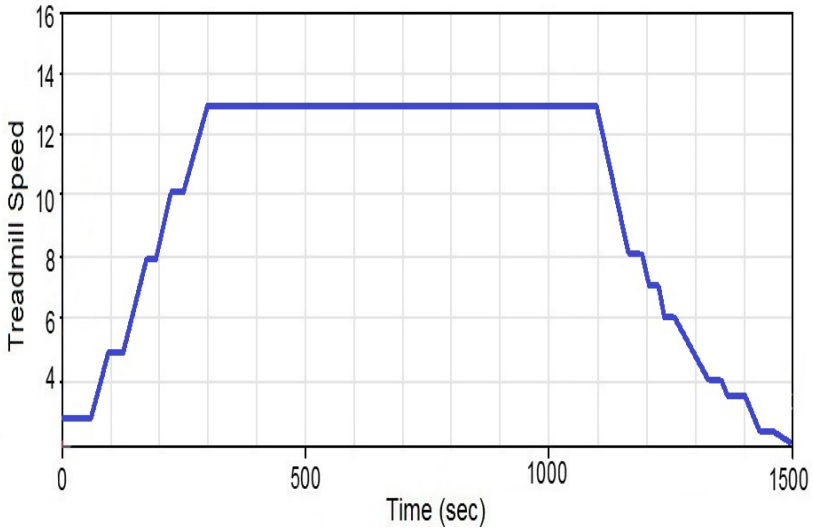

FIGURE 4.20: Speed provided by the DTSTSMC controller.

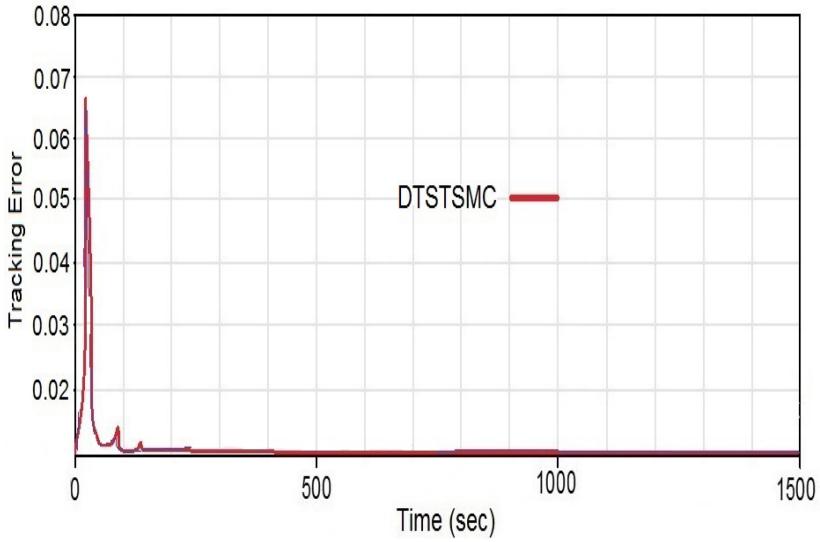

FIGURE 4.21: Tracking error of DTSTSMC.

4.4.10 Conclusion

The aim of this work is to design a discrete-time robust controller for the heart rate during treadmill exercise. In the first Section of this Chapter, we tried to design a feedback-linearization which is a very good strategy to design a controller but we faced into the not good robustness response in the result. Thus, for solving this problem we used Joint parameter-state estimation that has a good response. On the other hand in this controller, we reached to the complexity of this algorithm and problem of the estimation process that we had in this algorithm. Although, regarding the stability of the system and good respond that we got from designing the super-twisting SMC in Chapter 3, we decided to use this technique and discretize it as a new model to solve the previous problems.

Eventually, we used the super-twisting sliding mode controller and discretized it. The previous problems were solved and the system has also very good results as you can see in the last section of Chapter 4. The benefits of this system are such as robust discrete-time controller without chattering and the stability of the system is great. Also, it has a very systematic design and it did not need to use an observer.

It is important to note that, the material of this Chapter contained with 3 published IEEE conference paper, **[88]**[**132**][**133**] and one journal paper which is under process.

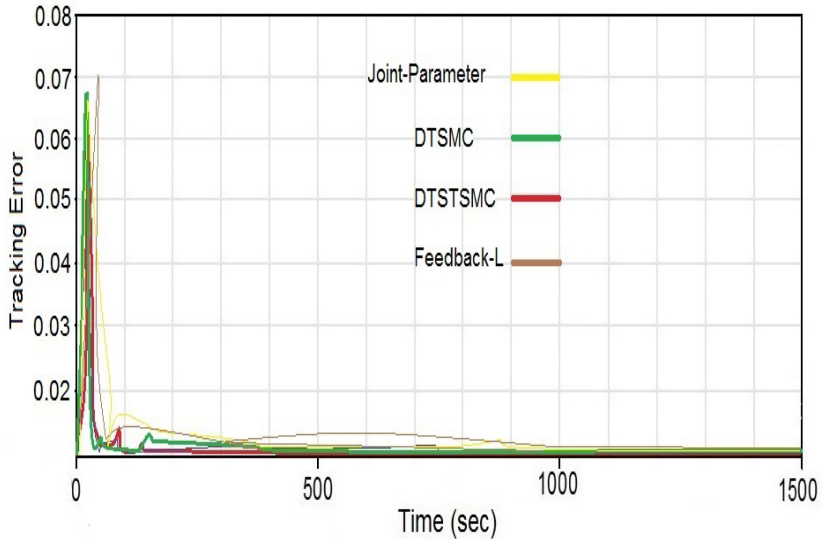

FIGURE 4.22: Evaluation of the Tracking errors of DTSTSMC, DTSMC, Joint-parameter and Feedback-Linearization.

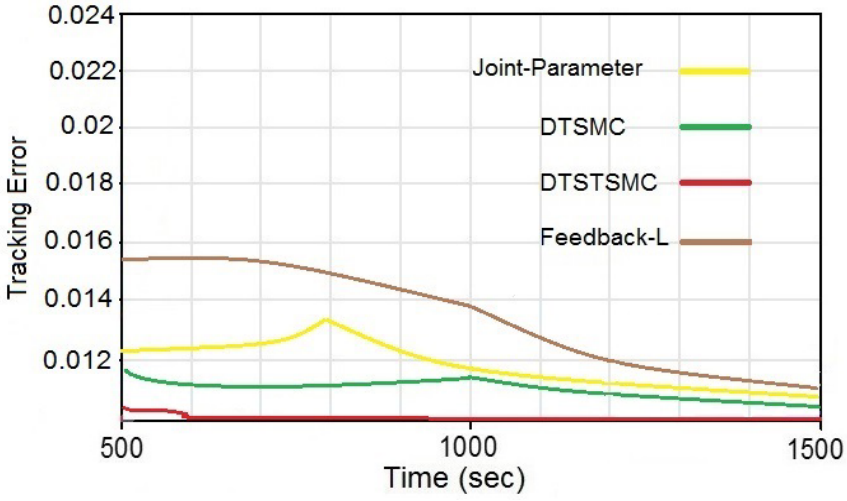

FIGURE 4.23: Zoom evaluation of the Tracking errors of DTSTSMC, DTSMC, Joint-parameter and Feedback-Linearization.

Chapter 5

Conclusions

Cardiac Rehabilitation has proven to be an effective tool in the recovery of cardiac patients and it has been shown that is not very widespread in the world.

In order to mitigate this issue, a system consisting of a treadmill is designed. The main component is the speed controller that is used between 2-14 km/h in this work. In order to complete the system, we need a model and a controller.

Chapter 2 of this work considered the parameter estimation problem formulated as an optimization one and solved by using Particle Swarm Optimization (PSO). This algorithm is used for the first time in this field. Numerical examples showed that the estimation procedure is able to obtain accurate values for the system's parameters and the achieved results and comparisons showed improvement with respect to other estimation methods.

In Chapter 3 the design of the controller has been done. The super twisting sliding mode control is used for the design of the controller. A super-twisting sliding mode controller is designed to perform the robust control of treadmill's speed in the presence of potential unmodelled dynamics of parametric uncertainties. The proposed control approach is able to obtain zero tracking error without chattering, definitely achieving the control objectives.

In the first section of Chapter 4 a feedback- linearization based control for the heart rate during treadmill exercise is designed. The set-up of the problem in discrete-time allows taking into consideration the effect of sampling during the controller design procedure instead of relegating it to the implementation stage. The control command requires the values of the parameters of the model along with the states. Thus, at this point parameters are assumed to be known and the state observer is designed for the unmeasurable-state.

It is shown that a linear state feedback controller is enough to make the nonlinear model's output track the reference profile regardless of its possibly complex time variation when the model parameters are known. However, the controller lacks of the robustness when there exists a mismatch between the nominal parameters and the actual ones.

Thus, the next section of this chapter (Section 4.3) a joint parameter-state estimation algorithm is designed to provide the values of the parameters and unmeasurable states to the control law. The use of this algorithm allows obtaining asymptotic perfect tracking in the presence of uncertainty in the model's parameters. Moreover, the identification of the parameters might allow monitoring the evolution of the coronary condition of the patients. However, the algorithm is not able to identify the actual values of the system's parameters and the output exhibits certain oscillation, that may be undesirable. The complexity of the algorithm, the lack of the identification of the parameters, the pursume of the oscillation and the great response the parameters and great response of the super-twisting controller in Chapter 3, made us make a decision to imply a new method to solve these problems.

In the last Section of Chapter 4 a discrete sliding mode system is tackled. We start by linearization SMC. The linear model is then discretized by using a Zero-Order Hold (ZOH) in order to obtain a discrete-time model. This discrete-time model is then used to design a sliding mode controller. Anyhow, the full state is not available for measurement and a reduced-order disturbance observer is incorporated into the discrete-time control law. Then, the continuous control command is generated by using a zero-order hold (ZOH). Simulation results presented that the designed controller is able to make the runner's heart rate follow the prescribed profile irrespective of the uncertainties in the model.

For the last part of the work a discrete-time, super-twisting sliding mode control is used and it is extended to the nonlinear case. This controller is designed for the first time and solves the difficulty of the oscillation of the outputs and chattering. The results such as reference tracking and tracking error that we achieved have a great response. Furthermore, simulation examples showed that the designed controller covered a wide range of speeds and results that are presented in this range are not usually employed in previous studies for heart rate control. The nonlinear system offered a great tracking property, an avoidance of state observer, no chattering, systematic design and robustness.

Eventually, with all of these reasons and improvements, we can say that this approach is the best one to solve all of these problems.

5.1 Future View

The work also has a great opportunity to be expanded in several ways. From the theoretical point of view, it has opened the door to the design of joint state-parameter estimators and to the mathematical demonstration of stability of the proposed schemes. From a practical point of view, the work can be extended with the implementation of the system on a real treadmill as well as the verification of the results obtained by simulation with real test subjects. I believe that the system developed contributes to the improvement of health care services for those patients who have suffered some heart disease and the system presented has a high application in real life. On the other hand, it is interesting to develop it as large system that it mentioned in the first Chapter. Developing the controller for conecting with other parts of the whole project.

Publications

1 **Ali Esmaeili**, Asier Ibeas, Jorge Herrera and Nazila Esmaeili. Identification and Robust Control of Heart Rate During Treadmill Exercise at Large Speed Ranges, Control Engineering and Applied Informatics Journal, CEAI, Vol.21, No. 1, pp. 51-60, 2019.

2 **Ali Esmaeili**, Asier Ibeas. Super-twisting Discrete-time Sliding Mode Control Technique to Control the Heart Rate in Treadmill Exercise, Journal paper in preparation.

3 **Ali Esmaeili**, Asier Ibeas. Discrete-time sliding mode control of heart rate during treadmill exercise, 24th IEEE Conference on Emerging Technologies and Factory Automation,Zaragoza, Spain, September 10th - 13th, 2019.

4 **Ali Esmaeili**, Asier Ibeas, Salim Ibrir and Pedro Balaguer. Joint Parameter-State Estimation-Based Control of Heart Rate During Treadmill Exercise, 24th IEEE Conference on Emerging Technologies and Factory Automation, Zaragoza, Spain, September 10th - 13th, 2019.

5 **Ali Esmaeili**, Asier Ibeas. Particle Swarm Optimization Modelling of the Heart Rate Response in Treadmill Exercise, IEEE ICSTCC Control system Conference 2016, Romania.

6 Asier Ibeas, **Ali Esmaeili**, Jorge Aurelio Herrera and Farouk Zouari. Discrete-Time Observer-Based State Feedback Control of Heart Rate During Treadmill Exercise, IEEE ICSTCC Control System Conference 2016, Romania.

7 Clement Girard, Asier Ibeas, Ramon Vilanova, **Ali Esmaeili**. Robust discrete-time linear control of heart rate during treadmill exercise, 24th Iranian Conference on Electrical Engineering (ICEE), 2016, Iran.

Bibliography

[1] Judith A. Finegold, Perviz Asaria, Darrel P. Francis, Mortality from ischaemic heart disease by country, region, and age: Statistics from World Health Organisation and United Nations, International Journal of Cardiology, vol. 168, pp. 934–945, 2013.

[2] J.M. Maroto R. Artigao, M.D. Morales, C. de Pablo and V. Abraira, Cardiac rehabilitation in patients with myocardial infarction. Results after 10 years of follow-up, Rev. Esp. De Cardiología, vol. 58, no.10, pp. 1181-7, 2005.

[3] Working Group of Cardiac Rehabilitation of the Spanish Society of Cardiology. Rehabilitation of the coronary patient. Secondary Prevention Rev Esp Cardiol, vol. 48, pp. 643-9, 1995.

[4] D. Nesic, A.R. Teel, Sampled-data control of nonlinear systems: an overview of recent results, in R.S.O. Moheimani (Ed.). Perspectives on robust Control, Springer-Verlag, New York, pp. 221-239, 2001.

[5] Soledad Márquez-Calderón, Román Villegas Portero, Eduardo Briones Pérez de la Blanca, Víctor Sarmiento González-Nieto, Margarita Reina Sánchez, Ignacio Sáinz Hidalgo, José A. Velasco Rami and Francisco Ridocci Soriano, Implementation and characteristics of cardiac rehabilitation programs in the Spanish National Health System, Rev Esp Cardiol, vol. 56, no. 8, pp. 775-82, 2003.

[6] NHS Centre for Reviews and Dissemination University of York. Cardiac rehabilitation. Eff Health Care, vol. 4, pp. 1-12, 1998.

[7] Euan Ashley, Josef Niebauer, Cardiology Explained, Ed. Remedica, 2004.

[8] Alberto Grima-Serrano, Esteban García-Porrero, Emilio Luengo-Fernández y Montserrat León Latre, Cardiología preventiva y rehabilitación cardíaca, Rev Esp Cardiol, vol. 64(Supl 1), pp. 66-72, 2011.

[9] Suaya JA, Stason WB, Ades PA, Normand SL, Shepard DS. Cardiac rehabilitation and survival in older coronary patients. J Am Coll Cardiol., 54:25-33, 2009.

[10] Hammill BG, Curtis LH, Schulman KA, Whellan DJ. Relationship between cardiac rehabilitation and long-term risks of death and myocardial infarction among elderly Medicare beneficiaries, Circulation, 121:63-70, 2010.

[11] Dalal HM, Zawada A, Jolly K, Moxham T, Taylor RS. Home based versus centre based cardiac rehabilitation: Cochrane systematic review and meta-analysis. BMJ, 340:b5631, 2010.

[12] Clark AM. Home based cardiac rehabilitation. BMJ, 340:b5510, 2010.

[13] Cortes-Bergoderi, M. et al., Availability and Characteristics of Cardiovascular Rehabilitation Programs in South America, Journal of Cardiopulmonary Rehabilitation Prevention, Volume 33 - Issue 1 - p 33–41, 2013.

[14] Yoel Korenfeld et al., Current status of cardiac rehabilitation in Latin America and the Caribbean, American Heart J., 158(3):480-7, 2009.

[15] Vanhees L, McGee HM, Dugmore LD, Vuori I, Pentilla UR, on behalf of the Carinex Group. The Carinex Survey. Current guidelines and practices in cardiac rehabilitation within Europe. Leuven: Uitgeverij Acco, 1999.

[16] Thompson DR, Bowman GS, Kitson AL, de Bono DP, Hopkins A. Cardiac rehabilitation services in England and Wales: a national survey. Int J Cardiol, 59:299-304, 1997.

[17] The heart Manual, NHS Lothian, http://www.theheartmanual.com/Pages /default.aspx, Fecha consulta, 2 de Febrero de 2015.

[18] Su, S.W., S. Huang ; L. Wang ; Celler, B.G. ; Savkin, A.V. ; Ying Guo ; Cheng, T., Nonparametric Hammerstein Model Based Model Predictive Control for Heart Rate Regulation, 29th Annual International Conference of the IEEE Engineering in Medicine and Biology Society, 2007, pp. 2984 – 2987, 2007.

[19] Cheng, TM, Savkin, AV, Celler, BG, Su, SW, Wang, L, Nonlinear Modeling and Control of Human Heart Rate Response During Exercise With Various Work Load Intensities, IEEE transactions on biomedical engineering Volume: 55 Issue: 11 Pages: 2499-2508 Published: NOV 2008.

[20] Cheng, TM, Savkin, AV, Celler, BG, Su, SW, Wang, L, Nonlinear modelling and control of heart rate response to treadmill walking exercise Edited by: Encarnacao, P; Veloso, A, Conference: 1st International Conference on Bio-Inspired Systems and Signal Processing Location: Funchal, PORTUGAL Date: JAN 28-31, 2008

[21] Cheng, TM, Savkin, AV, Celler, BG, Su, SW, Wang, L, A robust control design for heart rate tracking during exercise. Annual International Conference of the IEEE Engineering in Medicine and Biology Society. IEEE Engineering in Medicine and Biology Society. Annual Conference Volume: 2008 Pages: 2785-2788 Published: 2008

[22] R. A. Cooper , T. L. Fletcher-Shaw and R. N. Robertson, Model reference adaptive control of heart rate during wheel chair ergometry, IEEE Trans. on Control Systems Technology, vol. 6, no. 4, pp. 507- 514, 1998.

[23] S. Scalzi, P. Tomei, C.M. Verrelli, Nonlinear control techniques for the heart rate regulation in treadmill exercises, IEEE Trans. on Biomedical Engineering, vol. 59, no. 3, pp. 599- 603, 2012.

[24] S. W. Su, L. Wang, B.G. Celler, A.V. Savkin and Y. Guo, Identification and control for heart rate regulation during treadmill exercise, IEEE Trans. on Biomedical Engineering, vol. 54, no. 7, pp. 1238-1246, 2007.

[25] F. Mazenc, M. Malisoff and M. de Queiroz, Tracking control and robustness analysis for a nonlinear model of human heart rate during exercise, Automatica, vol. 47, pp. 968-974, 2011.

[26] M. Paradiso, S. Pietrosanti, S. Scalzi, P. Tomei and C. M. Verrelli, Experimental heart rate regulation in cycle-ergometer exercises, IEEE Trans. on Biomedial Engineering, vol. 60, no. 1, pp. 135-139, 2013.

[27] S. W. Wu, S. Huang, L. Wang, B. G. Celler, A.V. Savkin, Y. Guo and T. M. Cheng, Optimizing heart rate regulation for safe exercise, Annals of Biomedical Engineering, vol. 38, no. 3, pp. 758-768, 2010.

[28] Y. Zhang, K. T. Chong, N. Kazatzis and A. G. Parlos, Discretization of nonlinear input-driven dynamical systems using the Adomian decomposition method, Applied Mathematical Modelling, vol. 36, pp. 5856-5875, 2012.

[29] R. Vilanova, IMC based Robust PID design: Tuning guidelines and automatic tuning, J. of Process Control, vol. 18 no. 1, pp. 61-70, 2008.

[30] S Alcántara, WD Zhang, C Pedret, R Vilanova, S Skogestad, IMC-like analytical design with S/SP mixed sensitivity consideration: Utility in PID tuning guidance, Journal of Process Control vol. 21, no.6, pp. 976-985, 2011.

[31] VM Alfaro, R Vilanova, O Arrieta, Robust tuning of two-degree-of-freedom (2-DoF) PI/PID based cascade control systems, Journal of Process Control, vol. 19, no. 10, pp. 1658-1670, 2009.

[32] A. Ibeas, M. de la Sen and S. Alonso-Quesada, Robust sliding control of SEIR epidemic models, Mathematical Problems in Engineering, Article ID 104764, 11 pages, 2014.

[33] Stefanovic, Margareta, Safonov, Michael G., Safe adaptive control, Springer-Verlag, 2011.

[34] Esmaeili A., Ibeas A., Herrera J and Esmaeili N., Identification and Robust Control of Heart Rate During Treadmill Exercise at Large Speed Ranges, J. of Control Engineering and Applied Informatics, vol. 21, no. 1, pp.51-60, 2019.

[35] M. Ishitobi and M. Nishi, Sample-Data models for nonlinear Systems with a Fractional-Order Hold, 18th IEEE Int. Conf. on Control Applications, Saint Petersburg, Russia, July 8-10, 2009.

[36] JI Yuz, GC Goodwin, On sampled-data models for nonlinear systems, IEEE Transactions on Automatic Control vol. 50, no. 10, pp. 1477-1489, 2005.

[37] JI Yuz and G. C. Goodwin, Sampled-Data Models for Linear and Nonlinear Systems, Springer-Verlag, Berlin, 2014.

[38] C. D. Mathers, D. Loncar, Updated projections of global mortality and burden of disease, 2002-2030: Data sources, methods and results, World Health Organization, October, 2005.

[39] David J. Cook, Jeffrey E. Thompson, Sharon K. Prinsen, Joseph A. Dearani, Claude Deschamps, Functional Recovery in the Elderly After Major Surgery: Assessment of Mobility Recovery Using Wireless Technology, Ann Thorac Surg, vol. 96, pp. 1057–61, 2013.

[40] Ariel Diaz, Martial G. Bourassa, Marie-Claude Guertin and Jean-Claude Tardif, Long-term prognostic value of resting heart rate in patients with suspected or proven coronary artery disease, European Heart Journal, vol. 26, pp. 967–974, 2005.

[41] Guido Parodi, Benedetta Bellandi, Renato Valenti, Gentian Memisha, Gabriele Giuliani, Silvia Velluzzi, Angela Migliorini, Nazario Carrabba, David Antoniucci, Heart rate as an independent prognostic risk factor in patients with acute myocardial infarction undergoing primary percutaneous coronary intervention, Atherosclerosis, vol. 211, pp. 255–259, 2010.

[42] Jabre P, Roger VL, Weston SA, Adnet F, Jiang R, Vivien B, Empana JP, Jouven X, Resting heart rate in first year survivors of myocardial infarction and long-term mortality: a community study, Mayo Clin Proc, vol. 89, no. 12, pp. 1655-63, 2014.

[43] Hunt, Kenneth J., and Simon E. Fankhauser. "Heart rate control during treadmill exercise using input-sensitivity shaping for disturbance rejection of very-low-frequency heart rate variability." Biomedical Signal Processing and Control 30 (2016): 31-42.

[44] Weippert, M., Behrens, M., Rieger, A., Behrens, K. Sample entropy and traditional measures of heart rate dynamics reveal different modes of cardiovascular control during low intensity exercise,(2014). Entropy, 16(11), 5698-5711.

[45] Cheng TM, Savkin AV, Celler BG, Su SW, Wang L. Heart rate regulation during exercise with various loads: identification and nonlinear H infinity control. InIFAC World Congress 2008. 2008 IFAC.

[46] Yan, X., Wu, Q., Liu, H., Huang, W. (2013). An improved particle swarm optimization algorithm and its application. International Journal of Computer Science Issues (IJCSI), 10(1), 316.

[47] Jang, D. G., Ko, B. H., Sunoo, S., Nam, S. S., Park, H. Y., Bae, S. K. (2016, August). A preliminary study of a running speed based heart rate prediction during an incremental treadmill exercise. In Engineering in Medicine and Biology Society (EMBC), 2016 IEEE 38th Annual International Conference of the (pp. 5323-5326). IEEE.

[48] Zhang, Yudong, and Lenan Wu. "Crop classification by forward neural network with adaptive chaotic particle swarm optimization." Sensors 11.5 (2011): 4721-4743.

[49] Tian, Xiaomin, and Shumin Fei. "Robust control of a class of uncertain fractional-order chaotic systems with input nonlinearity via an adaptive sliding mode technique." Entropy 16.2 (2014): 729-746.

[50] Peter J. Huber, Robust Estimation of a Location Parameter , The Annals of Mathematical Statistics, Vol. 35, No. 1. (Mar., 1964), pp.73-101.

[51] Maronna, R.A. (1976). Robust M-estimators of Multivariate Location and Scatter, The Annals o Statistics 4, 51-67.

[52] Rini DP, Shamsuddin SM, Yuhaniz SS. Particle swarm optimization: Lari A, Khosravi A, Rajabi F. Controller design based on μ analysis and PSO algorithm. ISA transactions. 2014 Mar 31;53(2):517-23.

[53] Liu, W., Liu, L., Chung, I. Y., and Cartes, D. A. (2011). Real-time particle swarm optimization based parameter identification applied to permanent magnet synchronous machine. Applied Soft Computing, 11(2), 2556-2564.

[54] Bansal, J. C., Singh, P. K., Saraswat, M., Verma, A., Jadon, S. S., and Abraham. "Inertia weight strategies in particle swarm optimization." Nature and Biologically Inspired Computing (NaBIC),IEEE, 2011. 2011 Third World Congress on.

[55] Eswaran, T., and V. Suresh Kumar. "Particle swarm optimization (PSO)-based tuning technique for PI controller for management of a distributed static synchronous compensator (DSTATCOM) for improved dynamic response and power quality." Journal of Applied Research and Technology 15.2 (2017): 173-189.

[56] Hamed, E., Anushya, A., Alzoubi, R., and Vincy, B. A. (2017, August). An analysis of particle swarm optimization for feature selection on medical data. In 2017 International Conference on Energy, Communication, Data Analytics and Soft Computing (ICECDS) (pp. 227-231). IEEE.

[57] Ebrahimi, N., Ozgoli, S., and Ramezani, A. (2018). Model-free sliding mode control, theory and application. Proceedings of the Institution of Mechanical Engineers, Part I: Journal of Systems and Control Engineering, 0959651818780597.

[58] Meyer, Daniel, and Veit Senner. "Evaluating a heart rate regulation system for human–electric hybrid vehicles." Proceedings of the Institution of Mechanical Engineers, Part P: Journal of Sports Engineering and Technology 232, no. 2 (2018): 102-111.

[59] Shtessel, Yuri B. Super-twisting adaptive sliding mode control: A Lyapunov design. In: Decision and Control (CDC), 2010 49th IEEE Conference on IEEE, 2010. p. 5109-5113.

[60] Shtessel, Yuri B., Jaime A. Moreno, and Leonid M. Fridman. Twisting sliding mode control with adaptation: Lyapunov design, methodology and application. Automatica 75 (2017): 229-235.

[61] GAO, Xuehui. Variable gain super-twisting sliding mode control for Hammerstein system with Bouc-Wen hysteresis nonlinearity. In: Control Conference (CCC), 2016 35th Chinese. IEEE, 2016. p. 3369-3372.

[62] Kranjec, Beguš, Geršak , Drnovšek. "Non-contact heart rate and heart rate variability measurements: A review." Biomedical Signal Processing and Control 13 (2014): 102-112.

[63] Lu, C. H., Wang, W. C., Tai, C. C., and Chen, T. C. (2016). Design of a heart rate controller for treadmill exercise using a recurrent fuzzy neural network. Computer methods and programs in biomedicine, 128, 27-39.

[64] Abu-Rmileh, A., Garcia-Gabin, W., and Zambrano, D. (2010). Internal model sliding mode control approach for glucose regulation in type 1 diabetes. Biomedical Signal Processing and Control, 5(2), 94-102.

[65] Anselmino, M., Scarsoglio, S., Saglietto, A., Gaita, F., and Ridolfi, L. "A computational study on the relation between resting heart rate and atrial fibrillation hemodynamics under exercise." PloS one 12.1 (2017): e0169967.

[66] Yuan. B, Gallagher. M, (2003), Playing in Continuous Spaces: Some Analysis and Extension of Population-Based Incremental Learning, IEEE Evolutionary Computation, vol: 1, pp: 443-450.

[67] Swikir, Abdalla, and Vadim Utkin. "Chattering analysis of conventional and super twisting sliding mode control algorithm." Variable Structure Systems (VSS), 2016 14th International Workshop on. IEEE, 2016.

[68] Wang, X., Wang, S., and Ma, J. J. (2007). An improved co-evolutionary particle swarm optimization for wireless sensor networks with dynamic deployment. Sensors, 7(3), 354-370.

[69] Argha, A., Su, S. W., and Celler, B. G. (2017). Heart rate regulation during cycle-ergometer exercise via event-driven biofeedback. Medical and biological engineering and computing, 55(3), 483-492.

[70] Vaidyanathan, Sundarapandian. "Super-Twisting Sliding Mode Control of the Enzymes-Substrates Biological Chaotic System." Applications of Sliding Mode Control in Science and Engineering. Springer International Publishing, 2017. 435-450.

[71] Dan, A. M., and Dragomir, T. L. (2012, May). A model of the control function in the case of constant effort of the cardiovascular system. In Applied Computational Intelligence and Informatics (SACI), 2012 7th IEEE International Symposium on (pp. 169-173). IEEE.

[72] Belkaid, A., Gaubert, J. P., and Gherbi, A. (2016). An improved sliding mode control for maximum power point tracking in photovoltaic systems. Journal of Control Engineering and Applied Informatics, 18(1), 86-94.

[73] Xue, B., Zhang, M., and Browne, W. N. (2013). Particle swarm optimization for feature selection in classification: A multi-objective approach. IEEE transactions on Cybernetics, 43(6), 1656-1671.

[74] Suganthan PN (1999) Particle swarm optimizer with neighborhood operator. In: Proceedings of the IEEE congress on evolutionary computation, Washington, DC, pp 1958–1961

[75] Yang, H., Xu, Y., Peng, G., Yu, G., Chen, M., Duan, W., and Wang, X. (2017). Particle swarm optimization and its application to seismic inversion of igneous rocks. International Journal of Mining Science and Technology, 27(2), 349-357.

[76] Paul, Arun K., J. E. Mishra, and M. G. Radke. "Reduced order sliding mode control for pneumatic actuator." IEEE Transactions on Control Systems Technology 2, no. 3 (1994): 271-276.

[77] Guo, H., Liu, Y., Liu, G., and Li, H. (2008). Cascade control of a hydraulically driven 6-DOF parallel robot manipulator based on a sliding mode. Control Engineering Practice, 16(9), 1055-1068.

[78] B. Pavy, M-C. Iliou, B. Vergès-Patois, R. Brion, C. Monpère, F. Carré et al., "French Society of Cardiology guidelines for cardiac rehabilitation in adults,", Archives of Cardiovascular Diseases, vol. 105, no. 5, pp. 309-328, May 2012.

[79] M. Hajek, J. Potucek, and V. Brodan, "Mathematical model of heart rate regulation during exercise," Automatica, vol. 16, pp. 191-195, 1980. 2007.

[80] S. W. Su, S. Huang, L. Wang, B. G. Celler, A. V. Savkin, Y. Guo and T. Cheng, "Nonparametric Hammerstein Model Based Model Predictive Control for Heart Rate Regulation" Proc. of the 29^{th} Annual Int. Conf. of the IEEE EMBS, pp. 2984-2987, Lyon, France, August 23-26, 2007.

[81] E. F. Coyle and G. Alonso, "Cardiovascular drift during prolonged exercise: New perspectives", Exerc. Sport Sci. Rev. vol. 29, pp. 88-92, 2001.

[82] S. S. Sastry, Nonlinear systems: Analysis, Stability and Control, Springer-Verlag, 1999.

[83] World Health Organization, url: https://www.who.int/news-room/fact-sheets/detail/the-top-10-causes-of-death, date of access, March 13, 2019.

[84] B. Pavy, M-C. Iliou, B. Vergès-Patois, R. Brion, C. Monpere, F. Carre et al., "French Society of Cardiology guidelines for cardiac rehabilitation in adults", Archives of Cardiovascular Diseases, vol. 105, no. 5, pp. 309-328, May 2012.

[85] Corno, M., Giani, P., Tanelli, M. and Savaresi, S.M., 2015. Human-in-the-loop bicycle control via active heart rate regulation. IEEE Transactions on Control Systems Technology, 23(3), pp.1029-1040.

[86] Argha, A., Su, S.W., Nguyen, H. and Celler, B.G., 2015, August. Designing adaptive integral sliding mode control for heart rate regulation during cycle-ergometer exercise using bio-feedback. In Engineering in Medicine and Biology Society (EMBC), 2015 37th Annual International Conference of the IEEE (pp. 6688-6691). IEEE.

[87] Girard, C., Ibeas, A., Vilanova, R., and Esmaeili, A. (2016, May). Robust discrete-time linear control of heart rate during treadmill exercise. In Electrical Engineering (ICEE), 2016 24th Iranian Conference on (pp. 1113-1118). IEEE.

[88] Esmaeili, A., and Ibeas, A. . Particle Swarm Optimization modelling of the heart rate response in treadmill exercise. In System Theory, Control and Computing (ICSTCC), 2016 20th International Conference on (pp. 613-618). IEEE.

[89] Ibeas, A., Esmaeili, A., Herrera, J., and Zouari, F. (2016, October). Discrete-time observer-based state feedback control of heart rate during treadmill exercise. In System Theory, Control and Computing (ICSTCC), 2016 20th International Conference on (pp. 537-542). IEEE.

[90] Maroto J, De Pablo C, Artigao R, Morales M. Rehabilitación cardíaca. Barcelona: Olalla Ediciones, 1999.

[91] Ibrir S., Joint state and parameter estimation of non-linearly parameterized discrete-time nonlinear systems, Automatica, vol. 97, pp. 226-233, 2018.

[92] M. Farza, M. M'Saad, T. Maatoug and M. Kamoun, Adaptive observers for nonlinearly parameterized class of nonlinear systems, Automatica, vol. 45, pp. 2292-2299, 2009.

[93] M. Farza, M. M'Saad, T. Menard, A. Ltaief and T. Maatoug, Adaptive observer design for a class of nonlinear systems. Application to speed sensorless induction motor, Automatica, vol. 90, pp. 239-247, 2018.

[94] Abidi, K., Xu, J.X. and Xinghuo, Y., 2007. On the discrete-time integral sliding-mode control. IEEE Transactions on Automatic Control, 52(4), pp.709-715.

[95] Argha, A., Li, L. and Su, S.W., 2018. -based optimal sparse sliding mode control for networked control systems. International Journal of Robust and Nonlinear Control, 28(1), pp.16-30.

[96] Nguyen, T.N., Su, S., Celler, B. and Nguyen, H., 2014. Advanced portable remote monitoring system for the regulation of treadmill running exercises. Artificial intelligence in medicine, 61(2), pp.119-126.

[97] Jung, S.L. and Tzou, Y.Y., 1993, June. Sliding mode control of a closed-loop regulated PWM inverter under large load variations. In Power Electronics Specialists Conference, 1993. PESC'93 Record., 24th Annual IEEE (pp. 616-622). IEEE.

[98] Argha, A., Li, L., Su, S.W. and Nguyen, H., 2015, December. Robust output-feedback discrete-time sliding mode control utilizing disturbance observer. In Decision and Control (CDC), 2015 IEEE 54th Annual Conference on (pp. 5671-5676). IEEE.

[99] Pai, M.C., 2009. Robust tracking and model following of uncertain dynamic systems via discrete-time integral sliding mode control. International Journal of Control, Automation and Systems, 7(3), pp.381-387.

[100] Bhattacharyya, S.P., Keel, L.H. and Datta, A., 2009. Linear control theory: structure, robustness, and optimization. CRC press.

[101] Ren, Y., Liu, Z., Liu, X. and Zhang, Y., 2013. A chattering free discrete-time global sliding mode controller for optoelectronic tracking system. Mathematical Problems in Engineering, 2013.

[102] Du, H., Yu, X., Chen, M.Z. and Li, S., 2016. Chattering-free discrete-time sliding mode control. Automatica, 68, pp.87-91.

[103] Corno, M., Giani, P., Tanelli, M. and Savaresi, S.M., 2015. Human-in-the-loop bicycle control via active heart rate regulation. IEEE Transactions on Control Systems Technology, 23(3), pp.1029-1040.

[104] Argha, A., Su, S.W., Nguyen, H. and Celler, B.G., 2015, August. Designing adaptive integral sliding mode control for heart rate regulation during cycle-ergometer exercise using bio-feedback. In Engineering in Medicine and Biology Society (EMBC), 2015 37th Annual International Conference of the IEEE (pp. 6688-6691). IEEE.

[105] Wang, Honghai, Jianchang Liu, Xia Yu, Shubin Tan, and Yu Zhang. "New Results on PID Controller Design of Discrete-time Systems via Pole Placement." IFAC-PapersOnLine 50, no. 1 (2017): 6703-6708.

[106] Mizumoto, Ikuro, Daisuke Ikeda, Tadashi Hirahata, and Zenta Iwai. "Design of discrete time adaptive PID control systems with parallel feedforward compensator." Control Engineering Practice 18, no. 2 (2010), 168-176.

[107] P. Calabrese, A note on alternating series, Amer. Math. Monthly 69 (1962) 215–217.

[108] R. Johnsonbaugh, Summing an alternating series, Amer. Math. Monthly 86 (1979) 637–648.

[109] R. M. Young, The error in alternating series, Mathl. Gazette 69 (1985) 120–121.

[110] Utkin V. Sliding modes in control and optimization. Berlin: Springer-Verlag; 1992.

[111] Utkin V, Guldner J, Shi J. Sliding mode control in electro-mechanical systems. Autom. and control Eng. series. CRC Press; 2009 ISBN–13: 978-1420065602.

[112] Levant A. Sliding order and sliding accuracy in sliding mode control. Int J Control 1993;58(6):1247–63.

[113] Devant A. Principles of 2-sliding mode design. Automatica 2007;43(4):576–86.

[114] Drakunov SV, Utkin V. On discrete-time sliding mode. In: Proceedings of the IFAC symposium on nonlinear control systems design; 1989. p. 484–9.

[115] Miloslavjevic C. General conditions for the existence of a quasi-sliding mode on the sqitching hyperplane in discrete variable structure systems. Autom Remote Control 1985;46:679–84.

[116] Sira-Ramirez H. Nonlinear discrete variable structure systems in quasi-sliding mode. Int J Control 1991;54(5):1171–87.

[117] Bartoszewicz A. Discrete-time quasi-sliding mode control strategies. IEEE Transactions on Industrial Electronics encompasses the applications of electronics, controls and communications, 1998;45(4):633–7.

[118] Sarpturk SZ, Istefanopulos Y, Kaynak O. On the stability of discrete-time sliding mode control systems. IEEE Transactions on Industrial Electronics encompasses the applications of electronics, controls and communications, 1987;32(10):930–2.

[119] Chang J-L. Robust discrete-time model reference sliding-mode controller design with state and disturbance estimation. IEEE Transactions on Industrial Electronics encompasses the applications of electronics, controls and communications, 2008;55:4065–74.

[120] Chakravarthini M, Bandyopadhyay B, Unbehauen H. A new algorithm for discrete-time sliding mode control using fast output sampling feedback. IEEE Transactions on Industrial Electronics encompasses the applications of electronics, controls and communications 2002;49(2):518–23.

[121] Levant A. Finite differences in homogeneous discontinuous control. IEEE Transactions on Industrial Electronics encompasses the applications of electronics, controls and communications. 2007;52(7):1208–17.

[122] Wang B, Yu X, Li X. Zoh discretization effect on higher-order sliding mode control systems. IEEE Trans Ind Electron 2008;55(11):4055–64.

[123] Davila J, Fridman L, Levant A. Second-order sliding-mode observer for mechanical systems. IEEE Trans Autom Control 2005;50(11):1785–9.

[124] Salgado I, Kamal S, Chairez I, Bandyopadhyay B, Fridman L. Super-twisting-like algorithm in discrete time nonlinear systems. In The 2011 International conference on advanced mechatronic systems, Zhengzhou, China, August, 2011.

[125] Bartolini G, Ferrara A, Usai E, Utkin V. On multi input chattering-free second-order sliding mode control. IEEE Trans Autom Control 2000;45(9):1711–9.

[126] Orlov Y, Aguilar L, Cadiou C. Switched chattering vonytol vs backlash/friction phenomena in electrical servo-motors. Int J Control 2003;76:959–67.

[127] Levant A, Fridman L. High order sliding modes. Sliding mode in control in engineering. New York, USA: Marcel Dekker, Inc.; 2002. p. 53–101.

[128] Pisano A, Davila A, Fridman L, Usai E. Cascade control of pm dc drives via second-order sliding-mode technique. IEEE Trans Ind Electron 2008;55 (11):3846–54.

[129] Haddad WM, Chellaboina V. Nonlinear dynamical systems and control. Princeton University Press; 2008.

[130] Poznyak A. Advanced mathematical tools for automatic control engineers. In: Deterministic systems, vol. 1. Elsevier Science; Hungary, 2008.

[131] Dávila A, Moreno J, Fridman L. Variable gains super-twisting algorithm: a Lyapunov based design. In: American control conference; 2010

[132] Esmaeili. Ali, Ibeas. Asier, Salim Ibrir, and Pedro Balaguer. Joint Parameter-State Estimation-Based Control of Heart Rate During Treadmill Exercise, 24th IEEE Conference on Emerging Technologies and Factory Automation, Spain.

[133] Esmaeili. Ali, Ibeas. Asier, Discrete-time sliding mode control of heart rate during treadmill exercise, 24th IEEE Conference on Emerging Technologies and Factory Automation, Spain.

[134] Chalanga, Asif, Kamal, Shyam, Fridman, Leonid M, Bandyopadhyay, Bijnan, Moreno, Jaime A (2016). Implementation of super-twisting control: supertwisting and higher order sliding-mode observer-based approaches. IEEE Transactions on Industrial Electronics, 63(6), 3677–3685.

[135] Boiko, Igor, Fridman, Leonid, Pisano, Alessandro, and Usai, Elio (2007). Analysis of chattering in systems with second-order sliding modes. IEEE Transactions on Automatic Control, 52(11), 2085–2102.

[136] Plestan, Franck, Shtessel, Yuri, Bregeault, Vincent, and Poznyak, Alex (2010). New methodologies for adaptive sliding mode control. International Journal of Control, 83(9), 1907–1919.

[137] Brogliato, Bernard, Andrey Polyakov, and Denis Efimov. "The implicit discretization of the super-twisting sliding-mode control algorithm." 2018 15th International Workshop on Variable Structure Systems (VSS). IEEE, 2018.

[138] Koch, Stefan, and Markus Reichhartinger. "Discrete-time equivalents of the super-twisting algorithm." Automatica 107 (2019): 190-199.

[139] Chawengkrittayanont, Panitnart, and Chutiphon Pukdeboon. "Continuous higher order sliding mode observers for a class of uncertain nonlinear systems." Transactions of the Institute of Measurement and Control 41.3 (2019): 717-728.

[140] Roy S, Roy SB, Lee J, Baldi S. Overcoming the Underestimation and Overestimation Problems in Adaptive Sliding Mode Control. IEEE/ASME Transactions on Mechatronics. 2019 Jul 24.